AD A041158

NAVAL POSTGRADUATE SCHOOL
Monterey, California



THESIS

A MATHEMATICAL MODEL

FOR THE

LONGITUDINAL CONTROL SYSTEM

OF THE

SPACE SHUTTLE ORBITER

Approved for public release; distribution unlimited.

AD No.
DDC FILE COPY

DDC
RECEIVED
JUL 5 1977
D

UNCLASSIFIED

SECURITY CLASSIFICATION OF THIS PAGE (When Data Entered)

REPORT DOCUMENTATION PAGE		READ INSTRUCTIONS BEFORE COMPLETING FORM
1. REPORT NUMBER	2. GOVT ACCESSION NO. (9)	3. RECIPIENT'S CATALOG NUMBER
4. TITLE (and Subtitle) (6) A Mathematical Model for the Longitudinal Control System of the Space Shuttle Orbiter,		5. TYPE OF REPORT & PERIOD COVERED Master's thesis; March 1977
		6. PERFORMING ORG. REPORT NUMBER
7. AUTHOR(s) (10) Cole Jon PIERCE / Cole J., LCDR, USN		8. CONTRACT OR GRANT NUMBER(s)
9. PERFORMING ORGANIZATION NAME AND ADDRESS Naval Postgraduate School Monterey, California 93940		10. PROGRAM ELEMENT, PROJECT, TASK AREA & WORK UNIT NUMBERS (12) 192 p.
11. CONTROLLING OFFICE NAME AND ADDRESS Naval Postgraduate School Monterey, C lifornia 93940 (11)		12. REPORT DATE 25 Mar[illegible]1977
		13. NUMBER OF PAGES 192
14. MONITORING AGENCY NAME & ADDRESS(if different from Controlling Office)		15. SECURITY CLASS. (of this report) UNCLAS
		15a. DECLASSIFICATION/ DOWNGRADING SCHEDULE

16. DISTRIBUTION STATEMENT (of this Report)

Approved for public release; distribution unlimited

17. DISTRIBUTION STATEMENT (of the abstract entered in Block 20, if different from Report)

18. SUPPLEMENTARY NOTES

19. KEY WORDS (Continue on reverse side if necessary and identify by block number)

Model
Control system
Space Shuttle
Orbiter

20. ABSTRACT (Continue on reverse side if necessary and identify by block number)

The analysis of a fly-by-wire longitudinal control system, specifically that of the space shuttle orbiter, was undertaken in order to demonstrate the construction of a mathematical model depicting the relationships between forcing function and response. Each facet of modern control theory, including stability, was developed. Several computer programs were written, which should be of value to the Department of Aeronautics, for the HP9830 computer/plotter; these — next page

DD FORM 1 JAN 73 1473 (Page 1) EDITION OF 1 NOV 65 IS OBSOLETE S/N 0102-014-6601

UNCLASSIFIED

SECURITY CLASSIFICATION OF THIS PAGE (When Data Entered)

251 450

programs are basic to the study of control theory, demonstrate the importance of the transfer function, the characteristic equation, and the various forms of feedback, and will plot time and frequency (Bode) response graphs given the proper inputs. The Continuous System Modeling Program, version III, and the IBM360 were used to analyze the complex control system installed in the orbiter. The demonstration of the model and its interface with the CSMP program was given, and the efficiency of this procedure was made clear.

Approved for public release; distribution unlimited

A Mathematical Model for the Longitudinal Control System of the Space Shuttle Orbiter

by

Cole Jon Pierce
Lieutenant Commander
United States Navy

Submitted in partial fulfillment of the requirements for the degree of

MASTER OF SCIENCE IN AERONAUTICAL ENGINEERING

from the

NAVAL POSTGRADUATE SCHOOL
March 1977

DDC
JUL 5 1977
D

Author C. J. Pierce

Approved by: Daniel J. Collins
Thesis Advisor

Donald P. Layton
Second Reader

Richard W. Bell
Chairman, Department of Aeronautics

Robert M. Brown
Dean of Science and Engineering

ACCESSION for
NTIS White Section
DDC Buff Section
UNANNOUNCED
JUSTIFICATION
BY
DISTRIBUTION/AVAILABILITY CODES
Dist. AVAIL. and/or SPECIAL
A

ABSTRACT

The analysis of a fly-by-wire longitudinal control system, specifically that of the space shuttle orbiter, was undertaken in order to demonstrate the construction of a mathematical model depicting the relationships between forcing function and response. Each facet of modern control theory, including stability, was developed. Several computer programs were written, which should be of value to the Department of Aeronautics, for the HP9830 computer/plotter; these programs are basic to the study of control theory, demonstrate the importance of the transfer function, the characteristic equation, and the various forms of feedback, and will plot time and frequency (Bode) response graphs given the proper inputs. The Continuous System Modeling Program, version III, and the IBM360 were used to analyze the complex control system installed in the Orbiter. The demonstration of the model and its interface with the CSMP program was given, and the efficiency of this procedure was made clear.

TABLE OF CONTENTS

I. PHYSICAL DESCRIPTION OF THE ORBITER ---------- 7

II. DEFINITIONS AND SYMBOLOGY ---------- 14

III. MATHEMATICAL MODELS OF LINEAR SYSTEM ELEMENTS ---------- 28

IV. STABILITY ---------- 37

V. EQUATIONS OF MOTION ---------- 50

VI. COMPUTER METHODS OF ANALYSIS ---------- 63

VII. LONGITUDINAL FEEDBACK ---------- 101

VIII. THE ORBITER ---------- 141

BIBLIOGRAPHY ---------- 190

INITIAL DISTRIBUTION LIST ---------- 192

ACKNOWLEDGEMENTS

In appreciation of the help I have received while writing this paper, I would like to thank

Professor Schmidt
Department of Aeronautics

Professor Strum
Department of Electrical Engineering

especially

Professor Collins
Department of Aeronautics

most especially

my wife, [redacted]

I. PHYSICAL DESCRIPTION OF THE ORBITER

The space shuttle orbiter is the vanguard of a new generation and new concept of spacecraft, having been designed to fly as an atmospheric vehicle as well as to operate as a spacecraft in near-earth orbit. In order to function in this dual role, it requires the performance, stability, and control systems of both types.

For orbital flight, attitude control is achieved by means of a reaction control system such as those used in earlier spacecraft. Whereas earlier vehicles followed an unguided re-entry and parachute let-down, the orbiter is to be flown to a runway landing and therefore requires the conventional aerodynamic roll, pitch, and yaw controls for atmospheric flight. The longitudinal system for maintaining the desired pitch angle, pitch rate, and stability about the pitch axis is the subject of this paper.

The space shuttle orbiter is of conventional design, incorporating a low-mounted, highly swept delta wing and a small vertical stabilizer on a thick, rather square body. Sea level weight of the vehicle, in re-entry configuration, is approximately 186,000 lbs. The wetted area of the wing

is 2690 square feet, yielding a wing loading of 69 psf. Overall length is 122.3 ft, and wing span is 78 ft.[1] The landing speed of the orbiter, necessarily high because of the wing loading, is 190 knots.

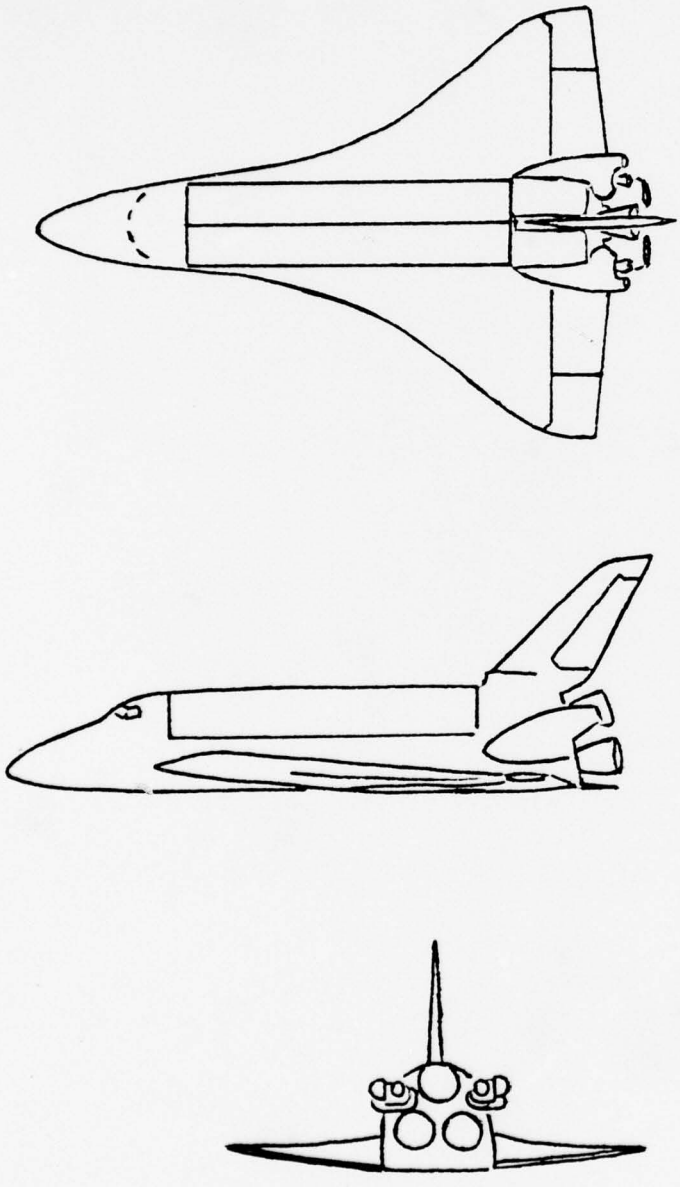
The primary aerodynamic control surfaces are split elevons at the trailing edge (to perform the functions of ailerons and elevators) and a combination rudder/speed-brake at the trailing edge of the vertical stabilizer. The rudder splits symmetrically along its vertical hinge to produce aerodynamic drag for speed control, hence its use as a speed brake. Body flaps are located at the trailing edge of the fuselage and, although they were originally intended to provide heat shielding for the main engines during re-entry, will be used as an active longitudinal trim device. Figure 1-1 is a three-view of the vehicle and shows the location of the primary control surfaces.

The elevons are split because of wing deflection and hinge moment considerations, and are quite large, comprising twenty per cent of the total wing area. Their maximum deflection is 35 degrees up and 20 down; maximum deflection

---

[1] By comparison, the commercial Douglas DC-9 measures 119.3 feet in length and has a span of 93.4 feet.

Figure 1-1



Three-view of the Orbiter

rate is twenty degrees per second.

The speed brake provides additional longitudinal control in some regimes by generating a pitching moment, but its primary use is for terminal area energy management.

The elevons are the primary pitch attitude control, but since their normal deflection is trailing edge down, the body flap is available to reduce the load on them. Use of the flap enables the elevons to trail as much as possible and minimizes their chances of overheating. The body flap is also an aid to longitudinal control at high angles of attack where the elevons lose much of their effectiveness. Due to rudder blanking, the orbiter is in fact directionally unstable in this regime (the early re-entry phase). The existence of a lightly damped dutch roll mode, however, provides dynamic stability for the vehicle.

The trajectory followed by the vehicle from orbit to touchdown is sensitive and complex as with former spacecraft and occurs as follows. Following de-orbit, the reaction control system engines orient the orbiter to a normal front-end-forward top-side-up attitude prior

to reaching re-entry interface at 400,000 feet. The angle of attack during re-entry varies between thirty and forty degrees. When the velocity decreases to 9000 feet per second, a slow pitch down maneuver commences which is completed by 70,000 feet; here, the angle of attack has been reduced to ten degrees and the velocity to 1500 feet per second. Terminal area energy management is then enabled to control airspeed and to position the orbiter to arrive on the final approach at 12,000 feet, six nautical miles from touchdown. Most of the phase prior to the final approach position will be flown at a large roll angle and at relatively high "g" in order to follow a steeper trajectory. This results in shortening the range and time to touchdown, which reduces the total heat load endured by the vehicle and extends the lifetime of the thermal protection system.

The flight control system itself has three modes: automatic, control stick steering, and direct. Each mode may be selected individually for longitudinal and/or lateral-directional control.

The automatic mode consists of hands-off coupling of guidance commands through the digital flight control system to the control surfaces. Control stick steering

is a pitch (roll) rate command system for the longitudinal (lateral-directional) channel with gain scheduled as a function of the dynamic pressure. This mode is further compensated for angle of bank and for the pitching moment created by the speed brake. The direct system relates controller deflections proportionally to the control surfaces; this mode will be hopefully unnecessary as the vehicle is marginally stable longitudinally, even with a forward center of gravity. "The aerodynamic characteristics of the orbiter, together with its total dependence on avionics for flight control, classify it as a digital fly-by-wire, control-configured vehicle."[2] The entire approach, from de-orbit to re-entry to touchdown, will normally be flown entirely in the automatic mode.

---

[2] LCOL C.G. Fullerton, USAF, "Space Shuttle Orbiter Approach and Landing Test Program," The Society of Experimental Test Pilots, 1975 Report, page 158

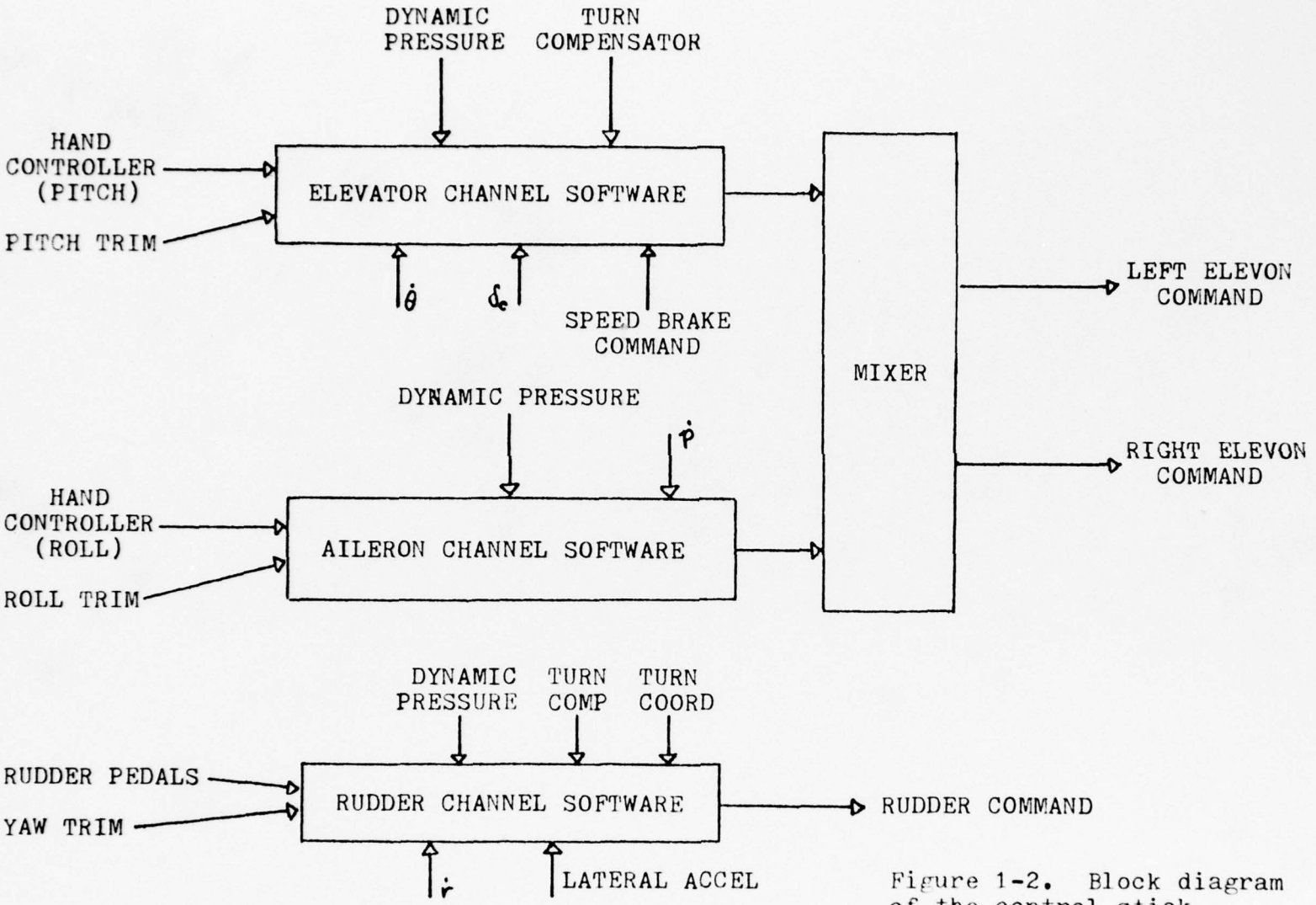


Figure 1-2. Block diagram of the control stick steering mode

II. DEFINITIONS AND SYMBOLOGY

As in any field of study, that of automatic control has many terms which have a particular meaning when used in this context. So that further references to some of these terms is facilitated, the following definitions apply:

Angle of attack: the angle between the fuselage reference line and the flight path; denoted by α.

Block diagram: a graphical representation, such as a schematic diagram, of the physical components of a system or a set of mathematical equations describing their input/output relationships.

Bode plot: a plot of the magnitude of response of a system to a sinusoidal input measured against the frequency of that input.

Characteristic equation: the denominator of a system's transfer function set equal to zero.

Closed-loop: a system in which the input is affected or modified by some stage of output.

Control matrix: describes how the control input affects the plant.

Control system: a set of physical components related in such a manner so as to control or regulate itself or

some other system.

Damping: frictional retardation of the magnitude of a deflection (displacement) or rate.

Damping ratio: the ratio of the amount of damping actually present in a system to the amount that would critically damp that system.

Error signal: the actual actuating signal of the system; it is generally the difference between the input and feedback signals.

Feedback: a signal, which is some form of the output signal, that is added to or subtracted from the original input in order to compare the desired output with that actually obtained.

Forcing function: see Input.

Frequency response: a measure of the output of the system as a function of input frequency.

Gain: the measure of magnitude of an input or feedback signal.

Initial condition: one of the two types of inputs to a system.

Input: a stimulus applied to a control system in order to produce a desired output.

Linear differential equation: one consisting of the sum of linear (first degree) terms; it has the property

that the response of a system due to several inputs acting at once is equal to the sum of the responses of each input acting alone. An equation may be linearized by making valid assumptions (approximations) about the system or by considering the system to operate in a restricted environment where the variations from linearity are small (piece-wise linearity).

Open-loop: a system in which the input is not affected or modified by any stage of output.

Output: the actual response of the system caused by the input reacting with the various components of the system; it is not necessarily the response implied by the input.

Plant: the object or system which is to be controlled.

Reaction control system: a control system which generates rolling, pitching, and/or yawing moments by venting jet, rocket, or compressor air exhaust about the axis desired.

Resolvent matrix: denoted by $\Phi(s)$; the matrix which, when multiplied by the control vector and the Laplace of the input, yields the Laplace of the output of the system.

Root locus: a method of graphing the roots of a characteristic equation as a function of gain; useful in stability analysis.

Stability, dynamic: the quality of a system that determines whether its response to any input will be bounded or unbounded.

Stability, static: the tendency of a system following displacement from a rest position, considered positive if the initial tendency is to return to the original position.

State variable: a variable which determines the state of the system; the state variables of a dynamic system are the smallest set of variables which completely determines the behavior of the system for any time $t \geq 0$.

Steady state response: that part of the total response which does not approach zero as time approaches infinity.

Terminal area energy management: a dynamic program using inputs of orbiter position and velocity to guide the vehicle to its final approach path, minimizing the heat load when possible.

Time constant: inverse of frequency.

Time-invariant differential equation: a differential equation inwhich none of the terms depends explicitly upon the independent variable, t.[3]

Time response: a measure of the output of the system as a function of time.

---

[3] Only linear, time-invariant differential equations will be considered in the development of the equations of motion in this study.

Transfer function: the ratio of the Laplace transform of the output (response) of a system to the Laplace transform of the input (forcing function) under the assumption that the initial conditions are zero.

Transfer matrix: the matrix of transfer functions for a multiple input/output system.

Transient response: that part of the total response which approaches zero as time approaches infinity.

Undamped natural frequency: the frequency at which a system would vibrate were it not damped.

Unit impulse: an input whose magnitude approaches infinity and whose duration approaches zero, but whose product of magnitude times duration equals one.

A glossary of symbols follows:

a lift curve slope, $\frac{\partial C_L}{\partial \alpha}$

b wing span

$\bar{c}$ mean aerodynamic chord

C_{L_α} $\frac{\partial C_L}{\partial \alpha}$, variation in lift with respect to angle of attack; generally linear at angles of attack below the stall region; coefficient of

C_{M_α} $\frac{\partial C_M}{\partial \alpha}$, variation of pitching moment about the center of gravity with respect to angle of attack; must be negative for positive static stability; coefficient of

C_{M_o} pitching moment that remains when lift forces equal zero, coefficient of

e span efficiency factor, relative to the elliptical wing and lift distribution

f any function, time domain, as f(t)

F any function, Laplace domain, as F(s)

g transfer function, time domain, as g(t)

G transfer function, Laplace domain, as G(s)

I moment of inertia, subscripted as to axis about which it is taken

K gain

$\mathcal{L}$ Laplace transform of, as $\mathcal{L}[f(t)]$

$\mathcal{L}^{-1}$ inverse Laplace transform of, as $\mathcal{L}^{-1}[F(s)]$

L,M,N moments about X-, Y-, and Z-axes, respectively

p,q,r perturbations in roll, pitch, and yaw rates

$\dot{p},\dot{q},\dot{r}$ perturbations in roll, pitch, and yaw accelerations

P,Q,R rates of roll, pitch, and yaw

S wing area

u,v,w perturbations in forward, side, and vertical velocities

$\dot{u},\dot{v},\dot{w}$ perturbations in forward, side, and vertical accelerations

U,V,W velocities in forward, side, and vertical directions

x,y,z distances along X-, Y-, and Z-axes

X,Y,Z axis system, right-handed; also force components in X, Y, and Z directions

α angle of attack

δ Dirac delta, unit impulse function $\delta(t)$

δ_e deflection, elevon

ζ damping ratio

$\theta, \dot{\theta}$ pitch angle, rate perturbations

Θ pitch angle, relative to earth, positive nose up

ρ air density

Φ roll angle, relative to earth, positive right wing down (see also resolvent matrix)

ω frequency

In order to derive the equations of motion of a system, a reference frame must be decided upon. The most natural of these would be a frame in which the axes were aligned with the physical structure of the vehicle, one which is called the body-fixed axis system. Such a system is depicted in Figure 2-1. Components of velocities, forces and moments, and distances relative to their respective axial motions are listed in Table 2-1.

In the development of the equations of motion for a vehicle, this reference frame has several advantages. The rotary inertial properties are constant (assuming

motion	velocity	applied forces and moments	distance
forward	U	X	x
side	V	Y	y
vertical	W	Z	z
roll	P	L	
pitch	Q	M	
yaw	R	N	

Table 2-1

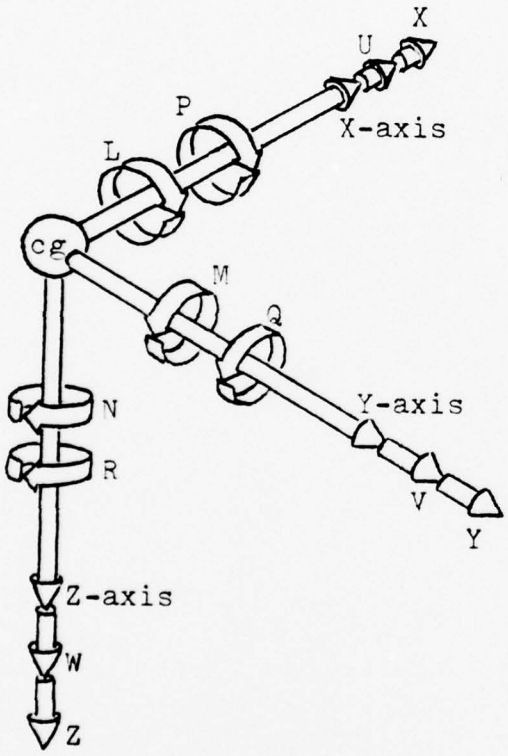


Figure 2-1[4]

[4] Adapted from McRuer, Ashkenas, and Graham, Aircraft Dynamics and Automatic Control, Princeton, 1973

constant mass) so that any derivatives with respect to time are zero. The pilot senses forces and moments with respect to the body-fixed frame, calculates his reactions to vehicular motion and to his changing external environment in terms of the body-fixed axes, and generally measures his position (attitude), velocities, and accelerations from a body-fixed system. This is especially true when he is dealing with primarily relative motion, as in air combat maneuvering.

An alternative to the body-fixed system is the space-fixed system where forces and moments are measured relative to an axis system oriented, for example, to a flat earth, as in Figure 2-2.

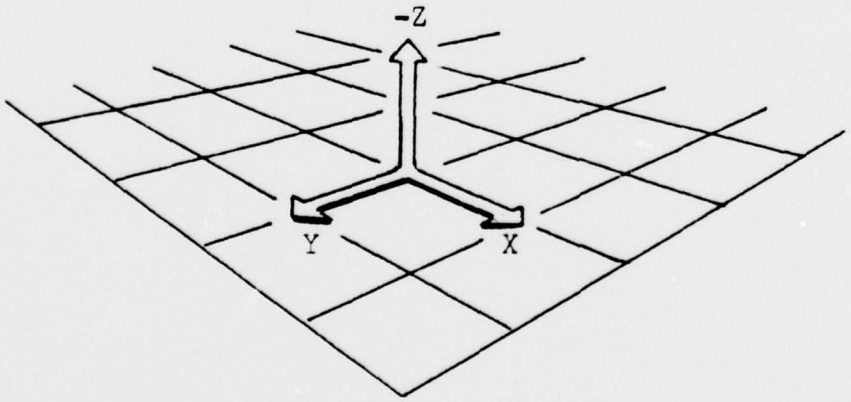


Figure 2-2

This system, however, has the very undesirable feature of requiring inclusion in the equations of motion the variations of moments of inertia of a vehicle as the vehicle changes its velocity vector and/or attitude. This system would be ideal for an aircraft which changed neither, but such is not the case in this study.

Corrections must also be made to the equations of motion in the body-fixed axis system, but these corrections are limited to inertial forces and accelerations and do not involve changing the apparent physical characteristics of the vehicle. Further simplifications are enabled by this choice of systems; one, the small angle assumption is made possible leading to the linearization of the equations of motion (see Chapter V); two, the symmetry of the aircraft across its X-Z plane eliminates several terms in the equations.

The body-fixed axis system is clearly the better selection for the development of the equations of motion of the vehicle.

A definition of "flight control" is necessary in

order to identify those parameters of the vehicle with which the study is concerned. The definition is borrowed from McRuer, Ashkenas, and Graham[5]:

> "Control: the development and application to a vehicle of appropriate forces and moments that
> 1. establish some equilibrium state of vehicle motion (operating point control)
> 2. restore a disturbed vehicle to its equilibrium (operating point) state and/or regulate, within desired limits, its departure from operating point conditions (stabilization)."

This definition includes the concept of stability and effectively excludes the domain of guidance.

In light aircraft, all functions of control (turning, climbing, accelerating) are performed by the pilot using the control wheel (or stick), the throttle, and various other aerodynamic controls, usually the flap handle, which are directly connected to the device which they operate. For example, the pilot desires to pull up; he uses some degree of back stick, the elevator responds immediately and in proportion to the amount of stick travel, and a pitch rate is generated. The pilot's environment remains

---

[5] Ibid.

relatively constant throughout the flight envelope of the airplane; a ten pound pull on the stick will give, for example, 1.3 g's at a given airspeed in every case.

Even for higher performance aircraft operating in the dynamic environment of air-to-air combat, this is an entirely satisfactory system.[6] Even though a given elevator deflection will not create the same pitch rate at 20000 feet as it does at sea level, the pilot quickly compensates for this by modifying control stick position. However, maintaining a particular pitch angle can better be performed by an automatic control system. Using a set of accelerometers to sense minute deviations from an operating (trim) condition, an automatic control system can command the rapid and precise control deflections necessary to maintain the vehicle near the desired flight condition. A pilot attempting to maintain a given pitch angle will find his sensory threshold much higher than (and his response on the controls much less precise than) an automatic system. This type of system is installed on many aircraft as an auto-pilot, engaged by the pilot when desired, to maintain certain flight conditions such as

---

[6] Present-day fighters have flight control systems augmented by 2- or 3-axis stabilization to minimize gust response and other oscillations.

heading and altitude.

The development and utilization of control systems may be taken one step further. When a vehicle, such as the orbiter, is required to fly in vastly different environments in the course of a mission, control stick inputs to obtain a given maneuver may require very different control deflections. Variations in dynamic pressure, Mach number, and altitude create changing values of control effectiveness, locations of aerodynamic forces, even stability. The automatic control system can use inputs such as air density, dynamic pressure, Mach number, and existing control deflection to compute precisely how much deflection is required to perform a particular maneuver and how rapidly the deflection should be applied. The system may also consider variations in stability under different flight conditions. It will then command that deflection, measure the response, and make further corrections if necessary, with far greater accuracy and efficiency than a human pilot.

This then is the principle by and for which the fly-by-wire system was developed. In an environment of changing flight conditions and stability where high

control precision is required, the automatic system significantly outperforms the best of pilots.

III. MATHEMATICAL MODELS OF LINEAR SYSTEM ELEMENTS

The Laplace transform is a major tool in the study and analysis of automatic control systems. It is the procedure by which time domain performance is connected to frequency response and results from the correspondence between the transfer function and the transient response. The transfer function itself is the ratio of the Laplace transform of a system's output to the transform of its input, assuming that all initial conditions are zero. A graphic representation of such an input-output relationship is provided by the block diagram. In the block diagram, of which the transfer function(s) is the heart, inputs and feedbacks are represented by their Laplace transforms, and the paths which the signals follow are depicted.

Several simplifications in computation occur when using the Laplace transform, among which are (1) differentiation in the time domain is represented by multiplication by s in the Laplace (frequency) domain; (2) integration becomes division by s (both with regard for initial conditions); and (3) convolution, or complex multiplication, becomes simple multiplication.

The equation linking the time domain to the frequency

domain is

$$\mathcal{L}[f(t)] \triangleq F(s) = \lim_{\substack{t_2 \to \infty \\ t_1 \to 0}} \int_{t_1}^{t_2} e^{-st} f(t)\, dt = \int_{0+}^{\infty} e^{-st} f(t)\, dt$$

When the equation of motion for a system can be expressed as a linear differential equation, the Laplace transform reduces the differential equation to an algebraic equation in the Laplace variable, s. To illustrate, a damped spring-mass system will be used.

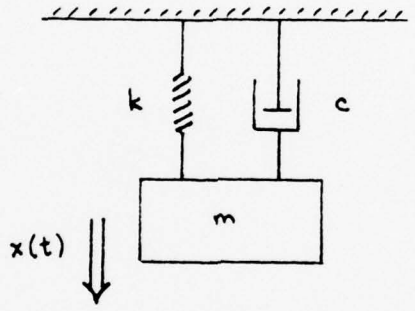


Figure 3-1

Here, $m\ddot{y} + c\dot{y} + ky = x(t)$. Each term is replaced by its Laplace transform:

$$m\ddot{y} \rightarrow m\left[s^2Y(s) - sy(0) - \frac{dy(0)}{dt}\right]$$

$$c\dot{y} \rightarrow c\left[sY(s) - y(0)\right]$$

$$ky \rightarrow kY(s)$$

$$x(t) \rightarrow X(s)$$

When coefficients of like powers of s are collected, the equation becomes

$$\left[mY(s)\right]s^2 - \left[my(0) - cY(s)\right]s - \left[m\frac{dy(0)}{dt} + cy(0) - kY(s)\right] = X(s)$$

The appropriate values of the initial conditions are entered, and a simple quadratic equation in s has replaced a second order differential equation.

Recalling the definition of a transfer function, all initial conditions are set equal to zero, and the ratio Y(s)/X(s) is found:

$$\left[mY(s)\right]s^2 + \left[cY(s)\right]s + kY(s) = X(s)$$

$$\left[ms^2 + cs + k\right]Y(s) = X(s)$$

$$\frac{Y(s)}{X(s)} = \frac{1}{ms^2 + cs + k} = G(s) \qquad (3\text{-}2)$$

where G(s) is a common symbol for the transfer function.

Figure 3-2 is the block diagram of this system where X(s) is the input or forcing function, Y(s) is the output, and G(s) is the transfer function (also called the plant matrix in multiple input/output systems). In this case, G(s) has been derived from mass properties of the system, the degree of damping, the spring stiffness, and fundamental laws of motion.

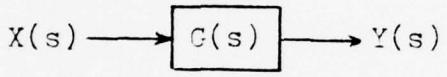


Figure 3-2

In modeling a system, G(s) will be found in a manner analogous to the above. All that remains in order to find the response to any input (neglecting feedback for the moment) is to multiply the transfer function by the Laplace transform of the input. The response may be left in the frequency domain, which is the usual case in stability analysis, or transformed back into the time domain to study the dynamic characteristics of the system, e.g. rise and settling times, maximum overshoot, etc.

Some of the more common inputs are listed in Table 3-1 with their time- and frequency-domain representations.

The transformations are linear; that is, if F(s) is the transform of f(t), then a•F(s) is the transform of a•f(t).

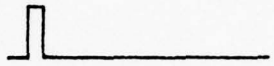
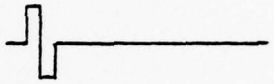
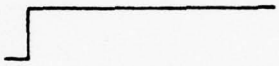
	time x(t)	frequency X(s)	graph
unit impulse	$\delta(t)$	1	
unit doublet	$\dot{\delta}(t)$	s	
unit step	1	$\frac{1}{s}$	
ramp	t	$\frac{1}{s^2}$	
sinusoidal	$\sin \omega t$	$\frac{\omega}{s^2+\omega^2}$	

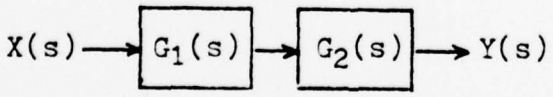
Table 3-1

It can be seen in the first column that the unit step is the time derivative of the ramp function, and the unit impulse (represented by the Dirac delta) is the derivative of the unit step. If the latter is not obvious, consider that the derivative of a function is the slope of that function at every point where the function is continuous. At t=0, the slope of the unit step approaches

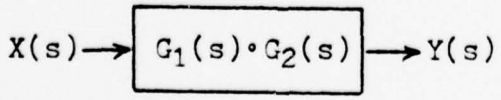
infinity, as does the magnitude of the unit impulse. At $t=0^+$, the slope of the unit step is zero, as is the magnitude of the impulse function.

Since an impulse function is an idealization, it must be approximated in the real world. When finding the Laplace transform of this approximation, any arbitrary magnitude may be assigned to the "impulse", as long as its duration is small compared to the time constant of the system. If the duration of the impulse is taken as the inverse of the magnitude, the area under its curve will equal one, hence the unit impulse.

Unless otherwise depicted, successive terms along a block diagram path are multiplied together; witness the correlation between equation (3-2) and Figure 3-2. This is true whether dealing with inputs, successive transfer functions, or other operations such as integration, delay, or differentiation. Diagramatically,



is identical to



The resulting transfer function $G(s) = G_1(s) \cdot G_2(s)$, or

the output $Y(s) = X(s) \cdot G_1(s) \cdot G_2(s)$.

A feedback signal, on the other hand, is not multiplied but rather employs a summing junction where certain signals downstream in the diagram are fed back and added to (or subtracted from) the input signal. A typical system with one feedback loop is depicted in Figure 3-3. The derivation of the complete, or closed loop, transfer function follows.

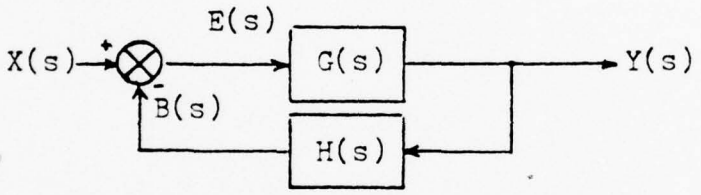


Figure 3-3

E(s) represents an error signal, the difference between the input signal and the feedback signal. B(s) is called the open loop transfer function; it is the input signal after being modified by any transfer functions and feedback terms up to the summing junction.

In this case

$$B(s) = G(s) \cdot H(s) \cdot E(s).$$

Since $Y(s) = G(s) \cdot E(s)$,

$$\text{and } E(s) = X(s) - B(s) = X(s) - G(s)\cdot H(s)\cdot E(s)$$

$$\text{then } E(s) + G(s)\cdot H(s)\cdot E(s) = X(s)$$

$$\text{or } E(s)\left[1 + G(s)\cdot H(s)\right] = X(s)$$

$$E(s) = \frac{X(s)}{1 + G(s)\cdot H(s)}$$

Substituting the error signal above into $Y(s) = G(s)\cdot E(s)$, the transfer function of the system due to feedback becomes $G'(s) = \frac{Y(s)}{X(s)} = \frac{G(s)}{1 + G(s)\cdot H(s)}$.

The second order system defined by the damped spring-mass system has the unique definition among its properties that $\frac{c}{m} = 2\zeta\omega_n$ and $\frac{k}{m} = \omega_n^2$ where ζ = damping ratio and ω_n = undamped (natural) frequency. If the equation of motion is divided through by m, the result is

$$\ddot{y} + \frac{c}{m}\dot{y} + \frac{k}{m}y = \frac{k}{m}x(t)$$

$$\text{or, } \ddot{y} + 2\zeta\omega_n\dot{y} + \omega_n^2 y = \omega_n^2 x(t)$$

where, for convenience, the input function x(t) has absorbed a constant 1/k. Taking the Laplace transform as before and letting the initial conditions equal zero,

$$\frac{Y(s)}{s^2 + 2\zeta\omega_n s + \omega_n^2} = X(s)$$

$$\text{or } \frac{Y(s)}{X(s)} = \frac{\omega_n^2}{s^2 + 2\zeta\omega_n s + \omega_n^2} .$$

If, then, the transfer function of a system may be written in the format $b/(s^2 + as + b)$, the physical characteristics of the system are immediately evident.

As will be seen in the analysis of the orbiter, the system transfer function may be factored into two such second order terms yielding at once the periods and degrees of damping of both the phugoid and the short period motions. The damping term offers a further clue as to basic or inherent stability of the system. When the roots of the quadratics are obtained from $s = -\zeta\omega_n \pm \omega_n\sqrt{\zeta^2-1}$, the value of ζ determines whether or not those roots lie in the right half plane (RHP) according to Table 3-2.

value of ζ	roots are
$\zeta < 0$	in RHP
$\zeta = 0$	pure imaginary
$0 < \zeta < 1$	complex with negative real parts
$\zeta = 1$	equal, negative, and real
$\zeta > 1$	negative and real

Table 3-2

The significance of a root or roots in the right half plane will be discussed in the section on stability.

IV. STABILITY

One of the prime indices of a vehicle's performance is the measure of its stability, or how, how much, and how quickly it responds to external forces or control inputs.

Two types of stability are generally defined, static and dynamic. Static stability is the vehicle's tendency to return to its original flight condition after being disturbed from that condition. A common representation of the three degrees of static stability, positive, negative, and neutral, is shown in Figure 4-1. The ball possessing positive static stability will return to its original position when displaced, the ball with negative static stability will continue to move away from its

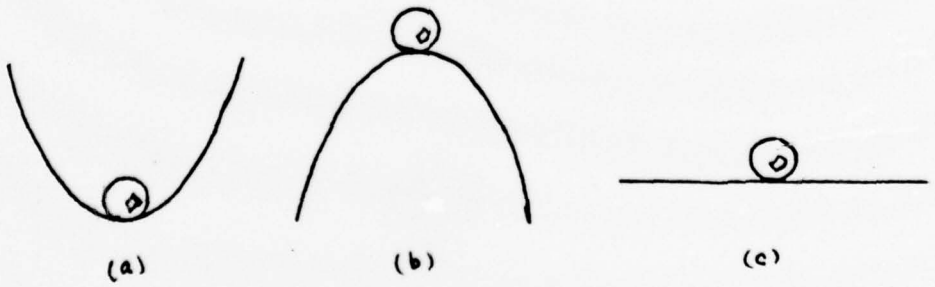


Figure 4-1

original position, and the ball with neutral stability will simply remain in its new position.

The parallel may be drawn with respect to an aircraft's longitudinal (pitch) response when displaced from trimmed flight[7] by a control input or external force. Figure 4-2 illustrates the longitudinal forces acting on a vehicle where L is the sum of lift forces produced by the wing and tail and is located on the aircraft so as to create the same total moment about the center of mass as would the individual forces. C_{m_o} is the pitch moment remaining when the lift forces are zero.

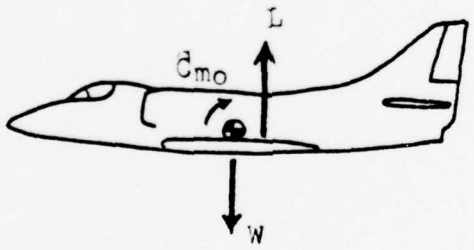


Figure 4-2

---

[7] Trimmed flight is defined as that flight condition where the sum of all moments acting about the longitudinal axis is zero, i.e., $C_M = 0$.

In equilibrium flight, the moment produced by L is balanced by C_{m_o}, and no pitch rate is generated. Suppose a gust causes a momentary increase in the angle of attack. If the lift curve slope is positive (that is, a higher angle of attack generates more lift), as are all modern conventional airfoils, the increased lift will cause the total moment about the center of mass to be nose down, or stabilizing. The vehicle will tend to return to its original condition.

If the center of mass should move aft of the lift vector, the aircraft could still be stable if C_{m_o} were negative (nose down). However, if that gust were to hit this aircraft, the increased lift would cause a nose UP moment, increasing the angle of attack, further increasing the lift, etc. This vehicle then would be clearly unstable.

Three quantities are necessary to this discussion, the lift curve slope, the pitching moment coefficient, examples of which are shown in Figure 4-3, and C_{m_o}. A vehicle must have a positive lift curve slope ($\frac{\partial C_L}{\partial \alpha}$), a negative pitching moment slope (which means an angle of attack above the trim point causes a pitch down and vice

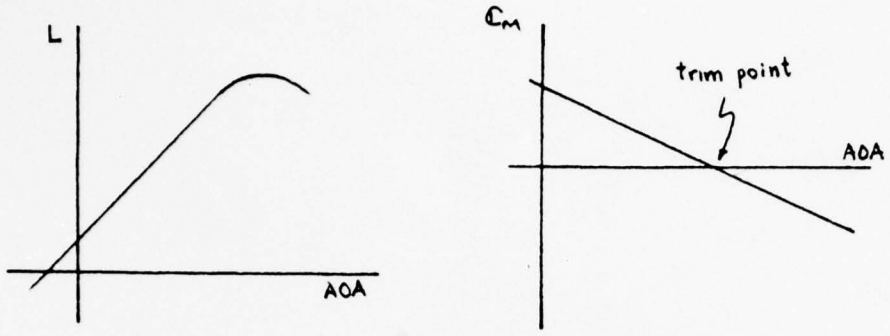


Figure 4-3

versa), and a positive C_{m_0} in order to be statically stable. C_{m_α} is negative when the aerodynamic center of the vehicle lies behind the center of mass, and a positive C_{m_0} is designed into the airframe.

Given that a vehicle has positive static stability, its dynamic stability may be studied[8]. The ball in Figure 4-1(a) is dynamically stable; if displaced from equilibrium, it would return to the bottom, probably overshoot, overshoot again coming back (but at a smaller magnitude), and eventually come to rest. If there were no friction, the system would be dynamically neutrally stable; the amount of overshoot would not vary from cycle to cycle. If, on the other hand, a magnetic

---

8 An exception to this requirement for positive static stability is the orbiter itself. Early in the reentry phase, at an angle of attack of 45°, the orbiter is laterally unstable due to the blanking of the vertical stabilizer. However, the presence of a lightly damped Dutch roll gives it positive dynamic stability.

device were installed under the bowl which was timed to attract the ball as it descended and repel it as it ascended, enough velocity could be imparted to the ball to finally shoot it over the side. As long as the force supplied by the magnet was by any degree greater than the forces of friction, the ball would eventually be thrown from the bowl; this is an example of a statically stable but dynamically unstable system.

Each degree of stability can be exemplified by an aircraft. A sharp rap on the control stick of a trimmed aircraft causes a pitch oscillation which quickly damps out and disappears (positive stability). Most aircraft have some degree of Dutch roll, a continuous but mild combination of rolling and yawing (neutral stability). High performance aircraft, whose stability may be marginal under certain conditions, can be susceptible to PIO (pilot induced oscillation) where the pilot plays the rôle of the aforementioned magnetic device and amplifies the pitching motion of the vehicle, with sometimes catastrophic results (negative dynamic stability).

In the more complicated realm of automatic control

systems involving feedback, high precision approach and landing sequences, etc., more than just "positive" or "negative" as regards stability must be known. For one reason or another, it may be desireable to utilize a high gain for a particular feedback signal, but there may be a limit as to how high the gain may be before it causes the system to become unstable. Certain types of inputs, generally frequency related, may cause large increases in the magnitude of response (resonance) and may require a certain amount of feedback to minimize these excursions.

Two of the basic tools used for studying the effects of feedback on a system are the root locus graph and the Bode plot.

The root locus is a locus of roots; the roots are those of the characteristic equation of the system. If the real parts of these roots are all negative, then the solution of the differential equation describing the system will involve negative (decaying) exponents, and the system will be stable. This is the rationale behind requiring roots to be in the left half plane for stability. Feedback gain can change the location of these roots and cause a system to become unstable.

An example is in order. Consider the system shown in Figure 4-4 where the plant transfer function is

$$\frac{(s-2)}{(s+1)(s+2)}$$

and where the feedback is linear and variable in magnitude.

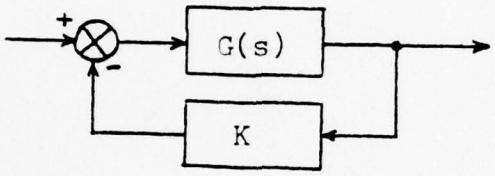


Figure 4-4

The closed loop transfer function becomes

$$\frac{(s-2)}{(s+1)(s+2) + K(s-2)} \quad ,$$

and the characteristic equation is

$$s^2 + (3+K)s + (2-2K) = 0.$$

The roots, for varying values of K, are given in Table 4-1.

K	root #1	root #2
0	-1	-2
0.5	-0.314	-3.186
1.0	0	-4
1.5	0.212	-4.712
2.0	0.372	-5.372

Table 4-1

Figure 4-5 is a graph of the root locus of the system. It may be seen that, as K exceeds the value of 1, one of the roots moves into the right half plane. That this

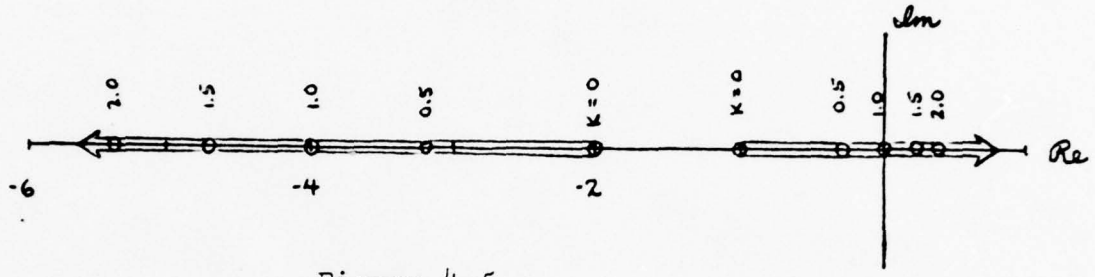


Figure 4-5

results in instability is shown by solving the corresponding differential equation for a value of $K > 1$. Let $K=2$; the characteristic equation becomes

$$s^2 + 5s - 2 = 0.$$

Converting this equation to the time domain by taking the inverse Laplace transform yields

$$\ddot{y} + 5\dot{y} - 2y = 0,$$

one of the solutions to which is $y = e^{0.372t}$. Since y is the output, it may be seen that the output increases without bound as the time increases. The system is unstable for this value of feedback gain.

The Bode plot depicts how the system will respond to a sinusoidal input. Gain and phase margins, which are measures of relative stability, are shown directly by the plot, as is the magnitude of response at resonance. By comparison with templates of the proper scale, the degree of damping may be read from the graph.

The standard representation of the magnitude of the response is $20 \cdot \log |G(j\omega)|$ where $j\omega$ has replaced s in the transfer function expression. This magnitude is plotted against the frequency of the input, which is on a logarithmic scale so that wide frequency ranges may be plotted with accuracy. The phase angle, φ, is likewise plotted against the logarithmically scaled frequency. A stable, time-invariant system, when energized by a sinusoidal input, will have a steady state output of the same frequency as the input although the magnitude and phase angle will likely be different.

Since the magnitude of the response is plotted in logarithmic form, finding the response curve of a complicated transfer function such as

$$G(s) = \frac{s^2 + 3s + 2}{s^3 + 6s^2 + 19s + 13}$$

is reduced to writing the function as the product of

first-order factors, finding the magnitude of each, and then adding (not multiplying) the logarithms of the magnitudes. From this, it is seen that an increase in gain merely raises the magnitude curve and does not affect the phase angle.

In the above example, writing the transfer function as a function of $j\omega$,

$$G(j\omega) = \frac{(j\omega)^2 + 3j\omega + 2}{(j\omega)^3 + 6(j\omega)^2 + 19(j\omega) + 13} = \frac{(2-\omega^2) + 3j\omega}{(13-6\omega^2) + j(19\omega - \omega^3)} .$$

Letting $\omega = 0.1$ yields

$$G(j0.1) = \frac{1.99 + j0.3}{12.94 + j1.899} \quad \text{and} \quad |G(j0.1)| = \frac{2.012}{13.079} = 0.1538 .$$

Then $20\ln|G(j0.1)| = -37.438$, the measure of magnitude of the response when the input frequency is 0.1 radian per second.

The phase angle is

$$\varphi = \tan^{-1}\frac{0.3}{1.99} - \tan^{-1}\frac{1.899}{12.94} = 8.57° - 8.35° = 0.22° .$$

Computing the values of the magnitude and phase angle over a wide range of frequencies, say from 0.001 to 10 radians per second, enables the construction of

the Bode diagram.

If the function is factored into

$$G(s) = \frac{(s+1)(s+2)}{(s+3+j2)(s+3-j2)(s+1)}$$

and each term written as a function of $j\omega$, the terms become

$$j\omega+1 \quad j\omega+2 \quad \left[3+j(\omega-2)\right]^{-1} \quad \left[3+j(\omega+2)\right]^{-1} \quad \left[j\omega+1\right]^{-1}.$$

The magnitudes at $\omega = 0.1$ are, respectively,

1.005 2.002 0.282 0.273 0.995.

The logarithms of these magnitudes are

0.005 0.694 -1.266 -1.298 -0.005.

which, when summed, total -1.870. Multiplying by 20, as before, yields -37.4, the same answer.

The sum of the phase angles is

$5.71^\circ + 2.86^\circ - (-32.3^\circ) - 34.99^\circ - 5.71^\circ = 0.17^\circ$,

approximately the same answer as before.

The factoring method is desired when the Bode plot is to be approximated by asymptotes, or straight lines which follow the trend of the function. It does not consider damping. The former method is entirely sufficient for plotting the exact function and will be the one used in this study.

A third type of graph used in the analysis of a system is the time response graph, or time history. Any forcing function (not just sinusoidal) for which a Laplace transform exists can be applied to a system, the output calculated, and the output inverted into the time domain. This yields a function of magnitude with respect to time, the plot of which depicts period(s), overshoot(s), rise times, decay times, steady state response, and gives an indication of the degree of damping in the system. Its drawback is that its degree of stability is not easily derived, although it is usually apparent whether or not the response is bounded.

As has been seen, gain will move the locus of roots on a root locus plot, sometimes changing the stability of a system; gain will move the Bode magnitude plot up or down, changing the relative stability. When gain is applied to a system, the time history plot reflects amplification of the magnitude of the response in proportion to the amount of gain, i.e., twice the gain yields twice the magnitude.[9] For example, if 5^{o} of elevator deflection create 50 lbs of force and 1000

---

9 Since we are dealing with linear systems

ft-lbs of moment, then 10^{o} of deflection will generate 100 lbs of force and 2000 ft-lbs of moment; the pitch rate created by the latter moment will be double that created by the former. However, when the gain to be varied is in a feedback loop, as described above for the root locus and Bode diagrams, the effects on the time history are generally unpredictable. The time history is therefore of limited value in designing a system; its asset is rather in analysis. All three types of plots will be used in this study.

V. EQUATIONS OF MOTION

In confining the study to the longitudinal case, only the X and Z forces and the pitching moment, M, are of interest. Each of these may have derivatives with respect to (1) forward velocity, u, (2) pitch angle, q, (3) vertical velocity, w, (4) vertical acceleration, $\dot{w}$, and (5) elevon deflection, δ_e . These derivatives are labelled, respectively, X_u, X_q, X_w, $X_{\dot{w}}$, X_{δ_e} , Z_u, etc. The lower case subscripts refer to perturbations from steady state.

The linearized equations of motion in state variable format, in terms of the derivatives defined above, are:

$$\begin{aligned}
\dot{u} &= X_u u + X_w w + X_q q - g\theta + X_{\delta_e}\delta_e \\
\dot{w} &= Z_u u + Z_w w + (U_o + Z_q) q + Z_{\delta_e}\delta_e \\
\dot{q} &= (M_u + Z_u M_{\dot{w}})u + (M_w + Z_w M_{\dot{w}})w \\
&\quad + \left[M_q + (U_o + Z_q)M_{\dot{w}}\right] q + (M_{\delta_e} + Z_{\delta_e} M_{\dot{w}})\delta_e \\
\dot{\theta} &= q
\end{aligned} \tag{5-1}$$

The state variables are written in the format

$$\{x\} = \begin{Bmatrix} u \\ w \\ q \\ \theta \end{Bmatrix}$$

and the equations of motion become

$$\begin{Bmatrix} \dot{u} \\ \dot{w} \\ \dot{q} \\ \dot{\theta} \end{Bmatrix} = \begin{bmatrix} X_u & X_w & X_q & -g \\ Z_u & Z_w & (U_o + Z_q) & 0 \\ (M_u + Z_u M_{\dot{w}}) & (M_w + Z_w M_{\dot{w}}) & [M_q + (U_o + Z_q) M_{\dot{w}}] & 0 \\ 0 & 0 & 1 & 0 \end{bmatrix} \begin{Bmatrix} u \\ w \\ q \\ \theta \end{Bmatrix}$$

$$+ \begin{Bmatrix} X_{\delta e} \\ Z_{\delta e} \\ (M_{\delta e} + Z_{\delta e} M_{\dot{w}}) \\ 0 \end{Bmatrix} \delta_e .$$

Or, $\{\dot{x}\} = [A]\{x\} + \{B\}\delta_e$

where $[A]$ is the plant matrix and $\{B\}$ is called the control matrix.

Some justification is in order for the linearization of the system equations of motion. Assumptions are also made to simplify the development and/or to define the scope of the study. Reference is made to Figure 2-1 for sign convention and notation in a body-fixed axis system; linear and angular velocities and applied forces and moments are identified.

The first assumption, which both simplifies the development and defines the environment, is that the earth is fixed in space. In orbital flight, a universal inertial frame is necessary due to the spinning of the earth on its axis and to the more pronounced effects of the gravitational fields of the sun and moon on a spacecraft. However, for the relatively short-term control analysis of this study, a geo-inertial frame of reference is assumed.

The airframe is assumed to be rigid. This enables the description of vehicular motion as a translation of and rotation about the vehicle's center of mass. The method of application of the thermal protection layer of the orbiter requires an absolute minimum of relative motion between and within various sections of the body, so this assumption of rigidity is especially valid.

The mass and mass distribution of the vehicle is assumed to be constant. Actually, since no fuel is being burned in producing thrust and no stores expended during that part of the trajectory under study, this, too, is an especially valid assumption.

For body-fixed axes, the inertial equations of motion (neglecting gravity) are:

$$\Sigma F_x = m(\dot{U} + QW - RV) \triangleq X$$
$$\Sigma F_z = m(\dot{W} + PV - QU) \triangleq Z$$
$$\Sigma M_y = \dot{Q} I_y + PR(I_x - I_z) + (P^2 - R^2) I_{xz} \triangleq M$$

The gravity force, acting only at the vehicle's center of mass, produces no moments but does contribute to the external forces; due to gravity,

$$\Delta X = mg \sin(-\Theta) = -mg \sin\Theta$$
$$\Delta Z = mg \cos(-\Theta)\cos\Phi = mg \cos\Theta \cos\Phi$$

The combination of the inertial and gravitational forces on the vehicle yields:

$$X = m(\dot{U} + QW - RV + g\sin\Theta)$$
$$Z = m(\dot{W} + PV - QU - g\cos\Theta\cos\Phi)$$
$$M = \dot{Q} I_y + PR(I_x - I_z) - R^2 I_{xz} + P^2 I_{xz}$$

Differentiating these equations yields equations of perturbed motion (where, for example, dU = u):

$$dX = m[\dot{u} + W_o q + Q_o w - V_o r - R_o v + (g\cos\Theta_o)\theta]$$
$$dZ = m[\dot{w} + V_o p + P_o v - U_o q - Q_o u + (g\cos\Theta_o \sin\Phi_o)\varphi + (g\sin\Theta_o \cos\Phi_o)\theta] \quad (5\text{-}2)$$
$$dM = \dot{q} I_y + (P_o r + R_o p)(I_x - I_z) - (2R_o r - 2P_o p) I_{xz}$$

where the quantities subscripted zero are the steady state (trimmed) values. To arrive at these equations, U was replaced by $U_o + u$, P by $P_o + p$, etc, and another assumption was made: the disturbances from steady flight are small enough so that the sine of an angle may be replaced by the angle itself and the cosine of an angle equals one. Any products of perturbations are neglected. The "small perturbation" concept has linearized the transcendental equations of the system.

Because of the symmetry of the airframe in the X-Z plane, and because there are no aerodynamic asymmetries such as propeller slipstream, it is assumed that longitudinal forces and moments due to lateral perturbations about the trim condition are negligible. Pitch rate at trim, Q_o, is defined to be zero. A further simplification, which now has no effect on the system, is that $P_o = R_o = V_o = \Phi_o$ = zero. This yields

$$dX = m[\dot{u} + \tilde{w}_o q + g\theta]$$
$$dZ = m[\dot{w} - U_o q]$$
$$dM = \dot{q} I_y$$

Since the aerodynamic forces and moments on the vehicle are dependent mainly upon the velocity of the

vehicle with respect to the air and not upon acceleration of the air mass, all derivatives with respect to acceleration are neglected. The exception is $\dot{w}$, an important one as it corresponds to the time lag between a vertical velocity perturbation at the leading edge and its effect at the trailing edge. It would not exist if downwash did not exist, but by this very fact, its magnitude cannot be disregarded. The flow is now assumed to be quasi-steady.

Altitude perturbations, being assumed small, allow the neglect of air density and temperature perturbations.

If the body axes are now rotated so that the x-axis points into the relative wind, W_o may be set equal to zero. This orientation forms a stability axis system. (Since small angle assumptions have been made, perturbations can still be measured in the body-fixed axis system.) Applying this rotation of axes to equations (5-2) and taking the Laplace transform of each yields

$$(s-X_u)u - (X_{\dot{w}}s + X_w)w + (-X_q s + g\cos\Theta_o)\theta = X_{\delta_e}\delta_e$$

$$-Z_u u + (s - Z_{\dot{w}}s - Z_w)w + [(-U_o - Z_q)s + g\sin\Theta_o]\theta = Z_{\delta_e}\delta_e$$

$$-M_u u - (M_{\dot{w}}s + M_w)w + s(s - M_q)\theta = M_{\delta_e}\delta_e$$

A vector diagram of the forces acting on the vehicle will aid in the discussion of the derivative terms in the above equations; see Figure 5-1. Note that there is no thrust force present.

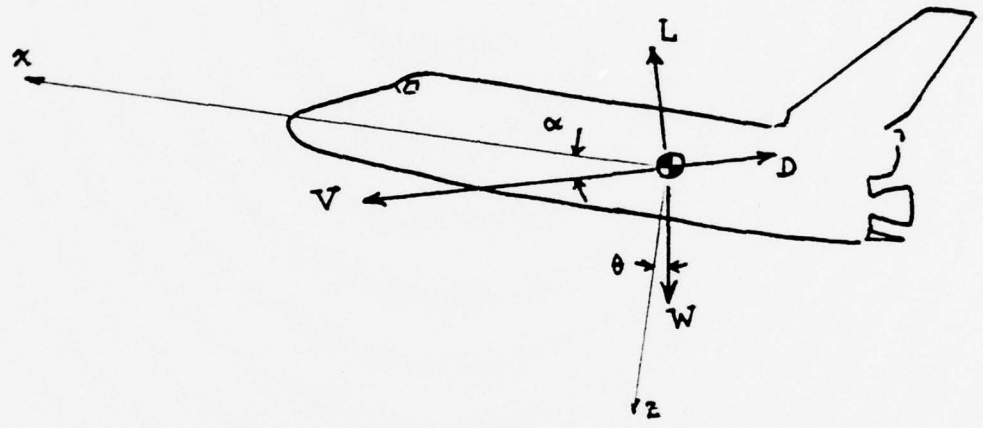


Figure 5-1

The sums of forces in the x- and z-directions is,

for small α $$X = L \sin\alpha - D\cos\alpha \approx L\alpha - D$$

$$Z \approx -(L + D\alpha)$$

The velocity, $\vec{V}$, is assumed to be equal to U_o. This assumption is justified by the following treatment:

$$\vec{V} = \sqrt{(U_o + u)^2 + v^2 + w^2}$$

$$= \sqrt{U_o^2 + 2U_o u + u^2 + v^2 + w^2}$$

Since u, v, and w are perturbations and are small when compared to U_o, their products may be neglected:

$$\vec{V} = \sqrt{U_o^2 + 2U_o u} = U_o\sqrt{1 + u/U_o} \approx U_o$$

Since $\Delta X = \frac{\partial X}{\partial u} u$, then

$$\frac{\partial X}{\partial u} u = \left(\frac{\partial L}{\partial u}\alpha_o + L\frac{\partial \alpha_o}{\partial u} - \frac{\partial D}{\partial u}\right)u = -\frac{\partial D}{\partial u} u$$

where α_o is assumed to be zero. Using the definitions

$X_u \triangleq \frac{1}{m}\cdot\frac{\partial X}{\partial u}$ and $D = \frac{1}{2}\rho U_o^2 S C_D$, then

$$X_u = -\frac{\rho S}{2m}\left(U_o^2\frac{\partial C_D}{\partial u} + 2U_o C_D\right)$$

$$= -\frac{\rho S U_o}{m}\left(\frac{U_o}{2}\frac{\partial C_D}{\partial u} + C_D\right)$$

Similarly $\Delta Z = \frac{\partial Z}{\partial u} u = -\left(\frac{\partial L}{\partial u} + \frac{\partial D}{\partial u}\alpha_o + \frac{\partial \alpha_o}{\partial u} D\right) = -\frac{\partial L}{\partial u}$

$$Z_u \triangleq \frac{1}{m}\cdot\frac{\partial Z}{\partial u} = -\frac{1}{m}\frac{\partial L}{\partial u}$$

Since lift = $L = \frac{1}{2}\rho U_o^2 S C_L$, then

$$Z_u = -\frac{\rho S U_o}{m}\left(\frac{U_o}{2}\frac{\partial C_L}{\partial u} + C_L\right)$$

Finally, where the moment = $M = \frac{1}{2}\rho U_o^2 S\bar{c} C_m$,

$$M_u = \frac{\rho U_o S\bar{c}}{I_y}\left(\frac{U_o}{2}\frac{\partial C_m}{\partial u} + C_m\right)$$

Using the same substitution and differentiation techniques as above, the rest of the force derivatives are found.

The q-derivatives:

$$X_q = -\rho\frac{U_0 S\bar{c}}{4m}\cdot\frac{\partial C_D}{\partial(q\bar{c}/2U_0)} \qquad [10]$$

$$Z_q = -\frac{\rho U_0 S\bar{c}}{4m}\cdot\frac{\partial C_L}{\partial(q\bar{c}/2U_0)}$$

$$M_q = \frac{\rho U S\bar{c}^2}{4I_y}\cdot\frac{\partial C_m}{\partial(q\bar{c}/2U_0)}$$

The w-derivatives:

$$X_w = \frac{\rho U_0 S}{2m}\left(C_L - \frac{\partial C_D}{\partial\alpha}\right)$$

$$Z_w = -\frac{\rho U_0 S}{2m}\left(\frac{\partial C_L}{\partial\alpha} + C_D\right)$$

$$M_w = \frac{\rho U_0 S\bar{c}}{2I_y}\cdot\frac{\partial C_m}{\partial\alpha}$$

The $\dot{w}$-derivatives:

$$X_{\dot{w}} = -\frac{\rho S\bar{c}}{4m}\cdot\frac{\partial C_D}{\partial(\dot{\alpha}\bar{c}/2U_0)}$$

$$Z_{\dot{w}} = -\frac{\rho S\bar{c}}{4m}\cdot\frac{\partial C_L}{\partial(\dot{\alpha}\bar{c}/2U_0)}$$

$$M_{\dot{w}} = \frac{\rho S\bar{c}^2}{4I_y}\cdot\frac{\partial C_m}{\partial(\dot{\alpha}\bar{c}/2U_0)}$$

---

[10] The non-dimensionalization procedure is discussed later in this chapter.

The δ_e-derivatives:

$$X_{\delta_e} = -\frac{\rho U_0^2 S}{2m} \cdot \frac{\partial C_D}{\partial \delta_e}$$

$$Z_{\delta_e} = -\frac{\rho U_0^2 S}{2m} \cdot \frac{\partial C_L}{\partial \delta_e}$$

$$M_{\delta_e} = \frac{\rho U_0^2 S \bar{c}}{2 I_y} \cdot \frac{\partial C_m}{\partial \delta_e}$$

Since the forces and moments are proportional to, respectively, mass and moment of inertia, the stability derivatives are non-dimensionalized by dividing the force/moment equations by these quantities; hence, the appearance of $1/m$ and $1/I_y$ in the results.

Some of the derivatives have particular significance or are named according to their effect on the motion of the system. Others may be neglected for various reasons. A discussion of these items is in order.

The quantity $\frac{\partial C_D}{\partial u}$ is called the speed damping derivative.

The quantity $\frac{\partial C_L}{\partial u}$ is generally small except at transonic speeds, the subject of this paper.

The quantity $\frac{\partial C_m}{\partial u}$ results from aeroelastic effects,

which are being neglected, and from compressibility effects, which are not. It, too, is largest at transonic speeds.

C_{m_q} is damping in pitch and is negative for a stable vehicle. Its primary effect is on short period damping.

The quantity $\frac{\partial C_m}{\partial \alpha}$ is the static stability derivative, the prime indicator of static longitudinal stability. Given an increase in angle-of-attack, the increased lift on the wing (normally, a tail contribution is dominant) will cause a negative pitching moment (nose down) about the center of mass of the vehicle. If this is the case, the center of mass must be forward of the aerodynamic center of the wing, and the vehicle is statically stable. Considering the tailless orbiter, it is expected that C_{m_α} will be small compared to a conventional aircraft, becoming somewhat more negative (more stable) as the vehicle becomes supersonic and the aerodynamic center moves further aft on the wing.

The quantity $\frac{\partial C_L}{\partial \alpha}$ is the lift curve slope and is positive and generally linear at angles-of-attack

below stall.

Since a change in drag on a horizontal tail is the main contributor to a change in $X_{\dot{w}}$, and since this drag increment is small anyway compared to the total drag, $X_{\dot{w}}$ is neglected in further discussion.

Because of the time lag between a change in angle-of-attack at the leading edge and the change in pressure distribution at the trailing edge, $\frac{\partial C_L}{\partial \dot{\alpha}}$ is produced. However, it is a negligible quantity.

The quantity $\frac{\partial C_m}{\partial \dot{\alpha}}$ will increase short period damping when it is negative, as is normally the case. It is non-dimensionalized as $\frac{\partial C_m}{\partial(\dot{\alpha}\bar{c}/2V_o)}$.

The quantities $\frac{\partial C_L}{\partial \delta_e}$ and $\frac{\partial C_D}{\partial \delta_e}$ are both significant in tailless vehicles, the first being always positive, the second smaller and sometimes negative. Their ratio may be likened to L/D. $C_{m_{\delta_e}}$ is elevator control effectiveness and, as the name implies, is quite important. It determines how much pitching moment will be generated for a given elevon deflection. It is sensitive to center of mass travel, aerodynamic center travel (as when a vehicle becomes supersonic), and $C_{L_{max}}$. It is

a negative quantity for elevons aft of the center of gravity.

Since $\alpha = \tan^{-1}(w/U_o) \doteq w/U_o$, the terms α and w may be interchanged (as may their derivatives) with due respect for the constant of proportionality.

The non-dimensional stability derivatives introduced on page 61 will be used wherever practical. In accordance with McRuer's definitions, they are called <u>basic</u> derivatives because they do not involve any inertial quantities. They are called non-dimensional because they involve force and moment coefficients rather than the forces and moments themselves. They are useful in that study of the vehicle under different flight conditions is most easily correlated. It may be seen that, for example, $\dot{\alpha}\bar{c}/2U_o$ is the non-dimensional form of $\dot{\alpha}$.

The other type of derivative, of which X_u is an example, is called a dimensional stability derivative parameter. It will be used in the study of airframe transfer functions.

VI. COMPUTER METHODS OF ANALYSIS

The concept of state variable analysis was made possible with the advent and refinement of the high speed digital computer. The arithmetical operations involved in dealing with just a 4x4 matrix are copious; they include inverting, factoring, solving the equations the matrix represents (which are often differential equations), and applying the results to state variable procedures for obtaining such things as the resolvent matrix, the state transition matrix, and the time response. In addition, most of these results must be computed for many instances of time, say every 0.1 second for 200 seconds, or for a wide range of frequencies in order that meaningful data may be plotted and analyzed.

Before the computer methods can be presented, a description of the underlying state variable theory and mathematics is necessary.

Conventional control theory, exemplified by the damped spring mass system in chapter III (pp 29 et seq.), is adequate for single-input-single-output

operations but is wholly inadequate for multiple-input-multiple-output systems. Each additional parameter introduced as an input or output increases the number of mathematical operations many-fold.

The set of state variables must first be specified. In accordance with the equations of motion (p 53), the set will be (u,w,q,θ). The state vector is seen to be $\{x\} = \begin{Bmatrix} u \\ w \\ q \\ \theta \end{Bmatrix}$, the control vector is $u = \delta_e$, and the plant matrix and control matrix are shown as $[A]$ and $\{B\}$ respectively on page 5-2. The state equation for the system is then

$$\{\dot{x}\} = [A]\{x\} + \{B\}u \quad .$$

The Laplace transform is used to solve this non-homogeneous equation of state:

$$s\underline{X}(s) - \underline{x}(0) = [A]\underline{X}(s) + \underline{B}\underline{U}(s)$$

$$s\underline{X}(s) - [A]\underline{X}(s) = \underline{x}(0) + \underline{B}\underline{U}(s)$$

$$[sI - A]\underline{X}(s) = \underline{x}(0) + \underline{B}\underline{U}(s)$$

$$\underline{X}(s) = [sI - A]^{-1}\underline{x}(0) + [sI - A]^{-1}\underline{B}\underline{U}(s)$$

Since $(sI-A)^{-1} = \frac{I}{s} + \frac{A}{s^2} + \frac{A^2}{s^3} + \cdots$

and $\mathcal{L}^{-1}\left[(sI-A)^{-1}\right] = I + At + \frac{A^2t^2}{2!} + \frac{A^3t^3}{3!} + \cdots = e^{At}$

then $\underset{\sim}{X}(s) = \mathcal{L}\left[e^{At}\right]\underset{\sim}{x}(0) + \mathcal{L}\left[e^{At}\right]\underset{\sim}{B}\underset{\sim}{U}(s)$

Taking the inverse Laplace,

$$\underset{\sim}{x}(t) = e^{At}\underset{\sim}{x}(0) + \int_0^t e^{A(t-\tau)}\underset{\sim}{B}\underset{\sim}{u}(\tau)\,d\tau \qquad (6\text{-}1)$$

where τ is a dummy variable.

The matrix e^{At} is written as $\Phi(t)$ and called the state transition matrix. Its Laplace counterpart, $\Phi(s)$, is called the resolvent matrix. The first term on the right hand side of equation (6-1) is the time response due to initial conditions; the second term is that due to the input, $\underset{\sim}{B}\underset{\sim}{u}$.

Just as in the single-input-single-output system, where $Y(s) = G(s)\cdot X(s)$, here, $X(s) = G(s)\cdot U(s)$, but $G(s)$ is now a matrix and is called the transfer matrix. The corresponding closed loop system is depicted in Figure 6-1.

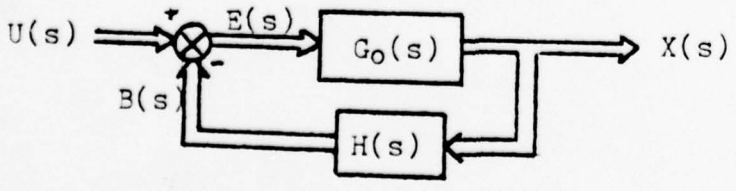


Figure 6-1

As was developed for the single input/output case,

$$B(s) = H(s) \cdot X(s)$$

or, dropping the "(s)" for convenience,

$$B = HG_oE$$

$$\text{Since} \quad X = G_o[U - B]$$

$$= G_o[U - HX]$$

$$\text{then} \quad X + G_oHX = G_oU$$

$$[I + G_oH]X = G_oU$$

$$\text{and} \quad X = [I + G_oH]^{-1} G_oU$$

Writing X as GU shows the closed loop transfer matrix to be $G(s) = [I + G_o(s) \cdot H(s)]^{-1} \cdot G_o(s)$.[11]

In order to solve the equations of motion, a computer program will use the above relationships and some form of numerical integration. The programs written by Melsa and Jones[12] were used in this study, the main two of which were BASMAT and RTRESP.

---

[11] Since, in general, $[A][B] \neq [B][A]$, care must be exercised in developing the equations by insuring that both sides are pre- or post-multiplied by a matrix in the same order.

[12] J.L. Melsa and S.K. Jones, Computer Programs for Computational Assistance in the Study of Linear Control Theory, 2nd edition, McGraw-Hill, 1973

Given a basic matrix, $[A]$, in this case the plant matrix, BASMAT produces

a. the determinant of $[A]$, $\det[A]$

b. the inverse of $[A]$, $[A]^{-1}$

c. the characteristic polynomial, $\det(sI-A)$

d. the eigenvalues of $[A]$, λ_i

e. the state transition matrix, $\Phi(t) = e^{At}$

f. the resolvent matrix, $\Phi(s) = (sI-A)^{-1}$

Once the state transition matrix is known, the time response may be found by equation (6-1) whether the input is in the form of an initial condition(s), a forcing function, or both. The other Melsa-Jones program, RTRESP (Rational Time RESPonse), was used for this purpose.

After the mathematical formulation of the time response is obtained, it is left to graph the results to see the time history of the system. In order to facilitate this operation, a program named GRAPH was written, in BASIC language, for execution on the HP9830 computer. See Figure 6-2. An explanation of the variables and operations in GRAPH follows:

```
REM     PROGRAM GRAPH

10 DIM C[9],P[9],Q[9],R[9]
20 FOR I=1 TO 9
30 C[I]=P[I]=Q[I]=R[I]=0
40 NEXT I
50 DISP "HOW MANY REAL ROOTS";
60 INPUT R1
70 DISP "HOW MANY COMPLEX ROOTS";
80 INPUT R2
90 IF R1=0 THEN 140
100 FOR I=1 TO R1
110 DISP "INPUT REAL ROOT #"I
120 INPUT P[I]
130 NEXT I
140 FOR I=R1+1 TO R1+R2 STEP 2
150 DISP "REAL/IMAG PARTS OF CPLX ROOT #"I;
160 INPUT Q[I],R[I]
170 Q[I+1]=Q[I]
180 R[I+1]=-R[I]
190 NEXT I
200 WRITE (15,210)
210 FORMAT 45"*"
220 PRINT "ROOTS OF CHAR EQN ARE"
230 PRINT "      REAL PART      IMAG PART"
240 FOR I=1 TO R1
250 WRITE (15,310)P[I],0
260 NEXT I
270 PRINT
280 FOR I=R1+1 TO R1+R2
290 WRITE (15,310)Q[I],R[I]
300 NEXT I
310 FORMAT 4X,F10.5,4X,F10.5
320 IF R1=0 THEN 370
330 FOR I=1 TO R1
340 DISP "COEFF OF EXP("P[I]"T)";
350 INPUT C[I]
360 NEXT I
370 FOR I=R1+1 TO R1+R2 STEP 2
380 R[I]=ABS(R[I])
390 DISP "COEFF OF EXP("Q[I]"T)*COS("R[I]"T)";
400 INPUT C[I]
410 DISP "COEFF OF EXP("Q[I]"T)*SIN("R[I]"T)";
420 INPUT C[I+1]
430 NEXT I
440 DISP "MAXIMUM MAGNITUDE OF RESPONSE";
450 INPUT G9
```

Figure 6-2

```
460 SCALE -5,12,-1.1*G9,1.1*G9
470 XAXIS 0,5,0,10
480 YAXIS -0.8,G9/4,-G9,G9
490 LABEL (*,2.5,1.7,0,10/7)
500 FOR X=0 TO 10 STEP 5
510 PLOT X,0,1
520 CPLOT -2.5,-2
530 LABEL (770)X
540 NEXT X
550 FOR Y=-G9 TO G9 STEP 2*G9
560 PLOT 0,Y,1
570 CPLOT -7,-0.3
580 LABEL (780)Y
590 NEXT Y
600 FOR T=0 TO 10 STEP 0.25
610 Y=0
    GOSUB 1080
    PLOT T,Y
    NEXT T
650 PEN
660 DISP "RESET PLOTTER FOR PHUGOID"
670 STOP
    SCALE -15,215,-1.1*G9,1.1*G9
690 XAXIS 0,25,0,200
700 YAXIS -8,G9/4,-G9,+G9
710 LABEL (*,2.5,2,0,7/10)
720 FOR X=0 TO 200 STEP 50
730 PLOT X,0,1
740 CPLOT -2.5,-2
750 LABEL (770)X
760 NEXT X
770 FORMAT F4.0
780 FORMAT F8.3
790 FOR T=0 TO 10 STEP 0.25
800 Y=0
810 GOSUB 1080
820 PLOT T,Y
830 NEXT T
840 FOR T=10 TO 50 STEP 1
850 Y=0
860 GOSUB 1080
870 PLOT T,Y
880 NEXT T
890 FOR T=50 TO 200 STEP 2
900 Y=0
```

Figure 6-2 (continued)

```
910 GOSUB 1080
920 PLOT T,Y
930 NEXT T
940 PEN
950 DISP "INPUT LETTER SIZE FOR LABELLING";
960 INPUT Z
970 LABEL (*,Z,1.7,0,7/10)
980 DISP "YOU ARE IN THE LETTER MODE"
990 LETTER
1000 DISP "ANY MORE LABELLING";
1010 INPUT Z
1020 IF Z=1 THEN 950
1030 DISP "ANY MORE GRAPHS WITH THESE ROOTS";
1040 INPUT Z
1050 IF Z=1 THEN 320
1060 DISP "     - - - - THE END - - - -"
1070 STOP
1080 REM SUBROUTINE TO COMPUTE MAGNITUDE OF RESPONSE
1090 IF R1=0 THEN 1140
1100 FOR I=1 TO R1
1110 IF P[I]*T<-225 THEN 1130
1120 Y=Y+C[I]*EXP(P[I]*T)
1130 NEXT I
1140 FOR I=R1+1 TO R1+R2 STEP 2
1150 IF Q[I]*T<-225 THEN 1180
1160 Y=Y+C[I]*EXP(Q[I]*T)*COS(R[I]*T)
1170 Y=Y+C[I+1]*EXP(Q[I]*T)*SIN(R[I]*T)
1180 NEXT I
1190 RETURN
1200 END
```

Figure 6-2 (continued)

C_i: coefficients of the exponential and sinusoidal terms, the sum of which describe the time response

G9: maximum absolute magnitude of the response; used to scale and label the time history plot

I: counting element

P_i: purely real roots

Q_i: real part of complex roots

R_i: imaginary part of complex roots

R1: number of purely real roots

R2: number of complex roots

T: time; see "X"

X: horizontal (time) axis

Y: vertical (magnitude) axis

Z: yes(1)/no(0) value; used to answer various questions which the program asks of the operator

lines 10-40: dimensions C, P, Q, and R and initializes their value at zero

ll 50-310: inputs roots, categorizes them as real or complex, and prints results

ll 320-430: inputs coefficients of exponential and sinusoidal terms

ll 440-590: scales, draws, and labels the axes of the graph

ll 600-650: plots short period magnitude-vs-time graph, using subroutine 1080

ll 660-940: plots phugoid graph, using subroutine 1080

ll 950-1020: allows for labeling

ll 1030-1070: allows drawing of other graphs with the same roots

ll 1080-1190: subroutine which computes magnitude of response at a given time

line 1200: END statement

. The values of the coefficients and roots (C_i, P_i, Q_i, R_i) are obtained from the program RTRESP.

The text Aircraft Dynamics and Automatic Control, referenced previously, contains an input/output analysis of an early operational Air Force interceptor, the F-89 Scorpion. In order to validate the GRAPH program, this example was run through the BASMAT and RTRESP programs and the results plotted using GRAPH.

From the given stability derivatives, the plant matrix and control vector were constructed in accordance with the state equations on page 50 ; for

altitude = 20000ft
weight = 30500lb
Mach = 0.638
TAS = 660fps

$X_u = -0.0097$	$Z_u = -0.0955$	$M_u = 0.0$
$X_w = 0.0016$	$Z_w = -1.430$	$M_w = -0.0235$
$X_{\delta_e} = 0.0$	$Z_{\delta_e} = -69.8$	$M_{\dot{w}} = -0.0013$
		$M_q = -1.920$
		$M_{\delta_e} = -26.009$

the plant matrix [A] was

$$\begin{bmatrix} -0.0097 & 0.0016 & 0.0 & -32.2 \\ -0.0955 & -1.430 & 660.0 & 0.0 \\ 0.000124 & -0.0216 & -2.778 & 0.0 \\ 0.0 & 0.0 & 1.0 & 0.0 \end{bmatrix}$$

and the control vector was

$$\begin{Bmatrix} 0.0 \\ -69.8 \\ -26.009 \\ 0.0 \end{Bmatrix}$$

The input to the system consisted of an elevator deflection of 0.02 radian commencing at t=0 with a duration of one second; initial conditions were equal to zero. The text results are shown in Figure 6-3.

In order to utilize the RTRESP program, a proper Laplace transform of the input had to be found. The first choice was a multiple of the unit impulse, in this case $0.02\,\delta(t)$. The Laplace of this input is $0.02(1/1)$. However, the Melsa-Jones program requires that the denominator of the Laplace of the input be one or more orders greater that that of the numerator. Since this prerequisite could not be satisfied, it was decided to use a step function input and take the derivative with respect to time of the output, since the

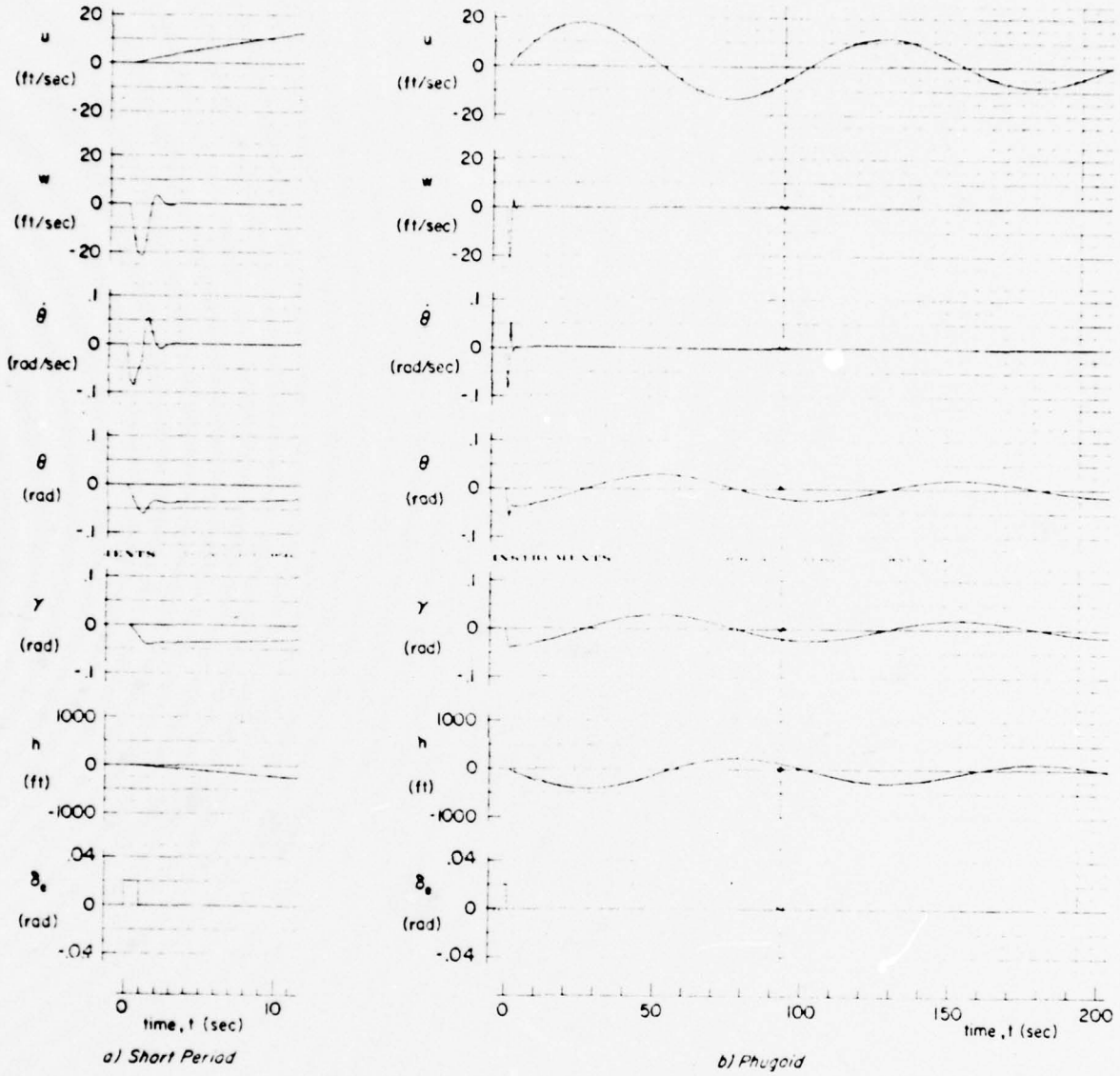


Figure 6-3

impulse is the derivative of the step function. The results of the system's matrix analysis are given in

Figure 6-4. The results of the step function input are shown in Figure 6-5, and Table 6-1 shows that the periods and damping ratios of the short period and the phugoid agree quite closely with the text results.

	SHORT PERIOD		PHUGOID	
	BASMAT	text	BASMAT	text
ω_n	4.2693	4.27	0.0629	0.0630
ζ	0.4928	0.493	0.0717	0.0714

Table 6-1

The differentiation of the results of the step function input yielded:

$$\text{let } a_1 = -2.104339 \qquad b_1 = 3.714746$$

$$a_2 = -0.004510971 \qquad b_2 = 0.06274506$$

$$u = -0.599148\exp(a_1 t)\cos(b_1 t) - 0.678176\exp(a_1 t)\sin(b_1 t) + 0.599209\exp(a_2 t)\cos(b_2 t) + 20.063997\exp(a_2 t)\sin(b_2 t)$$

```
BASIC MATRIX PROGRAM
PROBLEM IDENTIFICATION-     POWER EXAMPLE

***********************************************

THE A MATRIX

-9.6999966E-03      1.5999998E-03      0.0                -3.2199997E 01
-9.5499992E-02     -1.4299994E 00      6.0000000E 02       0.0
 1.2410000E-04     -2.1599997E-02     -2.7779999E 00       0.0
 0.0                0.0                1.0000000E 00       0.0

THE DETERMINANT OF THE MATRIX

 7.2136363E-02

THE INVERSE OF THE MATRIX

 1.5258789E-05     -9.6117233E 00      6.3031719E 02       9.1779785E 03
 0.0               -5.5305664E-02     -1.9539999E 01      -9.1667969E 01
-3.7252903E-09      2.3283064E-10     -5.0981665E-09       0.0000000E-01
-3.1055905E-03      2.0017338E-03     -1.9440031E-01      -2.8559999E 00

***********************************************

THE MATRIX COEFFICIENTS OF THE NUMERATOR OF THE RESOLVENT MATRIX

THE MATRIX COEFFICIENT OF S**3

 1.0000000E 00      0.0                0.0                0.0
 0.0                1.0000000E 00      0.0                0.0
 0.0                0.0                1.0000000E 00      0.0
 0.0                0.0                0.0                1.0000000E 00
```

Figure 6-4

```
 THE MATRIX COEFFICIENT OF S**2

  4.20709836E 00        1.59999998E-03        0.0                  -3.21999997E 01
 -9.54999992E-02        2.78760397E 00        6.60000000E 02        0.0
  1.24100000E-04       -2.15999997E-02        1.43960332E 00        0.0
  0.0                   0.0                   1.00000000E 00        4.21760016E 00

 THE MATRIX COEFFICIENT OF S**1

  1.82285316E 01        4.44470220E-03       -3.11439997E 01       -1.35407546E 02
 -1.83392388E-01        2.60470216E-02        6.40185555E 00        3.07500000E 00
  2.24026220E-03       -2.09316616E-04        1.40222237E-02       -3.00601235E-03
  1.24100000E-04       -2.15999997E-02        1.43960332E 00        1.82605016E 01

 THE MATRIX COEFFICIENT OF S**0

  5.06046455E-02        6.25510200E-01       -4.50465050E 01       -5.26052505E 02
  9.53674332E-07        3.00245916E-03        3.07466730E 00        5.00535535E 00
  0.0                  -2.21100011E-02        5.72204500E-05       -7.21363437E-02
  2.24026220E-03       -2.09316616E-04        1.40222237E-02        1.77110002E-01

**********************************************

 THE CHARACTERISTIC POLYNOMIAL - IN ASCENDING POWERS OF S

  7.21363437E-02        1.21100000E-01        1.82605016E 01        4.21760016E 00        1.00000000E

**********************************************

 THE EIGENVALUES OF THE A MATRIX
    REAL PART          IMAGINARY PART

 -2.1043377E 00        -3.7147436E 00
 -2.1043377E 00         3.7147436E 00
 -4.5110235E-03        -6.2747061E-02
 -4.5110235E-03         6.2747061E-02
```

Figure 6-4 (continued)

```
**********************************************

      THE ELEMENTS OF THE STATE TRANSITION MATRIX

      THE MATRIX COEFFICIENT OF EXP(-2.104330E 00)T*COS( 3.711744E 00)T

      -5.2974035E-05        8.5681075E-03        1.1999175E 00       -1.5999573E-03
       1.0039744E-02        1.0000267E 00       -1.2770457E-02       -9.4943513E-03
      -1.2310687E-04        1.2794000E-05        1.0000058E 00       -6.9429444E-04
       2.1560263E-05        1.1842430E-03       -7.9529258E-03       -5.7177473E-05

      THE MATRIX COEFFICIENT OF EXP(-2.104330E 00)T*SIN( 3.711744E 00)T

      -2.1243360E-04       -5.0083250E-03        1.3171759E 00       -4.4204205E-04
      -2.0048536E-02        1.8164849E-01        1.7765311E 02       -1.4041209E-01
      -3.6054349E-05       -5.8148727E-03       -1.8121606E-01        6.7383423E-04
      -2.0920542E-05        6.7169225E-04        2.2473659E-01       -2.1027751E-04

      THE MATRIX COEFFICIENT OF EXP(-4.511020E-03)T*COS( 6.274706E-02)T

       1.0000525E 00       -8.5682571E-03       -1.1999776E 00        1.5999575E-03
      -1.0039255E-02       -7.9118472E-05        1.0021961E-02        9.4943905E-03
       1.2310731E-04       -1.2794014E-05       -2.8773727E-05        6.9429447E-04
      -2.1559963E-05       -1.1842395E-03        7.9519722E-02        1.0000557E 00

      THE MATRIX COEFFICIENT OF EXP(-4.511020E-03)T*SIN( 6.274706E-02)T

      -7.1802017E-02        6.0273556E-01       -4.0203644E 01       -5.1319004E 02
       9.0856897E-04       -6.0513621E-03        3.0179455E-01        5.1598787E 00
      -7.4048729E-05        7.5133168E-05       -4.0005411E-03       -5.2194255E-02
       1.0604028E-03       -1.1502220E-04        4.2762756E-03        8.2060305E-02
D; T=3.06/4.17 21.34.20
```

Figure 6-4 (continued)

```
RATIONAL TIME RESPONSE
PROBLEM IDENTIFICATION - MCRUER EXAMPLE

**********************************************

THE A MATRIX

      -0.0097000          0.0016000          0.0          -32.2000000
      -0.0955000         -1.4300000        600.0000000      0.0
       0.0001240         -0.0210000         -2.7700000      0.0
       0.0                0.0                1.0000000      0.0

THE B MATRIX

       0.0               -69.8000000        -20.0090000      0.0

THE C MATRIX

       1.0000000          0.0                0.0            0.0

FEEDBACK COEFF.

       0.0                0.0                0.0            0.0

GAIN =  1.00000000D 00

**********************************************

INITIAL CONDITIONS - X(0)

       0.0                0.0                0.0            0.0

RGAIN =  2.00000000-02
```

Figure 6-5

```
NUMERATOR POLYNOMIAL OF R(S) - ASCENDING POWERS OF S
        1.0000000

DENOMINATOR POLYNOMIAL OF R(S) - ASCENDING POWERS OF S
        0.0                 1.0000000

DENOMINATOR ROOTS ARE
  REAL PART         IMAG. PART
        0.0                 0.0

**********************************************

THE TIME RESPONSE OF THE STATE X(T)

THE VECTOR COEFFICIENT OF EXP(-2.1043390 00)T*COS(3.7147460 00)T
        0.2073815          19.0449924          0.0391937          0.0194909

THE VECTOR COEFFICIENT OF EXP(-2.1043390 00)T*SIN(3.7147460 00)T
       -0.0438111          10.4154682         -0.1178410          0.0215921

THE VECTOR COEFFICIENT OF EXP(-4.5109710-03)T*COS(6.2745080-02)T
     -318.8088989           3.1114909         -0.0391704          0.0774104

THE VECTOR COEFFICIENT OF EXP(-4.5109710-03)T*SIN(6.2745080-02)T
      -13.3704338           0.1375328         -0.0023220         -0.0190052

THE VECTOR COEFFICIENT OF EXP( 0.0         )T
      318.8020508         -22.2811090          0.0001477         -0.0971559

**********************************************
```

Figure 6-5 (continued)

$$
\begin{aligned}
w &= -1.386301\exp(a_1 t)\cos(b_1 t) \\
&\quad -92.664985\exp(a_1 t)\sin(b_1 t) \\
&\quad -0.005406\exp(a_2 t)\cos(b_2 t) \\
&\quad -0.195852\exp(a_2 t)\sin(b_2 t)
\end{aligned}
$$

$$
\begin{aligned}
q &= -0.520226\exp(a_1 t)\cos(b_1 t) \\
&\quad +0.102383\exp(a_1 t)\sin(b_1 t) \\
&\quad +0.000031\exp(a_2 t)\cos(b_2 t) \\
&\quad +0.002468\exp(a_2 t)\sin(b_2 t)
\end{aligned}
$$

$$
\begin{aligned}
\theta &= +0.039993\exp(a_1 t)\cos(b_1 t) \\
&\quad -0.117850\exp(a_1 t)\sin(b_1 t) \\
&\quad -0.039189\exp(a_2 t)\cos(b_2 t) \\
&\quad -0.002065\exp(a_2 t)\sin(b_2 t)
\end{aligned}
$$

Figure 6-6 shows the time history of this system. The magnitudes of vertical velocity, pitch angle, and to a lesser degree, pitch rate were decidedly in error. Furthermore, the initial condition of zero pitch rate was not reflected in the results.

The discrepancies are due to the improper description of the input. Clearly, the effect of a maximum elevator deflection acting over a short period of time ($\Delta t \ll 1$) is different from a much smaller deflection for one second, hence the magnitude errors. The initial condition error is due to the indefinite integration of the input. When the input is integrated (multiplied by s), the denominator loses a root at s=0 and its associated eigenvalue. The time response

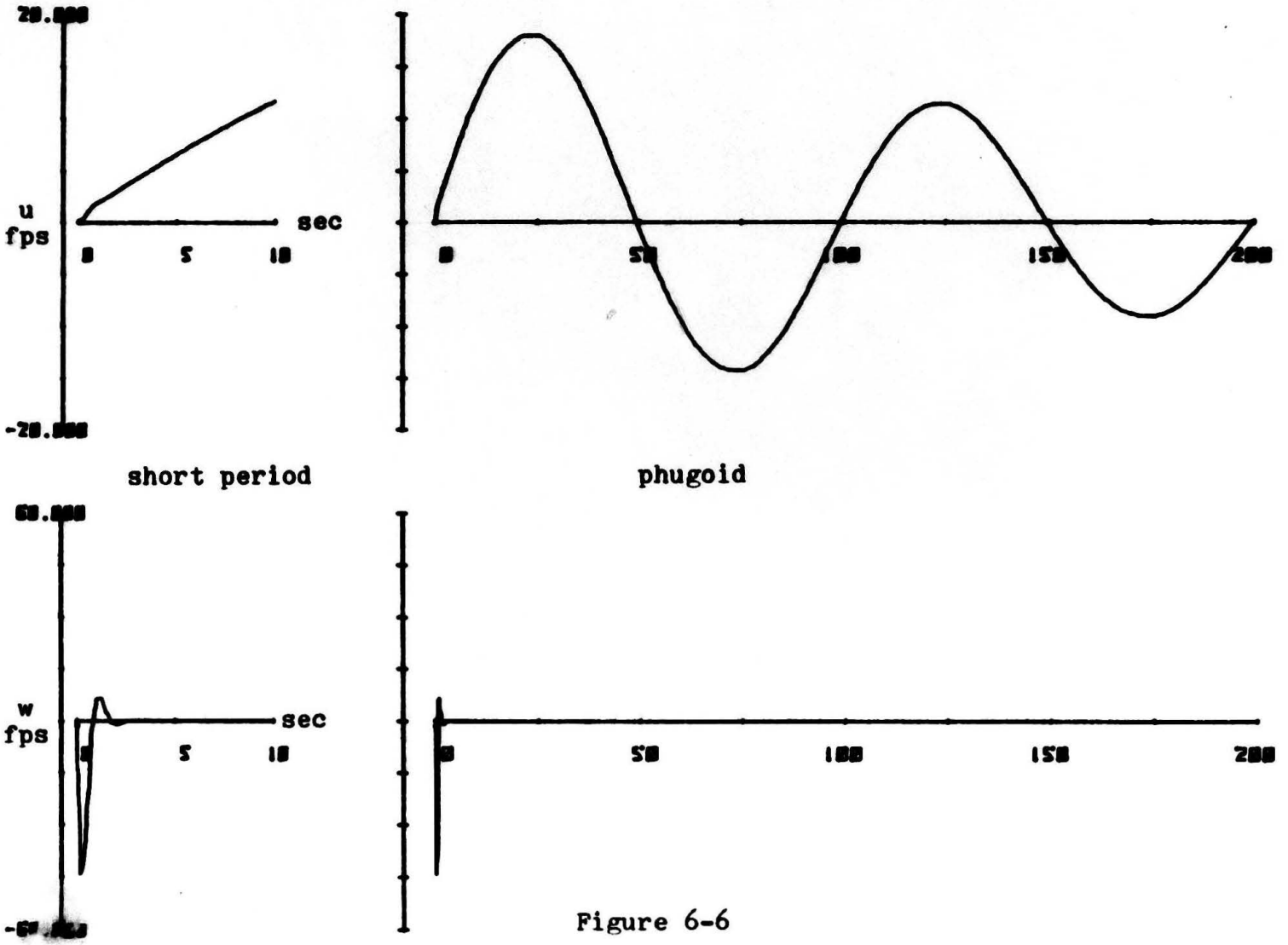
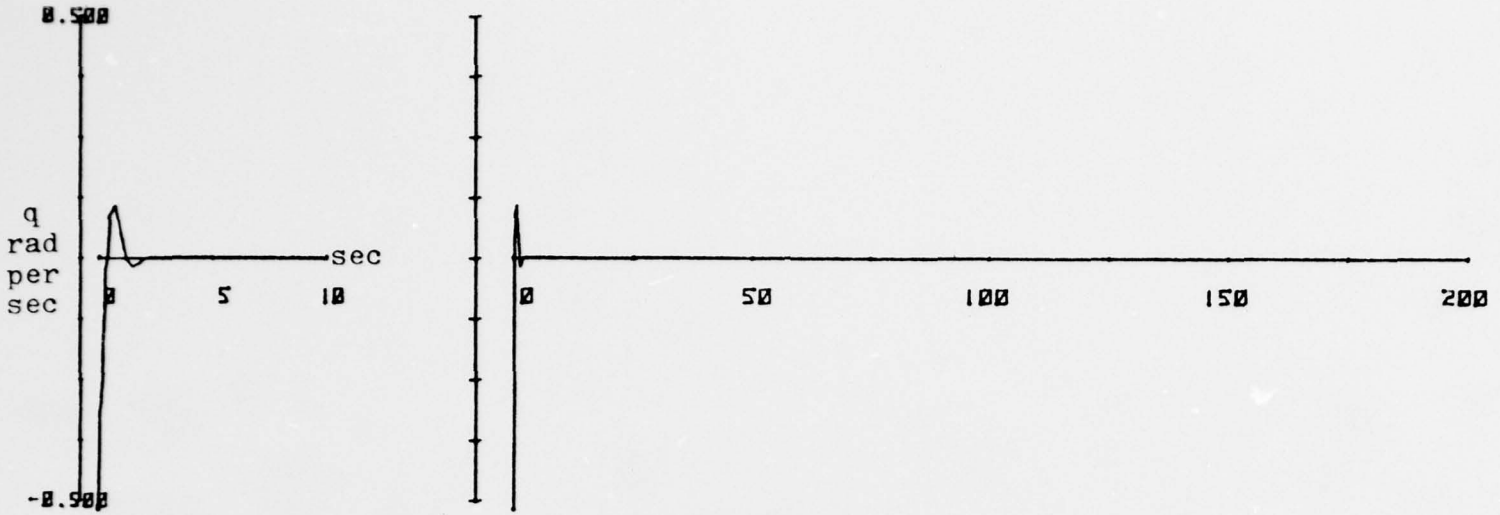


Figure 6-6



short period phugoid

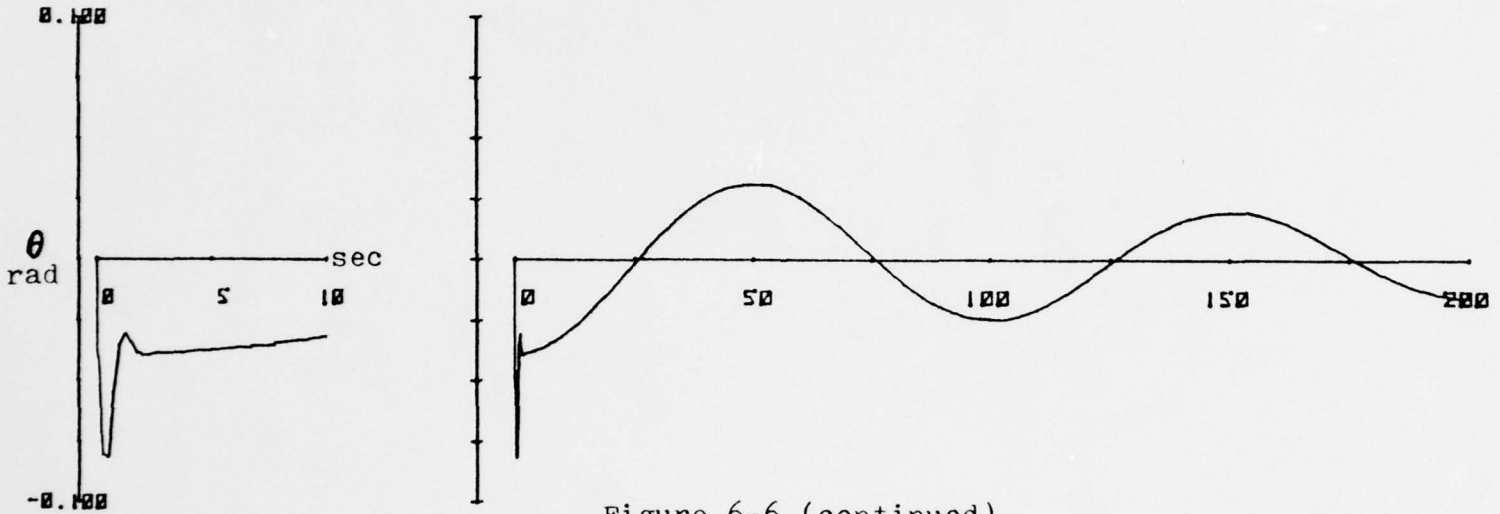
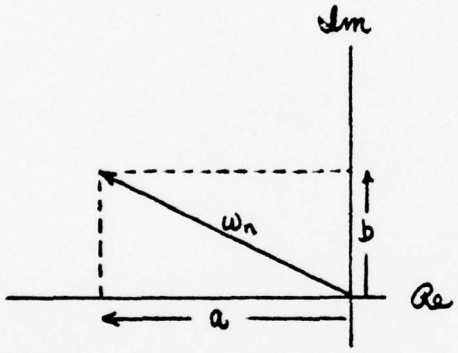


Figure 6-6 (continued)

therefore loses an exponential term, and the initial conditions are not satisfied.

The undamped natural frequencies and damping ratios are calculated from the roots (eigenvalues) of the characteristic equation by considering the roots in vector form.



$$\omega_n = \sqrt{a^2 + b^2}$$

$$\zeta = \frac{a}{\sqrt{a^2 + b^2}}$$

where the roots are expressed as $\lambda = a + jb$ and were calculated by BASMAT.

The second attempt to duplicate the given input function was to evaluate the results of the step function (x0.02) at t=1 and use these values as initial conditions for a zero-input system commencing at t=1. The values of the state variables at t=1, calculated from the RTRESP program (see Figure 6-5) were

$$\begin{Bmatrix} u \\ w \\ q \\ \theta \end{Bmatrix} = \begin{Bmatrix} 0.9938 \\ -21.8208 \\ -0.0035 \\ -0.0623 \end{Bmatrix}$$

When these values were run through RTRESP as initial conditions, with the input function now zero, the results were inconsistent with common sense. For example, the response of the system with an initial condition of 0.9938fps of forward velocity perturbation and no input yielded a change in U of over 300fps within ten seconds (the initial velocity of the aircraft was but 660fps).

Using the state transition matrix from BASMAT, a program called ICRESP was written to solve the response due to an initial condition with the equation

$$\underline{x}(t) = \Phi(t) \cdot \underline{x}(0) \ .$$

The results, shown in Figure 6-7, are much more consistent with the earlier figures. In the output portion of the print-out, A1 refers to the real part of the first root, B1 to the imaginary part of the first root, and likewise for A2 and B2. The matrix E is the matrix of coefficients of the state transition matrix,

```
PEM     PROGRAM  ICRESP


10 DIM E[16,4],D[4,1],X[4,4]
20 MAT READ E
30 DATA -5.2974E-05,0.0085681975,1.1288176,-0.0015909672
40 DATA 0.0100397,1,-0.018779,-0.0942425
50 DATA -0.000123106,1.87941E-06,1,-0.00069424
60 DATA 2.15602E-05,0.00118484,-0.078526,-5.71775E-05
70 DATA -0.000212434,-0.00500833,1.31718,-0.000442043
80 DATA -0.020049,0.18164849,177.653,-0.14041269
90 DATA -3.6054349E-05,-0.0058148727,-0.181217,0.000673634
100 DATA -2.09265E-05,0.000671698,0.224737,-0.000219278
110 DATA 1,-0.00856826,-1.128878,0.00154686
120 DATA -0.010039,-7.91185E-05,0.01062186,0.09424925
130 DATA 0.000123107,-1.8706E-06,-8.88737E-05,0.00069426
140 DATA -2.156E-05,-0.0011849,0.078517,1
150 DATA -0.071893,0.60873556,-40.203644,-513.19824
160 DATA 0.0009086,-0.00605144,0.39170456,5.1588783
170 DATA -7.49E-06,7.5133E-05,-0.004889544,-0.063124955
180 DATA 0.0019604028,-0.000115022,0.00427627,0.0829603
190 MAT READ D
200 DATA 0.9937896,-21.820808,-0.035139,-0.0623077
210 FOR I=1 TO 4
220 FOR J=1 TO 4
230 X[I,J]=0
240 NEXT J
250 NEXT I
260 FOR I=1 TO 4
270 FOR J=1 TO 4
280 FOR K=1 TO 4
290 X[I,J]=E[I+4*J-4,K]*D[K,1]+X[I,J]
300 NEXT K
310 NEXT J
320 NEXT I
330 PRINT " EXP(A1*T) *     EXP(A1*T) *     EXP(A2*T) *      EXP(A2*T) *"
340 PRINT "  COS(B1*T)       SIN(B1*T)       COS(B2*T)        SIN(B2*T)"
350 PRINT
360 MAT PRINT X
370 END

 EXP(A1*T) *     EXP(A1*T) *     EXP(A2*T) *      EXP(A2*T) *
  COS(B1*T)       SIN(B1*T)       COS(B2*T)        SIN(B2*T)

-0.226584030     0.062817847     1.220327219     20.03436953

-21.80429874    -10.21744129    -0.014495920    -0.202251680

-0.035259095     0.133175189     1.23026E-04     2.45808E-03

-0.023069852    -0.022561160    -0.039232660    -8.61228E-04
```

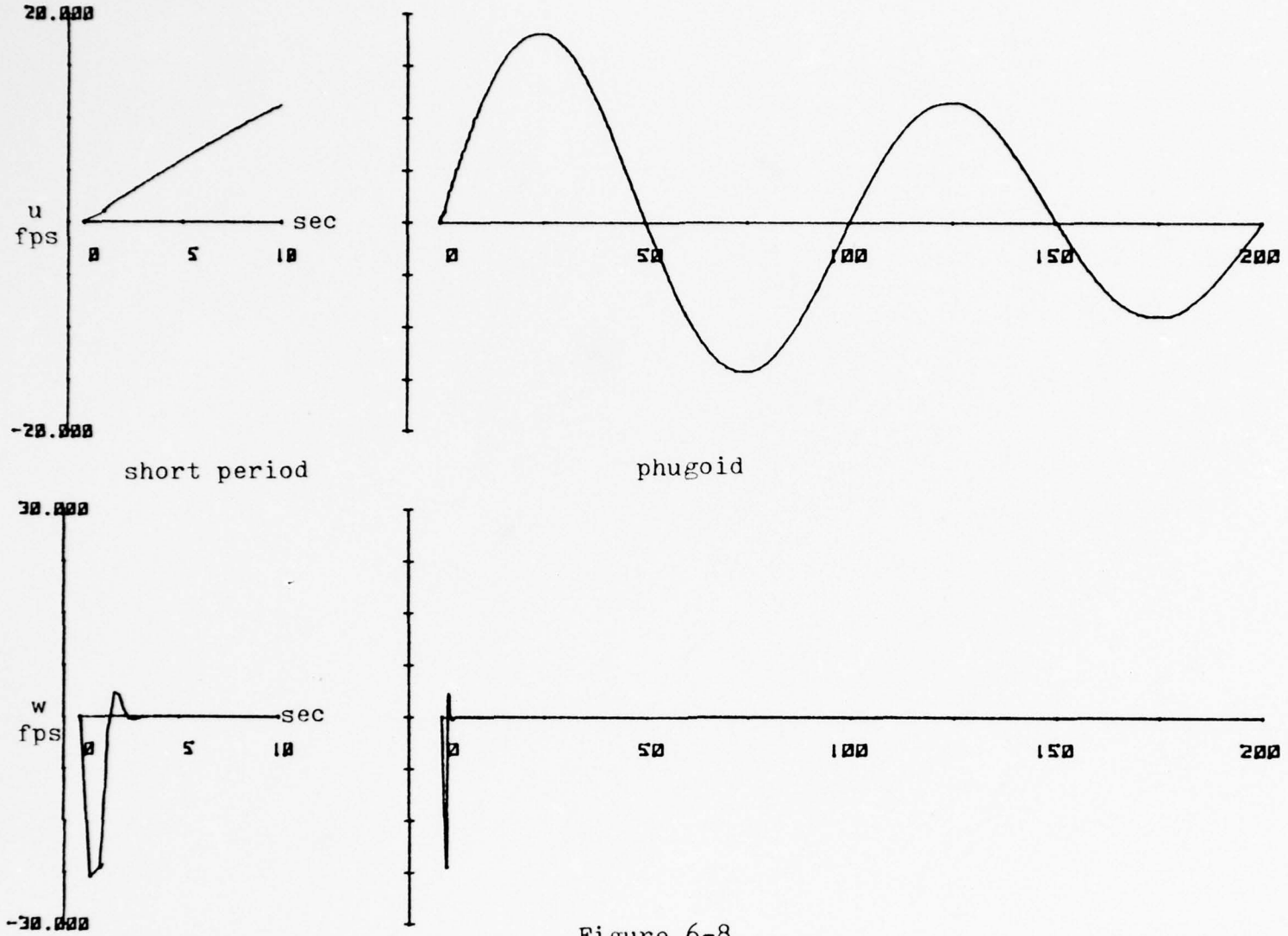
Figure 6-7

D is the matrix of initial conditions, and X is the matrix of coefficients of the output. The time history plots of the results are shown in Figure 6-8. Since the results were so consistent with the earlier program, it appeared as though the reason these figures were not coinciding with those of the text was that an error existed in one of the two Melsa-Jones programs.

The results of BASMAT (the determinant, the inverse, the characteristic polynomial, the eigenvalues, and the resolvent matrix) were computed by hand and found to be correct. The program RTRESP calculated the same eigenvalues as did BASMAT; its only problem appeared to be in the coefficient of the sine term of the phugoid root in the forward velocity expression when initial conditions are present. The equations of state from RTRESP were verified on the HP9830 by writing a program called STRESP which calculated the response of a system to a step input by using the formula

$$\underline{x}(t) = \Phi(t)\cdot\underline{x}(0) + [A]^{-1}[\Phi(t) - I]\{B\}\cdot k$$

where $[A]$ is the plant matrix, $\{B\}$ the control vector, k the gain (magnitude) of the step input, and $\Phi(t)$ the



short period

phugoid

Figure 6-8

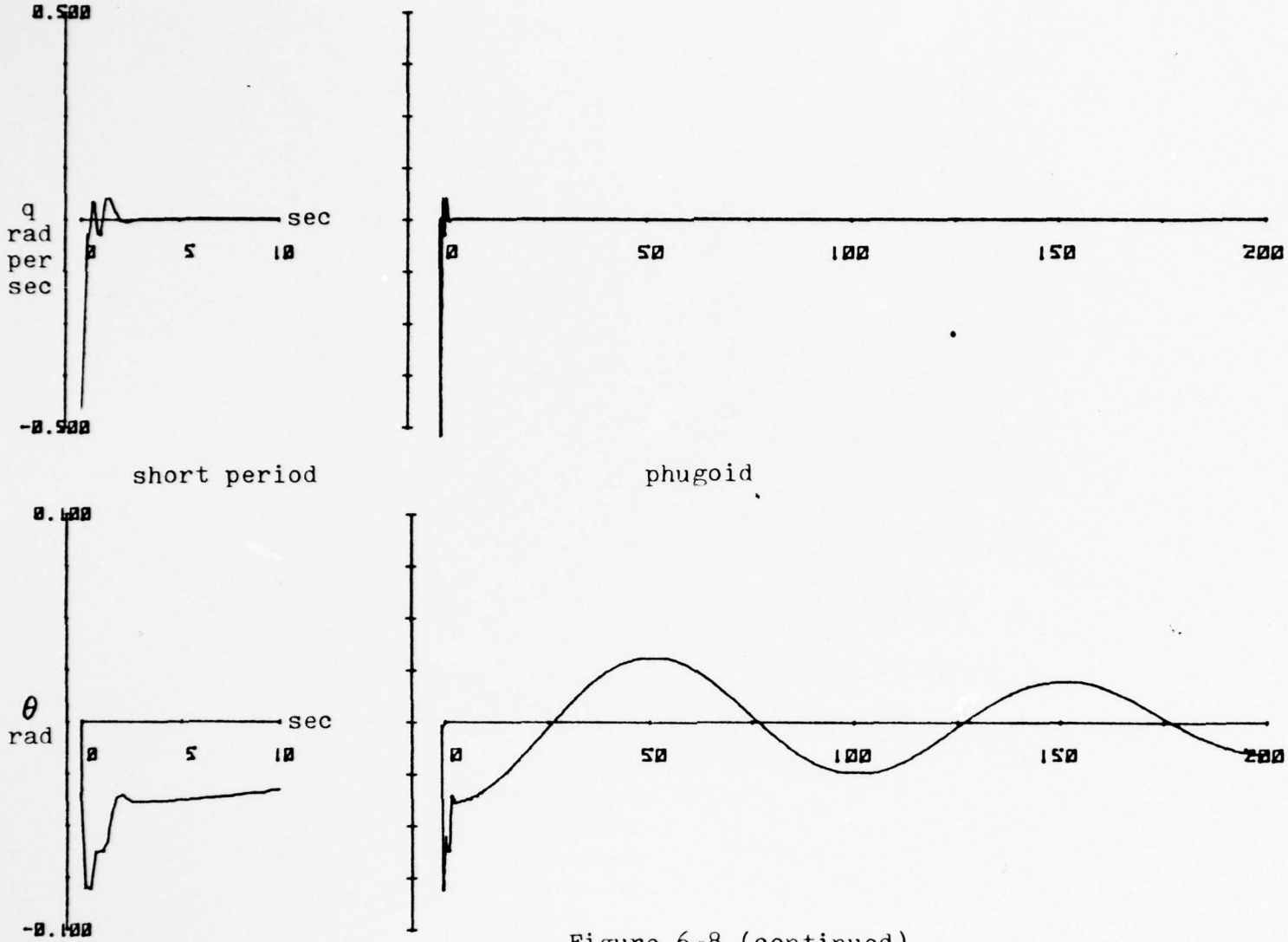


Figure 6-8 (continued)

state transition matrix. In this case, $\underset{\sim}{x}(0) = 0$. The program and results are shown in Figure 6-9.

Several other approximations to the desired input were tried, the first of which was

$$\delta(t) \approx \frac{1}{\tau} \exp\left[-\pi t^2/\tau^2\right] \quad \text{for} \quad \tau \ll 1$$

Transforming into the Laplace domain,

$$\mathcal{L}[f(t)] = \int_0^\infty e^{-st} f(t)\, dt = \int_0^\infty e^{-st} \frac{1}{\tau} \exp\left[-\pi t^2/\tau^2\right] dt$$

The solution was obtained by the use of Bonnet's Theorem (the Second Mean Value theorem) which states that

$$\int_a^b f(t)\, g(t)\, dt = f(b)\, G(b) - \int_a^b G(t)\, f'(t)\, dt$$

$$\text{where} \quad G(t) = \int_0^t g(t)\, dt$$

For $f(t) = e^{-\alpha t^2}$ where $\alpha = \frac{\pi}{\tau^2}$ and $g(t) = e^{-st}$

$$G(t) = \int_0^t e^{-st}\, dt = \frac{1}{s} - \frac{1}{s} e^{-st}$$

and $$f'(t) = -2\alpha t\, e^{-\alpha t^2}$$

```
KLM     PROGRAM  STRESP

10 DIM A[4,4],P[4,4],Q[4,4],R[4,4],S[4,4]
20 DIM B[4,4],C[4,4],D[4,4],E[4,4],F[4,1]
30 DIM W[4,1],X[4,1],Y[4,1],Z[4,1]
40 MAT READ B
50 DATA -5.2974E-05,0.0085681975,1.1288176,-0.0015909672
60 DATA 0.0100397,1,-0.018779,-0.0942425
70 DATA -0.000123106,1.87941E-06,1,-0.00069424
80 DATA 2.15602E-05,0.00118484,-0.078526,-5.71775E-05
90 MAT READ C
100 DATA -0.000212434,-0.00500833,1.31718,-0.000442043
110 DATA -0.020049,0.18164849,177.653,-0.14041269
120 DATA -3.6054349E-05,-0.0058148727,-0.181217,0.000673834
130 DATA -2.09265E-05,0.000671698,0.224737,-0.000219278
140 MAT READ D
150 DATA 1,-0.00856826,-1.128878,0.00154686
160 DATA -0.010039,-7.91185E-05,0.01062186,0.09424925
170 DATA 0.000123107,-1.8706E-06,-8.88737E-05,0.00069426
180 DATA -2.156E-05,-0.0011849,0.078517,1
190 MAT READ E
200 DATA -0.071893,0.60873556,-40.203644,-513.19824
210 DATA 0.0009086,-0.00605144,0.39170456,5.1588783
220 DATA -7.49E-06,7.5133E-05,-0.004889544,-0.063124955
230 DATA 0.0019604028,-0.000115022,0.00427627,0.0829603
240 MAT READ A
250 DATA 0,-9.64173,638.3179,8136.786
260 DATA 0,-0.055395,-42.6289,-81.86226
270 DATA 0,0,0,1
280 DATA -0.031056,0.0029017,-0.194407,-2.45521
290 MAT READ F
300 DATA 0,-69.8,-26.009,0
310 MAT P=A*B
320 MAT Q=A*C
330 MAT R=A*D
340 MAT S=A*E
350 MAT W=P*F
360 MAT W=(0.02)*W
370 MAT X=Q*F
380 MAT X=(0.02)*X
390 MAT Y=R*F
400 MAT Y=(0.02)*Y
410 MAT Z=S*F
420 MAT Z=(0.02)*Z
430 PRINT "THE TIME RESPONSE OF THE STATE, X(T)"
440 PRINT
450 PRINT "VECTOR COEFF OF EXP(-2.104338)T*COS(3.714744)T"
```

Figure 6-9

```
460 PRINT W[1,1],W[2,1],W[3,1],W[4,1]
470 PRINT
480 PRINT "VECTOR COEFF OF EXP(-2.104338)T*SIN(3.714744)T"
490 PRINT X[1,1],X[2,1],X[3,1],X[4,1]
500 PRINT
510 PRINT "VECTOR COEFF OF EXP(-0.004511029)T*COS(0.06274706)T"
520 PRINT Y[1,1],Y[2,1],Y[3,1],Y[4,1]
530 PRINT
540 PRINT "VECTOR COEFF OF EXP(-0.004511029)T*SIN(0.06274706)T"
550 PRINT Z[1,1],Z[2,1],Z[3,1],Z[4,1]
560 END
```

```
THE TIME RESPONSE OF THE STATE, X(T)

VECTOR COEFF OF EXP(-2.104338)T*COS(3.714744)T
 0.233872832     1.312519      0.039193618     0.019483841

VECTOR COEFF OF EXP(-2.104338)T*SIN(3.714744)T
-0.045144590     10.41547062   -0.117841383     0.021596520

VECTOR COEFF OF EXP(-0.004511029)T*COS(0.06274706)T
-318.7879228      .206305933   -0.039188853     0.077583489

VECTOR COEFF OF EXP(-0.004511029)T*SIN(0.06274706)T
-13.35349032     0.075818325   -2.06386E-03    -0.619060577
```

Figure 6-9 (continued)

Substituting,

$$\int_0^\infty f(t)\,g(t)\,dt = f(\infty)\,G(\infty) - \int_0^\infty G(t)\,f'(t)\,dt$$

$$= \int_0^\infty \left(\frac{1}{s} - \frac{1}{s}e^{-st}\right)\left(2\alpha t e^{-\alpha t^2}\right) dt$$

$$= \frac{2\alpha}{s}\int_0^\infty \left(1 - e^{-st}\right) e^{-\alpha t^2}\, dt$$

$$\int_0^\infty e^{-\alpha t^2} e^{-st}\, dt = \frac{2\alpha}{s}\int_0^\infty e^{-\alpha t^2}\, dt - \frac{2\alpha}{s}\int_0^\infty e^{-\alpha t^2} e^{-st}\, dt$$

Combining terms,

$$\left(\frac{2\alpha}{s} + 1\right)\int_0^\infty e^{-\alpha t^2} e^{-st}\, dt = \frac{2\alpha}{s}\int_0^\infty e^{-\alpha t^2}\, dt = \frac{2\alpha}{s}\,\frac{1}{2\sqrt{\alpha}}\sqrt{\pi}$$

$$\int_0^\infty e^{-st} e^{-\alpha t^2}\, dt = \frac{s}{2\alpha + s}\cdot\frac{2\alpha}{s}\sqrt{\frac{\pi}{\alpha}}\cdot\frac{1}{2} = \frac{\alpha}{2\alpha + s}\sqrt{\frac{\pi}{\alpha}}$$

For $\tau = 0.01$, $\alpha = \dfrac{\pi}{.0001} = 31416$

$$\int_0^\infty e^{-st} e^{-\alpha t^2}\, dt = \frac{31416}{62832 + s}\sqrt{.0001} = \frac{314.16}{62832 + s}$$

Multiplying by the magnitude of the input, 0.02, yielded

$$0.02\,\delta(t) = \frac{6.2832}{62832 + s}$$

The magnitudes of the results of this input were too small, the probable reason being that half of the function $\exp(\pi t^2/\tau^2)$ lies to the left of the t=0 axis and is contributing nothing to the input.

The application of a 0.001 second delay to this function would place 99% of it to the right of the t=0 axis, countering the problem that existed originally. A time delay of 0.001 seconds corresponds to multiplying the Laplace transform by $e^{-0.001s}$. Approximating $e^{-0.001s}$ by the series

$$1 - 0.001s + \frac{(0.001)^2 s^2}{2!} - \frac{(0.001)^3 s^3}{3!} + \cdots,$$

R(s) becomes $\left(\frac{0.000001s^2 - 0.0005s + 0.05}{2}\right)\left(\frac{6.2832}{62832 + s}\right)$

$= 79577.5\left(\frac{s^2 - 500s + 500,000}{s + 62832}\right).$

Again, N(s) is of greater order than D(s).

The correct answer was finally reached when a variation of an earlier idea (using the response at t=1 from a step function as initial conditions) was pursued. In this case, the two steps were combined into one by summing two step functions, one commencing at t=0, the other at t=1 and negative in sign. The graphical representation and summation is shown in Figure 6-14.

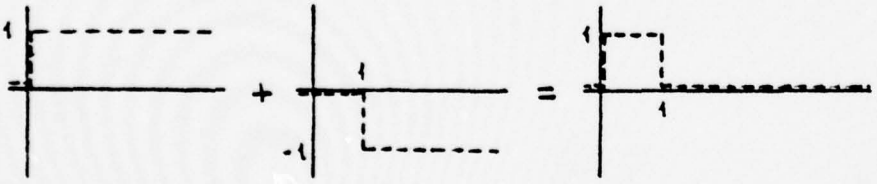


Figure 6-14

In the time domain, the result is written

$$r(t) = 1(t) - 1(t - \tau), \text{ where } \tau = 1.$$

The Laplace was easily found and was

$$R(s) = \frac{1}{s} - \frac{1}{s} e^{-\tau s}$$

Searching for an approximation of e^{-s} which would satisfy the requirement for the order of the numerator to be smaller than the order of the denominator led to[13]

$$e^{-s} = \frac{1 - \frac{s}{2} + \frac{s^2}{8} - \frac{s^3}{48} + \cdots}{1 + \frac{s}{2} + \frac{s^2}{8} + \frac{s^3}{48} + \cdots}$$

$$= \frac{48 - 24s + 6s^2 - s^3 + \cdots}{48 + 24s + 6s^2 + s^3 - \cdots}$$

Substituting into $R(s) = 0.02(\frac{1}{s} - \frac{1}{s}e^{-s})$ yielded

$$R(s) = 0.04\left[\frac{24 + s^2}{48 + 24s + 6s^2 + s^3}\right]$$

The results of the RTRESP computations and the time history plots are shown in Figures 6-15 and 6-16. Their agreement with the text figures confirmed the accuracy of the RTRESP (for other than initial condition inputs) and GRAPH programs and provided a valid approximation of a finite impulse-type input.

---

[13] Ogata, Modern Control Engineering, Prentice-Hall, 1970, p 414

```
RATIONAL TIME RESPONSE
PROBLEM IDENTIFICATION - HOPNER EXAMPLE

**********************************************

THE A MATRIX

      -0.0697000          0.0010000          0.0          -32.2000000
      -0.0955000         -1.4300000        [illegible]        0.0
       0.0001240         -0.0210000         -2.7700000        0.0
       0.0                0.0                1.0000000        0.0

THE B MATRIX

       0.0               -00.0000000        -20.0000000       0.0

THE C MATRIX

       1.0000000         0.0                0.0              0.0

FEEDBACK COEFF.

       0.0               0.0                0.0              0.0

GAIN =  1.00000000 00

**********************************************

INITIAL CONDITIONS - X(0)

       0.0               0.0                0.0              0.0

PGAIN =  4.00000000-02

NUMERATOR POLYNOMIAL OF H(S) - ASCENDING POWERS OF S
      24.0000000         0.0                1.0000000
```

Figure 6-15

```
 NUMERATOR ROOTS ARE
   REAL PART        IMAG. PART
         0.0              -4.8989795
         0.0               4.8989795

 DENOMINATOR POLYNOMIAL OF R(S) - ASCENDING POWERS OF S
        48.0000000       24.0000000        6.0000000        1.0000000

 DENOMINATOR ROOTS ARE
   REAL PART        IMAG. PART
        -1.4039284       -3.0140790
        -1.4039284        3.0140790
        -3.1921433        0.0

**********************************************

 THE TIME RESPONSE OF THE STATE X(T)

 THE VECTOR COEFFICIENT OF EXP(-2.1043390 00)T*COS(3.7147460 00)T
        -0.4502925       89.5084830       -1.0780095        0.1906888

 THE VECTOR COEFFICIENT OF EXP(-2.1043390 00)T*SIN(3.7147460 00)T
        -1.0082787     -175.2804871       -0.3249722       -0.1321901

 THE VECTOR COEFFICIENT OF EXP(-4.5109710-03)T*COS(6.2745000-02)T
        -0.0508000        0.0043945       -0.0000398       -0.0391895

 THE VECTOR COEFFICIENT OF EXP(-4.5109710-03)T*SIN(6.2745000-02)T
        20.1149292       -0.1923828        0.0025139       -0.0033016

 THE VECTOR COEFFICIENT OF EXP(-1.4039280 00)T*COS(3.0140790 00)T
         1.2746306        0.0067856        0.0125671       -0.0083148

 THE VECTOR COEFFICIENT OF EXP(-1.4039280 00)T*SIN(3.0140790 00)T
         1.1051407      140.1347351       -0.0314089        0.1982617

 THE VECTOR COEFFICIENT OF EXP(-3.1921430 00)T
        -0.7932987      -91.1166420        0.2455351       -0.0831330

**********************************************
```

Figure 6-15 (continued)

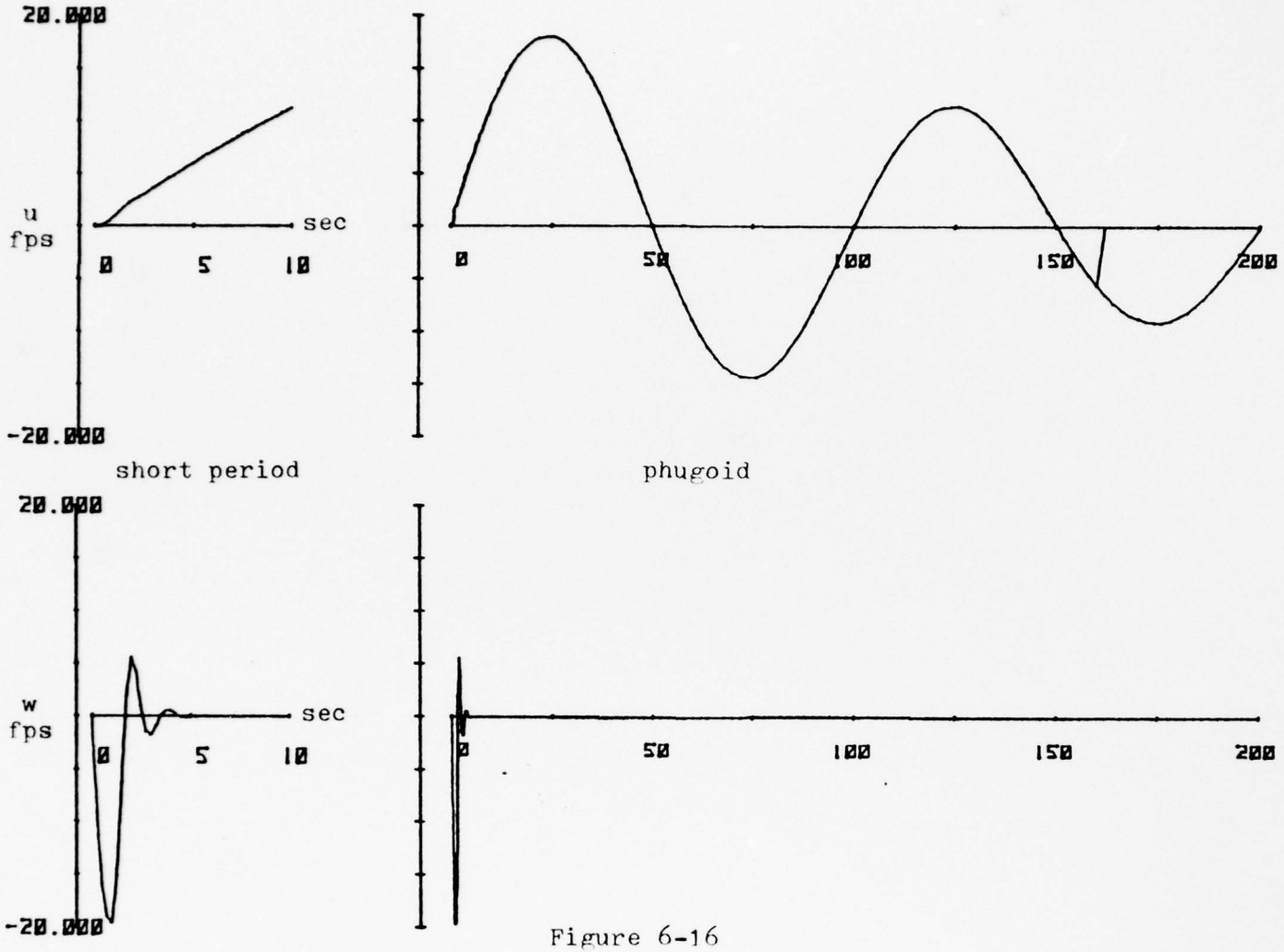

20.000
u
fps
sec
0
5
10
-20.000
short period
0
50
100
150
200
phugoid
20.000
w
fps
sec
0
5
10
-20.000
0
50
100
150
200

Figure 6-16

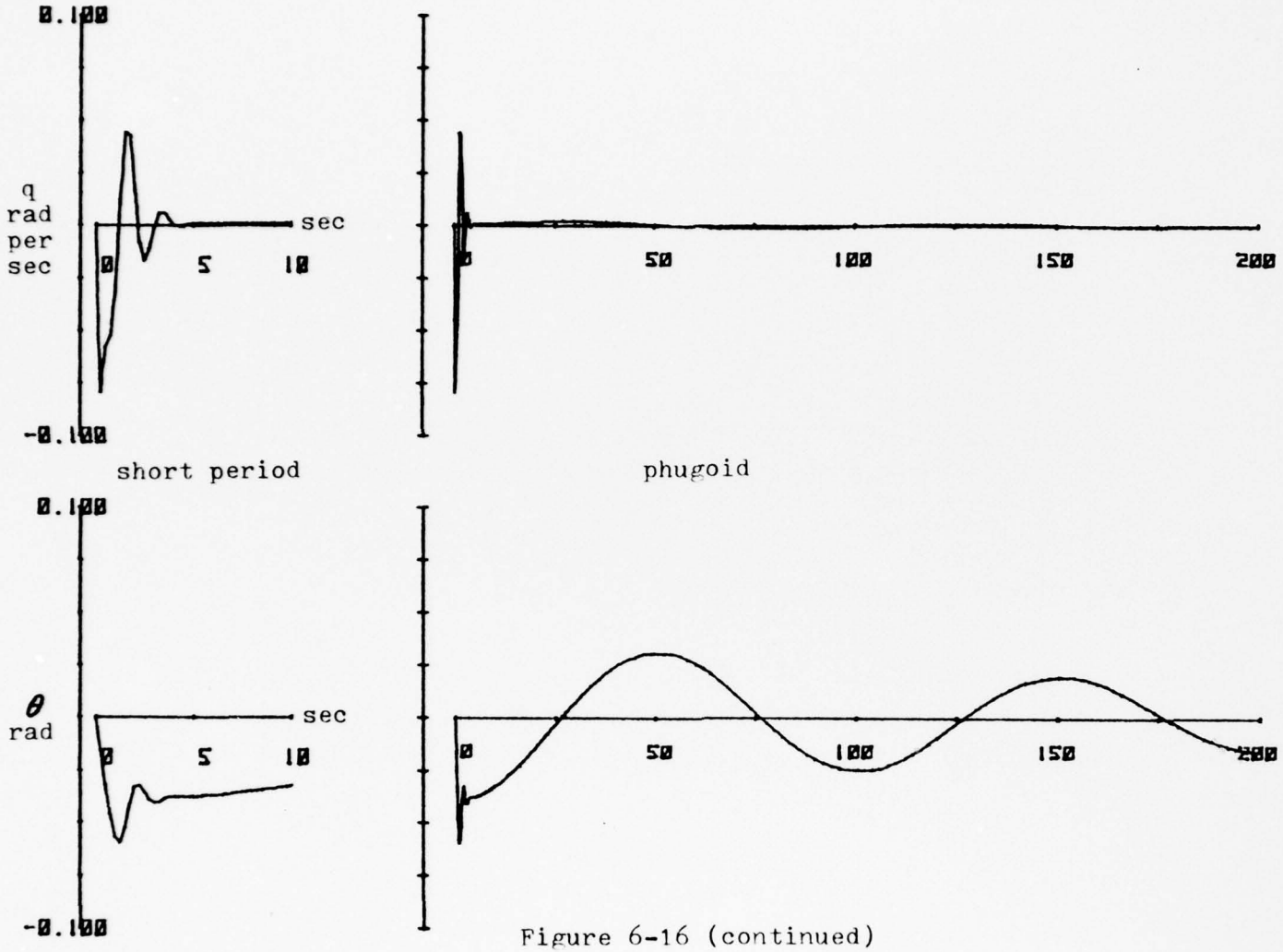


Figure 6-16 (continued)

VII. LONGITUDINAL FEEDBACK

The primary purpose in using feedback in a control system is to reduce the system's sensitivity to external perturbations. In the open loop system, the area of main concern is calibration; in the closed loop system, it is stability. Use of feedback can enhance the rapidity of response, reduce errors of response, and increase damping to satisfactory levels; it can also overcorrect errors or decrease damping to the point where an otherwise stable system becomes unstable. It is of interest, then, to be able to "measure" the stability of a system.

The stability of a system may be ascertained by an analysis of the characteristic equation of the system, that is, the denominator of its transfer function. Simply stated, if the real part of every root of the equation is negative in sign, the system is stable. That this is so is manifested by the relationship between the roots of the characteristic equation and the solution of the differential equation which it represents.

For a multiple input/output system, the feedback effects on the transfer functions must be dealt with by matrix manipulation

The solution to the system of differential equations

$$\dot{\underline{x}} = [A]\underline{x} + \{b\}u$$

was seen to be, in the Laplace domain,

$$x(s) = [sI-A]^{-1}\{b\}u(s) = [\Phi(s)]\{b\}u(s).$$

The open loop transfer function was then

$$G_o(s) = \frac{x(s)}{u(s)} = [\Phi(s)]\{b\}$$

where $\Phi(s)$ is the resolvent matrix. In a 4x4 system, the transfer function is written

$$G_O(s) = \frac{\begin{bmatrix} \varphi_{11} & \varphi_{12} & \varphi_{13} & \varphi_{14} \\ \varphi_{21} & \varphi_{22} & \varphi_{23} & \varphi_{24} \\ \varphi_{31} & \varphi_{32} & \varphi_{33} & \varphi_{34} \\ \varphi_{41} & \varphi_{42} & \varphi_{43} & \varphi_{44} \end{bmatrix} \begin{Bmatrix} b_1 \\ b_2 \\ b_3 \\ b_4 \end{Bmatrix}}{\Delta} = \begin{Bmatrix} \sum \varphi_{1j} b_j / \Delta \\ \sum \varphi_{2j} b_j / \Delta \\ \sum \varphi_{3j} b_j / \Delta \\ \sum \varphi_{4j} b_j / \Delta \end{Bmatrix}$$

$$j = 1, \ldots, 4$$

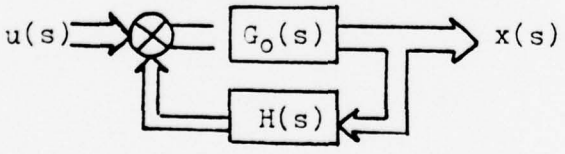
The last quantity will be written

$$\begin{Bmatrix} G_1 \\ G_2 \\ G_3 \\ G_4 \end{Bmatrix}_{open} \qquad \text{where } \Delta = \det[sI-A]$$

Applying the feedback signal to a particular parameter, for example, x_3, yields

$$H = \lfloor 0 \; 0 \; h \; 0 \rfloor$$

where the block diagram is



(The solid arrows are used to signify a multiple input/output system.) The closed loop transfer function is

$$G(s) = \frac{G_o(s)}{1 + G_oH}$$

In matrix format, $\left\{G(s)\right\} = \left[I + G_oH\right]^{-1}\left\{G_o(s)\right\}$.

To find this matrix product, the matrices were taken term by term:

$$\left[I + G_oH\right] = \begin{bmatrix} 1 & 0 & hG_1 & 0 \\ 0 & 1 & hG_2 & 0 \\ 0 & 0 & 1+hG_3 & 0 \\ 0 & 0 & hG_4 & 1 \end{bmatrix}$$

$$\left[I + G_oH\right]^{-1} = \frac{\begin{bmatrix} 1+hG_3 & 0 & -hG_1 & 0 \\ 0 & 1+hG_3 & -hG_2 & 0 \\ 0 & 0 & 1 & 0 \\ 0 & 0 & -hG_4 & 1+hG_3 \end{bmatrix}}{\Delta'}$$

where $\Delta' = \det\left[I + G_oH\right] = 1 + hG_3$.

Finally,

$$\left[I+G_oH\right]^{-1}\left\{G_o(s)\right\} = \frac{\begin{Bmatrix} G_1 \\ G_2 \\ G_3 \\ G_4 \end{Bmatrix}_{open}}{\Delta'} = \frac{\begin{Bmatrix} \Sigma\, b_j\varphi_{1j} \\ \Sigma\, b_j\varphi_{2j} \\ \Sigma\, b_j\varphi_{3j} \\ \Sigma\, b_j\varphi_{4j} \end{Bmatrix}}{(1+hG_3)\,\Delta} = \frac{\begin{Bmatrix} \Sigma\, b_j\varphi_{1j} \\ \Sigma\, b_j\varphi_{2j} \\ \Sigma\, b_j\varphi_{3j} \\ \Sigma\, b_j\varphi_{4j} \end{Bmatrix}}{\left(1 + h\,\frac{\Sigma\, b_j\varphi_{3j}}{\Delta}\right)\Delta}$$

$$= \frac{\begin{Bmatrix} \Sigma\, b_j\varphi_{1j} \\ \Sigma\, b_j\varphi_{2j} \\ \Sigma\, b_j\varphi_{3j} \\ \Sigma\, b_j\varphi_{4j} \end{Bmatrix}}{\Delta + h\,\Sigma\, b_j\varphi_{3j}}$$

The closed loop transfer function is then

$$\{G_c(s)\} = \frac{\left\{ \begin{array}{l} b_1\varphi_{11} + b_2\varphi_{12} + b_3\varphi_{13} + b_4\varphi_{14} \\ b_1\varphi_{21} + b_2\varphi_{22} + b_3\varphi_{23} + b_4\varphi_{24} \\ b_1\varphi_{31} + b_2\varphi_{32} + b_3\varphi_{33} + b_4\varphi_{34} \\ b_1\varphi_{41} + b_2\varphi_{42} + b_3\varphi_{43} + b_4\varphi_{44} \end{array} \right\}}{\Delta + h\left(b_1\varphi_{31} + b_2\varphi_{32} + b_3\varphi_{33} + b_4\varphi_{34}\right)}$$

In the general form, the first subscript of φ in the denominator will vary as the feedback parameter is varied. Regardless of the form or magnitude of h, only the denominator is affected; the numerator is a function solely of the openloop resolvent matrix, $\Phi(s)$, and the control vector, $\{b\}$.

The most important characteristic of the transfer function is that the frequency response may be obtained by letting $s = j\omega$, where ω is the applied sinusoidal forcing function. That this is so is shown by assuming that the output contains a sinusoidal component of the same frequency as the input in the form

$$A \cdot R(\omega) \cdot \sin\left[\omega t + \varphi(\omega)\right]$$

where A is a constant, $R(\omega)$ is the magnitude, and $\varphi(\omega)$

is the phase angle between the input and the response. For an input of $A\sin\omega t$, the Laplace of which is

$$\frac{A\omega}{s^2 + \omega^2}$$

the output is

$$y(s) = G(s)r(s) = \frac{A\omega G(s)}{s^2 + \omega^2} = \frac{A\omega G(s)}{(s + j\omega)(s - j\omega)}$$

Using partial fraction expansion:

$$y(s) = \frac{Z_1}{s+j\omega} + \frac{Z_2}{s-j\omega} + \text{transient terms}$$

Assuming the transient solution is stable allows the transient terms to be dropped, so

$$Z_1 = \left.\frac{A\omega G(s)}{s-j\omega}\right|_{s=-j\omega} = \frac{-AG(-j\omega)}{2j}$$

$$Z_2 = \left.\frac{A\omega G(s)}{s+j\omega}\right|_{s=+j\omega} = \frac{AG(j\omega)}{2j}$$

Solving for $y(t)$ by taking the inverse Laplace transform:

$$y(t) = \frac{-AG(-j\omega)}{2j} e^{-j\omega t} + \frac{AG(j\omega)}{2j} e^{+j\omega t} \qquad (7\text{-}1)$$

Since $G(j\omega)$ is complex, write it as

$$G(j\omega) = x(\omega) + jY(\omega) \quad \text{and} \quad G(-j\omega) = x(\omega) - jY(\omega)$$

where $|G(j\omega)| = \sqrt{X^2(\omega) + Y^2(\omega)}$ and $\arg G(j\omega) = \tan^{-1}\frac{Y(\omega)}{X(\omega)}$.

Substitute into equation (7-1):

$$y(t) = -\frac{A}{2j}\left[X(\omega) - jY(\omega)\right]e^{-j\omega t} + \frac{A}{2j}\left[X(\omega) + jY(\omega)\right]e^{+j\omega t}$$

$$= \frac{AX(\omega)}{2j}\left(e^{j\omega t} - e^{-j\omega t}\right) + \frac{AY(\omega)}{2j}\left(e^{j\omega t} + e^{-j\omega t}\right)$$

$$= AX(\omega)\sin\omega t + AY(\omega)\cos\omega t$$

$$= A\left[X^2(\omega) + Y^2(\omega)\right]^{1/2}\sin\left[\omega t + \alpha(\omega)\right]$$

where $\alpha = \tan^{-1}\frac{Y(\omega)}{X(\omega)}$.

This is the same form as the assumed input, so that R(s) becomes $\sqrt{X^2(\omega) + Y^2(\omega)} = |G(j\omega)|$ and the phase angle $\varphi(\omega)$ becomes $\tan^{-1}Y(\omega)/X(\omega) = \arg G(j\omega)$.

It becomes a simple matter to apply a feedback to a plant matrix, obtain the transfer functions in each of the variables, and plot the magnitude of the responses to a sinusoidal input against the frequency of that

input. This plot is termed a Bode (Bō′-dee) plot, named for its developer, H.W. Bode. One of the important uses of the plot is in measuring the stability of a system.

In order to facilitate construction of a Bode plot, and in order to avoid relying upon asymptotic approximations of magnitude and phase angle, a program named BODE was written for the HP9830 computer/plotter. Using, as input, the stability derivatives and the type and magnitude of feedback, the program prints out the resulting transfer functions (in the Laplace domain), repeats the feedback inputs, and, for given limits of frequency and magnitude, constructs the Bode diagram on semi-log paper. The feedback form may be linear, integration (1/s), or differentiation (s).

The program, listed in Figure 7-2, is explained:

line 10 dimensions open and closed loop matrices

ll 20-60 defines variables in terms of stability derivatives;

XU = X_u
XW = X_w
XDE = $X_{\delta e}$
MWDOT = $M_{\dot{w}}$, etc.

line 70 iterates program for x_1, x_2, x_3, and x_4 (u,w,q,θ) outputs

```
REM  PROGRAM  CODE  22NOV76

10 DIM ME8,8],SL8,8]
20 REM X1,X2,X3 ARE XU,XW,XDE
30 REM Z1,Z2,Z3 ARE ZU,ZW,ZDE
40 REM M1,M2,M3 ARE MU,MW,MWDOT
50 REM M4,M5,M6 ARE MA,MQ,MDE
60 REM X4 IS XQ
70 FOR J=1 TO 4
80 WRITE (15,90)
90 FORMAT 45"*"
100 PRINT
110 DEG
120 T0=0
130 U0=1016.9
140 G=32.073
150 X1=-0.0097
160 X2=0.0016
170 X3=0
180 X4=0
190 Z1=-0.0955
200 Z2=-1.43
210 Z3=-59.8
220 M1=-0
230 M2=-0.0235
240 M3=-0.0013
250 M4=U0*M2
260 M5=-1.92
270 M6=-26.1
280 FOR I=1 TO 7
290 D[I]=0
300 FOR K=1 TO 7
310 N[I,K]=0
320 NEXT K
330 NEXT I
340 D[5]=1
350 N[3,4]=M6+Z3*M3
360 N[4,2]=Z3
370 N[4,1]=X3
380 D[4]=-M5-Z2-X1
390 N[2,4]=X3*(Z1*M3+M1)+Z3*(M2-X1*M3)-M6*(X1+Z2)
400 N[3,2]=X3*Z1-Z3*(X1+M5)+M6*U0
410 N[3,1]=-X3*(Z2+M5)+Z3*X2+X4*M6
420 D[3]=Z2*M5-X2*Z1+X1*(M5+Z2)-M4-M1*X4
430 N[1,4]=X3*(Z1*M2-Z2*M1)+Z3*(M1*X2-M2*X1)+M6*(Z2*X1-X2*Z1)
440 N[2,2]=X3*(U0*M1-Z1*M5)+Z3*X1*M5-U0*M6*X1+X4*(M6*Z1-M1*Z3)
450 N[2,1]=X3*(Z2*M5-M4)-Z3*(X2*M5+G*M3)-M6*G+M6*X2*U0-M6*Z2*X4
460 D[2]=-X1*(Z2*M5-M4)+Z1*(X2*M5+G*M3)-M1*(X2*U0-G)+X4*(M1*Z2-M2*Z1)
470 N[5,4]=N[5,3]=0
480 N[4,3]=M6
490 N[3,3]=-M6*X1-M6*Z2+M1*X3+M2*Z3
500 N[2,3]=M6*X1*Z2+M2*X3*Z1+M1*X2*Z3-M1*X3*Z2-M6*X2*Z1-M2*X1*Z3
```

Figure 7-2

```
510 N[1,3]=0
520 N[1,2]=G*(Z3+M1-M6*Z1)
530 N[1,1]=G*(M6+Z2-Z3*M2)
540 D[1]=G*(Z1*M2-M1+Z2)
550 DISP "IS FDBK 0, LINEAR, S, OR 1/S";
560 INPUT Z
570 IF Z=0 THEN 940
580 IF Z=1 THEN 610
590 IF Z=2 THEN 680
600 IF Z=3 THEN 790
610 DISP "INPUT FEEDBACK GAIN";
620 INPUT K
630 PRINT "FEEDBACK IS LINEAR"
640 FOR I=1 TO 7
650 D[I]=D[I]-N[I,J]*K
660 NEXT I
670 GOTO 960
680 DISP "INPUT FEEDBACK GAIN";
690 INPUT K
700 PRINT "FEEDBACK FORM IS K*S"
710 FOR I=7 TO 1 STEP -1
720 S[I+1,J]=N[I,J]*K
730 NEXT I
740 S[1,J]=0
750 FOR I=1 TO 7
760 D[I]=D[I]-S[I,J]
770 NEXT I
780 GOTO 960
790 DISP "INPUT FEEBACK GAIN";
800 INPUT K
810 PRINT "FEEDBACK FORM IS K/S"
820 FOR I=7 TO 1 STEP -1
830 D[I+1]=D[I]
840 NEXT I
850 D[1]=0
860 FOR I=1 TO 7
870 D[I]=D[I]-N[I,J]*K
880 NEXT I
890 FOR I=7 TO 1 STEP -1
900 N[I+1,J]=N[I,J]
910 NEXT I
920 N[1,J]=0
930 GOTO 960
940 PRINT "FEEDBACK IS NOT APPLIED"
950 GOTO 970
960 PRINT "FEEDBACK GAIN IS "K
970 PRINT "TRANSFER FUNCTION COEFFICIENTS (INCREASING POWERS OF S)"
980 PRINT
990 PRINT "COEFFICIENTS OF NUMERATOR"
1000 FOR I=1 TO 7
```

Figure 7-2 (continued)

```
1010 PRINT N[I,J]
1020 NEXT I
1030 PRINT
1040 PRINT "COEFFICIENTS OF DENOMINATOR (CHAR END)"
1050 FOR I=1 TO 7
1060 PRINT D[I]
1070 NEXT I
1080 DISP "PLACE PAPER ON PLOTTER";
1090 STOP
1100 DISP "INPUT /G/ MAX (DB)";
1110 INPUT G9
1120 DISP "INPUT OMEGA MINIMUM";
1130 INPUT 00
1140 GOSUB 1650
1150 FOR L=LGT(00)+1 TO LGT(00)+5
1160 X=10↑L
1170 FOR W=X/10 TO X STEP X/50
1180 X[J]=(N[1,J]-N[3,J]*W↑2+N[5,J]*W↑4-N[7,J]*W↑6)↑2
1190 X[J]=X[J]+(N[2,J]*W-N[4,J]*W↑3+N[6,J]*W↑5)↑2
1200 X[J]=SQR(X[J])
1210 Y[J]=(D[1]-D[3]*W↑2+D[5]*W↑4)↑2
1220 Y[J]=Y[J]+(D[2]*W-D[4]*W↑3+D[6]*W↑5)↑2
1230 Y[J]=SQR(Y[J])
1240 R[J]=X[J]/Y[J]
1250 IF 20*LGT(R[J])<G9-140 THEN 1270
1260 PLOT LGT(W),20*LGT(R[J])
1270 NEXT W
1280 NEXT L
1290 PEN
1300 PLOT LGT(00)+0.1,G9-1,1
1310 LABEL (*,1.2,1.7,0,7/10)"DECIBELS"
1320 PLOT LGT(00)+2.2,G9-140,1
1330 LABEL (*,1.2,1.7,0,7/10)"RADIANS/SECOND"
1340 PEN
1350 GOSUB 1910
1360 FOR L=LGT(00)+1 TO LGT(00)+5
1370 X=10↑L
1380 FOR W=X/10 TO X STEP X/50
1390 T9=T3
1400 Q1=N[2,J]*W-N[4,J]*W↑3+N[6,J]*W↑5
1410 Q2=N[1,J]-N[3,J]*W↑2+N[5,J]*W↑4-N[7,J]*W↑6
1420 Q3=D[2]*W-D[4]*W↑3+D[6]*W↑5
1430 Q4=D[1]-D[3]*W↑2+D[5]*W↑4-D[7]*W↑6
1440 GOSUB 2080
1450 T3=T1-T2
1460 IF ABS(T3-T9)<180 THEN 1500
1470 T3=T3+360
1480 IF ABS(T3-T9)<180 THEN 1500
1490 T3=T3-720
1500 IF T3<-300 THEN 1520
```

Figure 7-2 (continued)

```
1510 PLOT LGT(W),T3
1520 NEXT W
1530 NEXT I
1540 PEN
1550 DISP "INPUT LETTER SIZE";
1560 INPUT Z
1570 LABEL (*,Z,2,0,7/10)
1580 DISP "YOU ARE IN THE LETTER MODE"
1590 LETTER
1600 DISP "ANY OTHER LETTERING";
1610 INPUT Z
1620 IF Z=1 THEN 1550
1630 NEXT
1640 STOP
1650 SCALE LGT(00)-0.5,LGT(00)+5.5,G9-145,G9+5
1660 DISP "CHECK ALIGNMENT OF PLOTTER"
1670 PLOT LGT(00),G9-140,1
1680 STOP
1690 PLOT LGT(00)+5,G9,1
1700 DISP "RE-CHECK ALIGNMENT?";
1710 INPUT Z
1720 IF Z=0 THEN 1740
1730 GOTO 1660
1740 YAXIS LGT(00),20,G9-140,G9
1750 LABEL (*,1,1.7,0,7/10)
1760 FOR Y=G9-140 TO G9 STEP 20
1770 PLOT LGT(00),Y,1
1780 CPLOT -5,-0.3
1790 LABEL (1800)Y
1800 FORMAT F4.0
1810 NEXT Y
1820 FOR X=LGT(00)+1 TO LGT(00)+5
1830 PLOT X,G9-140,1
1840 CPLOT -4.5,-1.5
1850 LABEL (1860)10↑X
1860 FORMAT F8.2
1870 NEXT X
1880 PEN
1890 RETURN
1900 STOP
1910 SCALE LGT(00)-0.5,LGT(00)+5.5,-325,425
1920 DISP "RE-CHECK ALIGNMENT OF PLOTTER";
1930 PLOT LGT(00),-300,1
1940 STOP
1950 PLOT LGT(00)+5,400,1
1960 STOP
1970 LABEL (*,1.2,1.7,0,7/10)
1980 FOR Y=-200 TO 100 STEP 100
1990 PLOT LGT(00)+4.7,Y,1
2000 CPLOT 0,-0.3
```

Figure 7-2 (continued)

```
2010 LABEL (2050)Y
2020 NEXT Y
2030 PLOT LGT(00)+4.95,95,1
2040 LABEL (*,1.2,1.7,0,7/10)"DEG"
2050 FORMAT F4.0
2060 RETURN
2070 STOP
2080 IF Q1>0 AND Q2<0 THEN 2130
2090 IF Q1<0 AND Q2<0 THEN 2150
2100 IF Q1<0 AND Q2>0 THEN 2170
2110 T1=ATN(Q1/Q2)-180
2120 GOTO 2180
2130 T1=ATN(Q1/Q2)
2140 GOTO 2180
2150 T1=ATN(Q1/Q2)
2160 GOTO 2180
2170 T1=180+ATN(Q1/Q2)
2180 IF Q3>0 AND Q4<0 THEN 2230
2190 IF Q3<0 AND Q4<0 THEN 2250
2200 IF Q3<0 AND Q4>0 THEN 2270
2210 T2=ATN(Q3/Q4)
2220 RETURN
2230 T2=180+ATN(Q3/Q4)
2240 RETURN
2250 T2=180+ATN(Q3/Q4)
2260 RETURN
2270 T2=360+ATN(Q3/Q4)
2280 RETURN
2290 END
```

Figure 7-2 (continued)

ll 80-110 format

ll 120-270 assigns values to variables, initializes T3 (phase angle, used for comparison)

ll 280-330 initializes numerator and denominator coefficients to zero

ll 340-540 computes values of numerator and denominator coefficients

ll 550-1070 inputs feedback type and magnitude, computes and prints closed loop numerator and denominator coefficients

ll 1080-1640 inputs frequency and magnitude limits (of response), labels graph, and plots magnitude and phase angle against applied frequency

ll 1650-1900 subroutine for scaling and labelling magnitude graph

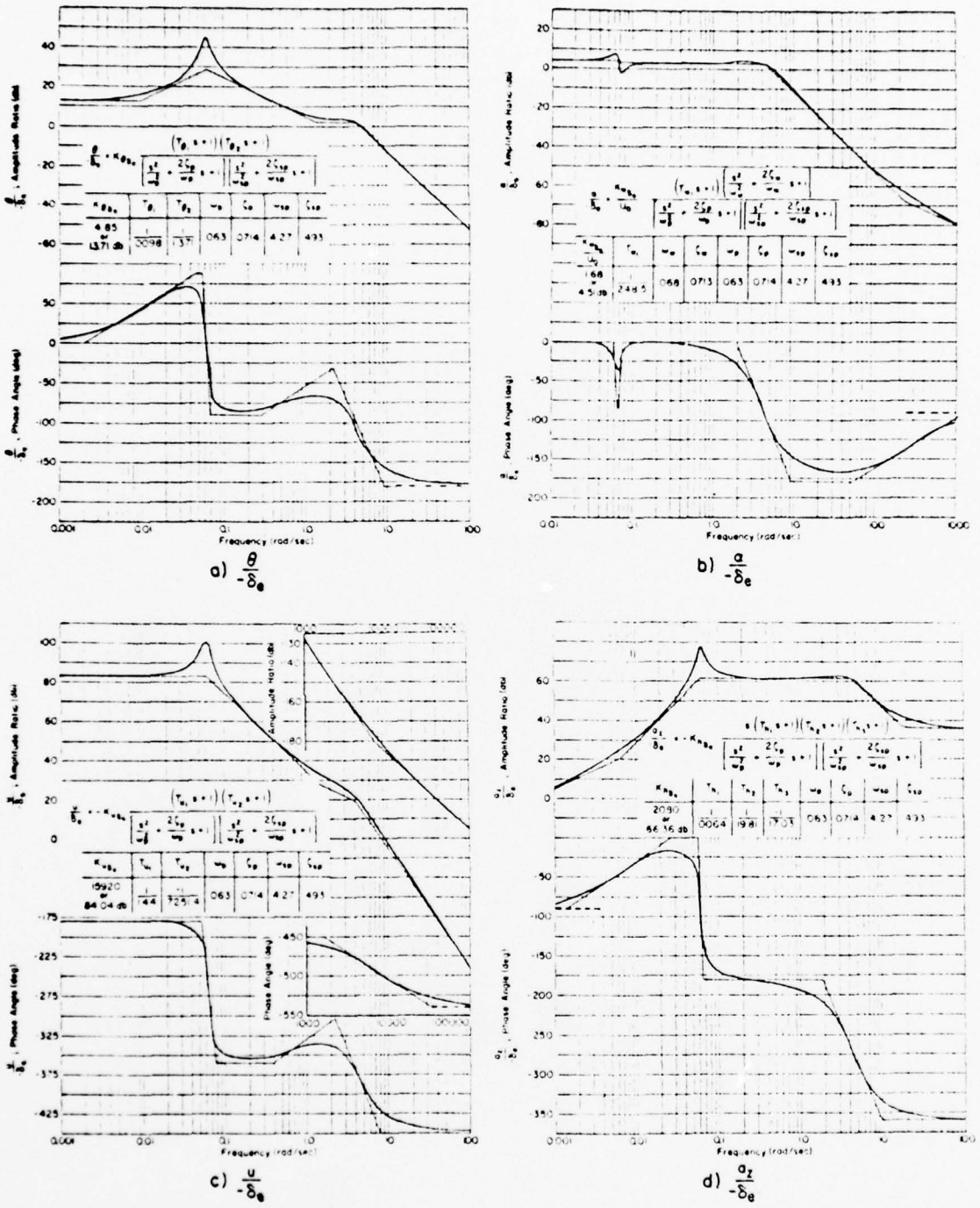
ll 1910-2070 subroutine for scaling and labelling phase angle graph

ll 2080-2280 subroutine which computes phase angle correct for sign and quadrant

line 2290 END statement

To verify the program, the McRuer example was again used. The text results are shown in Figure 7-3. The BODE results are shown in Figures 7-4, 7-5, and 7-6 for the three parameters common to both programs, θ, α, and u.

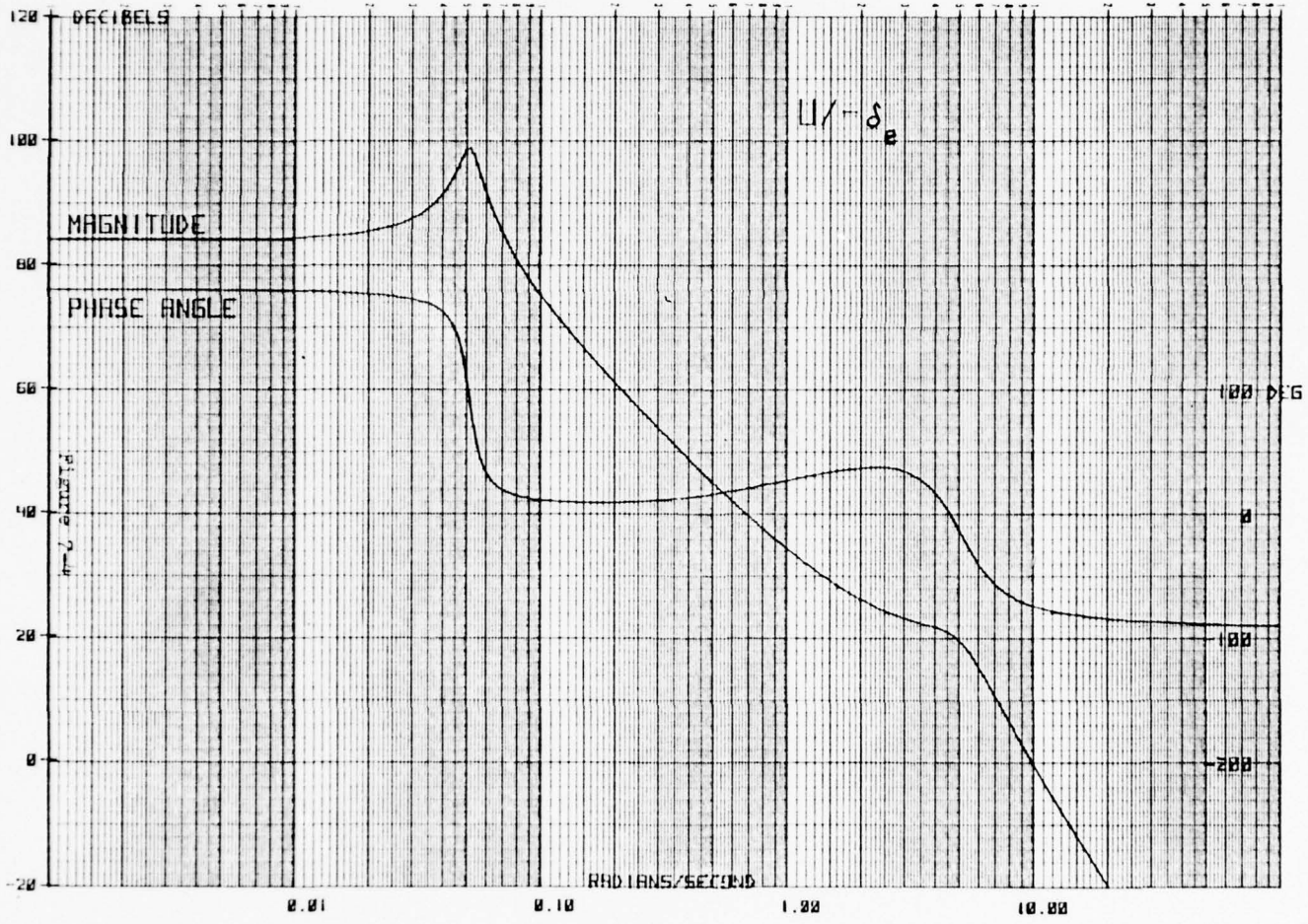
The comparison of the α values of the text and the graph of w from BODE needs some explanation. The text's



a) $\frac{\theta}{-\delta_e}$ b) $\frac{\alpha}{-\delta_e}$

c) $\frac{u}{-\delta_e}$ d) $\frac{a_z}{-\delta_e}$

Figure 7-3


SEMILOGARITHMIC 5 CYCLES X 10 DIVISIONS
DECIBELS
120
100
80
60
40
20
0
-20
MAGNITUDE
PHASE ANGLE
$U/-\delta_e$
100 DEG
0
-100
-200
RADIANS/SECOND
0.01
0.10
1.00
10.00

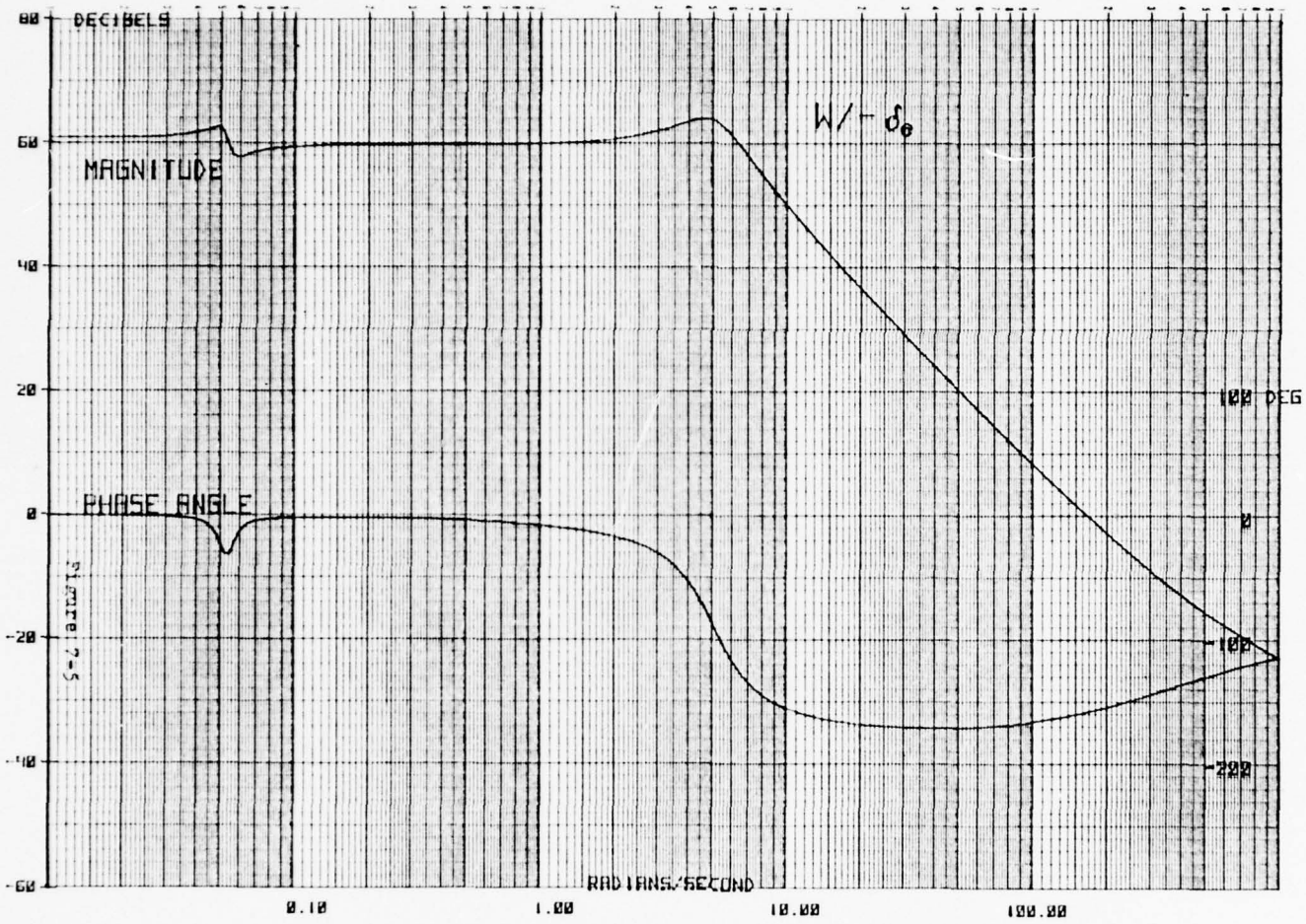
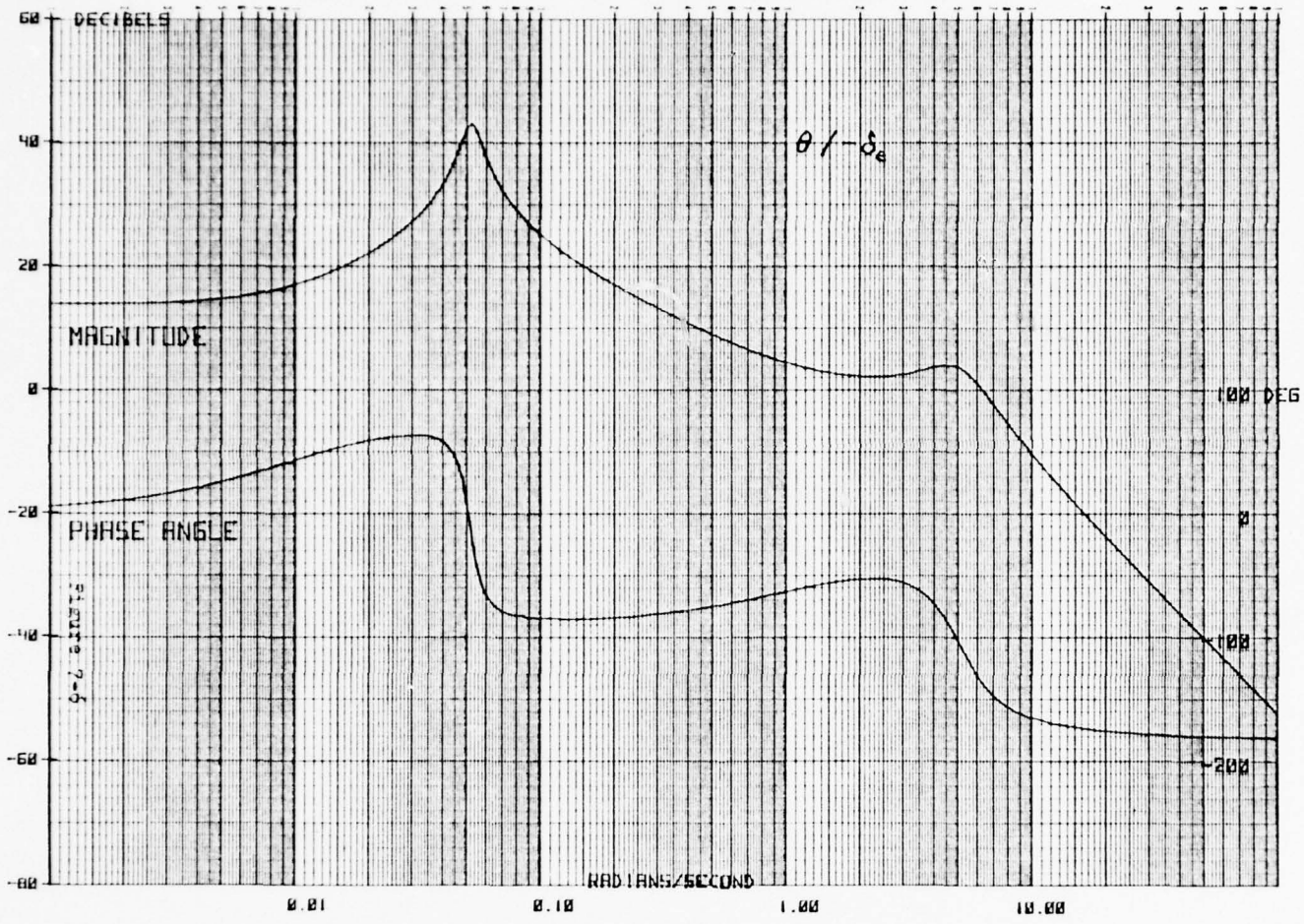

DECIBELS
MAGNITUDE
PHASE ANGLE
W/ - δ_e
80
60
40
20
0
-20
-40
-60
100 DEG
0
-100
-200
0.10
1.00
10.00
100.00
RADIANS/SECOND

Figure 7-5


DECIBELS
60
40
20
0
-20
-40
-60
-80
θ / -δe
MAGNITUDE
PHASE ANGLE
100 DEG
0
-100
-200
RADIANS/SECOND
0.01
0.10
1.00
10.00

magnitude for α at low frequency is ~ 4.0; the results of BODE showed the magnitude of w at low frequency to be ~ 61, a 57 decibel difference. For $U_o = 660$,

$$w = \alpha U_o = 660\alpha$$

$$\log(w) = \log(660) + \log(\alpha).$$

Since log(660) = 56.4, the 57 db difference is correct.

Table 7-2 compares the results of the BODE program's transfer function coefficients with those of the text.

		NUMERATORS
u	BODE	$0.11168s^2 - 791.5148s - 1144.4512$
	text	$0.1103s^2 - 799s - 1151$
w	BODE	$69.8s^3 + 26675.783s^2 + 258.7485s + 79.94357$
	text	$69.8s^3 + 17350s^2 + 168.6s + 80.2$
θ	BODE	$26.00926s^2 + 35.93499s + 0.35011$
	text	$26.12s^2 + 36.1s + 0.351$
		DENOMINATOR
	BODE	$s^4 + 3.3597s^3 + 26.6754s^2 + 0.26271s + 0.07198$
	text	$s^4 + 4.22s^3 + 18.28s^2 + 0.2097s + 0.0724$

Table 7-2

Inasmuch as the text figures appeared to be slide-rule accuracy, the results of BODE were considered more accurate. The BODE graphs, which were computed with zero feedback, compared very favorably with the text, and the program may be considered verified.

The transfer functions may also be written as functions of the stability derivatives, and, in this way, the effects of various types of feedback may be predicted. Writing the equations of motion (equations 5-1) in the Laplace domain:

$$
\begin{aligned}
(s-X_u)u \quad & -X_w w \quad & -X_q q + g\theta &= X_{\delta_e} \\
-Z_u u + (s-Z_w)w \quad & & -U_o q &= Z_{\delta_e} \\
-M_u u \quad & -M_w w + (s-M_q)q & &= M_{\delta_e} \\
& & -q + s\theta &= 0
\end{aligned}
$$

Use of Cramer's rule allows for the solution of each variable in terms of the stability derivatives. That is:

$$
\frac{u(s)}{\delta_e(s)} = \frac{\begin{vmatrix} X_{\delta_e} & -X_w & -X_q & g \\ Z_{\delta_e} & s-Z_w & -U_o & 0 \\ M_{\delta_e} & -M_w & s-M_q & 0 \\ 0 & 0 & -1 & s \end{vmatrix}}{\Delta}
$$

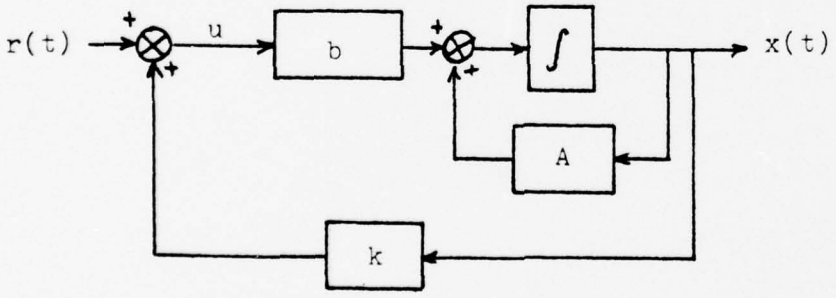
where $\Delta = \begin{vmatrix} s-X_u & -X_w & -X_q & g \\ -Z_u & s-Z_w & -U_0 & 0 \\ -M_u & -M_w & s-M_q & 0 \\ 0 & 0 & -1 & s \end{vmatrix}$

The transfer functions for $w(s)/\delta_e(s)$, $q(s)/\delta_e(s)$, and $\theta(s)/\delta_e(s)$ are similarly found. Compiling the coefficients for each of the numerators yields Table 7-3.

The time history response may be obtained by substituting the error signal for the input term to the plant matrix. In other words, where, for the open loop system,

$$\dot{\underline{x}}(t) = [A]\underline{x} + \{b\}u,$$

in the closed loop system



$u = r - kx$, and $\dot{x}(t) = [A]\underline{x} + \{b\}(r - [k]\{x\})$.

Rewriting,

$$\dot{x}(t) = (A - bk^T)\underline{x} + \underline{b}r.$$

NUMERATORS

	s^3	s^2	s^1	s^0
u	X_{δ_e}	$X_w Z$ $-X_{\delta_e}(Z_w + M_q)$	$X_{\delta_e}(Z_w M_q - M_w U_o)$ $-Z_{\delta_e} X_w M_q$ $+M_{\delta_e}(X_w U_o - g)$	$g(Z_w M_{\delta_e} - Z_{\delta_e} M_w)$
w	Z_{δ_e}	$X_{\delta_e} Z_u + M_{\delta_e} U_o$ $-Z_{\delta_e}(X_u + M_q)$	$X_{\delta_e}(M_u U_o - Z_u M_q)$ $+Z_{\delta_e}(X_u M_q - X_q M_u)$ $+M_{\delta_e}(X_q Z_u - X_u U_o)$	$g(Z_{\delta_e} M_u - Z_u M_{\delta_e})$
q	M_{δ_e}	$X_{\delta_e} M_u + Z_{\delta_e} M_w$ $-M_{\delta_e}(X_u + Z_w)$	$X_{\delta_e}(Z_u M_w - Z_w M_u)$ $+Z_{\delta_e}(X_w M_u - X_u M_w)$ $+M_{\delta_e}(X_u Z_w - X_w Z_u)$	
θ		M_{δ_e}	$X_{\delta_e} M_u + Z_{\delta_e} M_w$ $-M_{\delta_e}(X_u + Z_w)$	$X_{\delta_e}(Z_u M_w - M_u Z_w)$ $+Z_{\delta_e}(X_w M_u - X_u M_w)$ $+M_{\delta_e}(X_u Z_w - X_w Z_u)$

DENOMINATOR

$$\Delta = s^4 - (X_u + Z_w + M_q)s^3 + (X_u Z_w + X_u M_q + Z_w M_q - X_q M_u - X_w Z_u - M_w U_o)s^2 + (X_q Z_w M_u + X_w Z_u M_q - X_u Z_w M_q - X_q Z_u M_w - X_w M_u U_o + X_u M_w U_o + M_u g)s + g(Z_u M_w - Z_w M_u)$$

Table 7-3

As originally formulated,

$$[A] = \begin{bmatrix} X_u & X_w & X_q & -g \\ Z_u & Z_w & U_o+Z_q & 0 \\ M_u & M_w & M_q & 0 \\ 0 & 0 & 1 & 0 \end{bmatrix}$$

and

$$\{B\} = \begin{Bmatrix} X_{\delta_e} \\ Z_{\delta_e} \\ M_{\delta_e} \\ 0 \end{Bmatrix}$$

Assuming the input to be zero ($r = 0$), the effects of a speed error feedback can be seen by letting $\lfloor k \rfloor = \lfloor k_u \quad 0 \quad 0 \quad 0 \rfloor$ and solving for $\left[A - \underline{b}\underline{k}^T\right]$:

$$\{B\}\lfloor k \rfloor = \begin{bmatrix} X_{\delta_e} k_u & 0 & 0 & 0 \\ Z_{\delta_e} k_u & 0 & 0 & 0 \\ M_{\delta_e} k_u & 0 & 0 & 0 \\ 0 & 0 & 0 & 0 \end{bmatrix}$$

$$\left[A - \underline{B}\underline{k}^T\right] = \begin{bmatrix} X_u - X_{\delta_e} k_u & X_w & X_q & -g \\ Z_u - Z_{\delta_e} k_u & Z_w & U_o+Z_q & 0 \\ M_u - M_{\delta_e} k_u & M_w & M_q & 0 \\ 0 & 0 & 1 & 0 \end{bmatrix}$$

This is the new plant matrix from which the eigenvalues may be calculated and roots plotted. As k_u is varied, the roots move, and this movement is the critical factor in retaining, gaining, or improving stability. Plotting the roots also shows how variations in k affect the undamped natural frequencies and damping ratios and gives a rough idea of the sensitivity of the system.

In order that the roots of a given system subject to feedback could be quickly ascertained, a program named FDBK was written for the HP9830. Using as inputs the resolvent matrix of the open loop system, the control vector $\{b\}$, the coefficients of the open loop characteristic equation, and the type and magnitude (gain) of the feedback, the program computes $[A - \underline{b}\underline{k}^T]$, finds and prints the new roots, and calculates the resulting frequencies, periods, and damping ratios. See Figure 7-7 for a listing of FDBK. The REMark statements in the listing provide an explanation of the procedures used.

Figure 7-8 is an example of the program's output. In this case, the McRuer example was again used with no feedback applied; the results were in agreement with the example.

```
REM     PROGRAM  FDBK  08DEC76


10 REM  THIS PROGRAM TAKES A 4X4 RESOLVENT MATRIX FROM DATA
20 REM  STATEMENTS, CONSTRUCTS THE OPEN-LOOP TRANSFER FUNCTION,
30 REM  AND FINALLY, BY APPLYING FEEDBACK FROM ANY ONE OF THE
40 REM  FOUR PARAMETERS, CONSTRUCTS THE CLOSED-LOOP TRANSFER
50 REM  MATRIX; THE FEEDBACK MAY BE LINEAR, K/S, K*S, OR NOT
60 REM  APPLIED AT ALL.  ANY VALUE OF FEEDBACK GAIN MAY BE USED.
70 DIM A[4,4],B[4,4],C[4,4],D[4,4],E[4,4],F[4,4],M[4]
80 REM  INITIALIZE COEFFS TO ZERO
90 FOR I=1 TO 4
100 FOR J=1 TO 4
110 A[I,J]=B[I,J]=C[I,J]=D[I,J]=E[I,J]=F[I,J]=0
120 NEXT J
130 G[I]=H[I]=I[I]=J[I]=K[I]=M[I]=0
140 NEXT I
150 S=T=U=V=W=X=Y=X9=Y9=0
160 PRINT
170 WRITE (15,180)
180 FORMAT 45"*"
190 FORMAT 22" *"
200 PRINT
210 REM  ENTER RESOLVENT MATRIX IN INCREASING POWERS OF S
220 MAT READ B
230 DATA 0,0.7567,-46.046,-627.429
240 DATA 0,0.004061,3.0646,5.91353
250 DATA 0,0,0,-0.07797
260 DATA 0.00242,-0.00023,0.01401,0.1893
270 MAT READ C
280 DATA 19.4854,0.004448,-31.144,-135.5619
290 DATA -0.18365,0.02695,6.401856,3.075099
300 DATA 0.00242,-0.00023,0.01401,-0.0039928
310 DATA 0.000124,-0.0235,1.4397,19.52637
320 MAT READ D
330 DATA 4.21,0.0015,0,-32.2
340 DATA -0.0355,2.7897,660,0
350 DATA 0.000124,-0.0235,1.4397,0
360 DATA 0,0,1,4.2197
370 MAT READ E
380 DATA 1,0,0,0
390 DATA 0,1,0,0
400 DATA 0,0,1,0
410 DATA 0,0,0,1
420 REM  ENTER CONTROL VECTOR (B)
430 MAT READ M
440 DATA 0,-69.8,-26.009,0
450 REM  ENTER COEFFICIENTS OF ORIGINAL CHARACTERISTIC EQUATION
460 REM  IN INCREASING POWERS OF S
470 READ N0,N1,N2,N3,N4
480 DATA 0.07797,0.19329,19.52637,4.2197,1
490 DISP "IS FDBK 0, LINEAR, K*S, OR K/S";
500 INPUT L
```

Figure 7-7

```
510 DISP "WHICH PARAMETER DESIRED FOR FDBK";
520 INPUT Z
530 DISP "ENTER GAIN";
540 INPUT K
550 IF Z#1 THEN 570
560 PRINT "FEEDBACK PARAMATER IS HORIZ VELOCITY"
570 IF Z#2 THEN 590
580 PRINT "FEEDBACK PARAMETER IS VERT VELOCITY"
590 IF Z#3 THEN 610
600 PRINT "FEEDBACK PARAMETER IS PITCH RATE"
610 IF Z#4 THEN 630
620 PRINT "FEEDBACK PARAMETER IS PITCH ANGLE"
630 PRINT "GAIN = "K
640 REM  MULTIPLY PHI(S) TIMES B (CONTROL VECTOR) TO FORM
650 REM  NUMERATOR OF G0(S) (OPEN LOOP TX FN)
660 FOR I=1 TO 4
670 FOR J=1 TO 4
680 H[I]=B[I,J]*M[J]+H[I]
690 I[I]=C[I,J]*M[J]+I[I]
700 J[I]=D[I,J]*M[J]+J[I]
710 K[I]=E[I,J]*M[J]+K[I]
720 NEXT J
730 NEXT I
740 REM  DENOMINATOR OF G0(S) IS THE CHARACTERISTIC EQN (SEE
750 REM  LINES 440-470).  NUMERATOR OF CLOSED-LOOP TRANSFER
760 REM  MATRIX IS THE SAME AS THAT OF THE OPEN-LOOP MATRIX.
770 REM  THE DENOMINATOR IS OF THE FORM H TIMES SUM(B(J)*PHI
780 REM  (Z,J)) PLUS CHAR EQN OF PLANT MATRIX.
790 FOR J=1 TO 4
800 T=B[Z,J]*M[J]+T
810 U=C[Z,J]*M[J]+U
820 V=D[Z,J]*M[J]+V
830 W=E[Z,J]*M[J]+W
840 X=F[Z,J]*M[J]+X
850 NEXT J
860 IF L=0 THEN 990
870 IF L=1 THEN 1030
880 IF L=2 THEN 1110
890 IF L=3 THEN 900
900 PRINT "FEEDBACK MODE IS K/S"
910 PRINT
920 S=T*K
930 T=U*K
940 U=V*K
950 V=W*K
960 W=X*K
970 X=0
980 GOTO 1200
990 PRINT "FEEDBACK IS NOT APPLIED"
1000 PRINT
```

Figure 7-7 (continued)

```
1010 T=U=V=W=X=Y=0
1020 GOTO 1200
1030 PRINT "FEEDBACK MODE IS LINEAR"
1040 PRINT
1050 T=T*K
1060 U=U*K
1070 V=V*K
1080 W=W*K
1090 X=X*K
1100 GOTO 1200
1110 PRINT "FEEDBACK MODE IS K*S"
1120 PRINT
1130 Y=X*K
1140 X=W*K
1150 W=V*K
1160 V=U*K
1170 U=T*K
1180 T=0
1190 GOTO 1200
1200 REM  SUMMING TERMS IN DENOMINATOR OF CLOSED-LOOP TX MATRIX
1210 S=S
1220 T=T+N0
1230 U=U+N1
1240 V=V+N2
1250 W=W+N3
1260 X=X+N4
1270 Y=Y
1280 WRITE (15,190)
1290 PRINT
1300 PRINT "THE COEFFICIENTS OF THE NUMERATOR OF THE CLOSED-LOOP TX F
1310 PRINT "      (FROM S↑(0) TO S↑(3))"
1320 PRINT
1330 FOR I=1 TO 4
1340 PRINT "COEFFS OF G("I")"
1350 WRITE (15,1470)H[I],I[I],J[I],K[I]
1360 PRINT
1370 NEXT I
1380 WRITE (15,190)
1390 PRINT
1400 PRINT "COEFFICIENTS OF THE DENOMINATOR ARE:"
1410 PRINT "      (FROM S↑(-1) TO S↑(5))"
1420 PRINT
1430 WRITE (15,1470)S,T,U,V
1440 WRITE (15,1470)W,X,Y
1450 PRINT
1460 WRITE (15,190)
1470 FORMAT 4F15.7
1480 IF S=0 AND Y=0 THEN 1530
1490 GOTO 2140
1500 STOP
```

Figure 7-7 (continued)

```
1510 REM
1520 REM
1530 PRINT
1540 REM  THIS PROGRAM CALCULATES THE COMPLEX ROOTS OF A FOURTH
1550 REM  ORDER POLYNOMIAL USING THE MODIFIED BAIRSTOW METHOD.
1560 R9=1
1570 S9=1
1580 A4=X
1590 A3=W
1600 A2=V
1610 A1=U
1620 A0=T
1630 B4=A4
1640 B3=A3+R9*B4
1650 B2=A2+R9*B3+S9*B4
1660 B1=A1+R9*B2+S9*B3
1670 B0=A0+S9*B2
1680 IF ABS(B0)>1E-02 THEN 1700
1690 IF ABS(B1)<1E-02 THEN 1730
1700 S9=-A0/B2
1710 R9=-(A1+S9*B3)/B2
1720 GOTO 1630
1730 IF (R9↑2+4*S9)<0 THEN 1780
1740 X1=(R9+SQR(R9↑2+4*S9))/2
1750 X2=(R9-SQR(R9↑2+4*S9))/2
1760 X5=X6=0
1770 GOTO 1810
1780 X1=X2=R9/2
1790 X5=SQR(ABS(R9↑2+4*S9))/2
1800 X6=-X5
1810 IF (B3↑2-4*B4*B2)<0 THEN 1860
1820 X3=(-B3+SQR(B3↑2-4*B4*B2))/2
1830 X4=(-B3-SQR(B3↑2-4*B4*B2))/2
1840 X7=X8=0
1850 GOTO 1890
1860 X3=X4=-B3/2
1870 X7=SQR(ABS(B3↑2-4*B4*B2))/2
1880 X8=-X7
1890 PRINT "THE EIGENVALUES ARE"
1900 PRINT
1910 PRINT "      REAL PART       IMAG PART"
1920 WRITE (15,1990)X1,X5
1930 WRITE (15,1990)X2,X6
1940 WRITE (15,1990)X3,X7
1950 WRITE (15,1990)X4,X8
1960 PRINT
1970 PRINT
1980 WRITE (15,190)
1990 FORMAT 3X,F10.5,5X,F10.5
2000 FIXED 4
```

Figure 7-7 (continued)

```
2010 PRINT
2020 PRINT "MODE I FREQUENCY IS "SQR(X1↑2+X5↑2)"RADIANS PER SECOND"
2030 PRINT "           PERIOD IS "2*PI/SQR(X1↑2+X5↑2)"SECONDS"
2040 PRINT "    DAMPING RATIO IS "-X1/SQR(X1↑2+X5↑2)
2050 PRINT
2060 PRINT "MODE II FREQUENCY IS "SQR(X3↑2+X7↑2)"RADIANS PER SECOND"
2070 PRINT "           PERIOD IS "2*PI/SQR(X3↑2+X7↑2)"SECONDS"
2080 PRINT "    DAMPING RATIO IS "-X3/SQR(X3↑2+X7↑2)
2090 PRINT
2100 FORMAT 5F12.5
2110 X9=X
2120 Y9=Y
2130 STOP
```

Figure 7-7 (continued)

```
**********************************************

FEEDBACK PARAMETER IS PITCH RATE
GAIN =  0
FEEDBACK IS NOT APPLIED

 * * * * * * * * * * * * * * * * * * * * * *

THE COEFFICIENTS OF THE NUMERATOR OF THE CLOSED-LOOP TF FN ARE:
     (FROM S↑(0) TO S↑(3))

COEFFS OF G( 1     )
   1144.7927540    809.7138256     -0.1116800      0.0000000

COEFFS OF G( 2     )
    -79.9906392   -168.3869827 -17360.6610600    -69.8000000

COEFFS OF G( 3     )
      0.0000000     -0.3483321    -35.8048573    -26.0090000

COEFFS (  ,  4     )
     -0.          -35.8048573    -26.0090000      0.0000000

 * * * * * * * * * * * * * * * * * * * * * *

COEFFICIENTS OF THE DENOMINATOR ARE:
     (FROM S↑(0) TO S↑(5))

      0.0000000      0.0779700      0.1932900     19.5263700
      4.2197906      1.0000000      0.0000000

  * * * * *  * * * * * * * * * * * * * * * * *

THE EIGENVALUES ARE

     REAL PART       IMAG PART
     -0.03455         0.06308
     -0.03455        -0.06308
     -2.10532         3.87967
     -2.10532        -3.87967


 * * * * * * * * * * * * * * * * * * * * * *

MODE I FREQUENCY IS  0.0632  RADIANS PER SECOND
          PERIOD IS  99.3505    SECONDS
   DAMPING RATIO IS  0.0716

MODE II FREQUENCY IS  4.4141  RADIANS PER SECOND
           PERIOD IS  1.4234  SECONDS
    DAMPING RATIO IS  0.4770
```

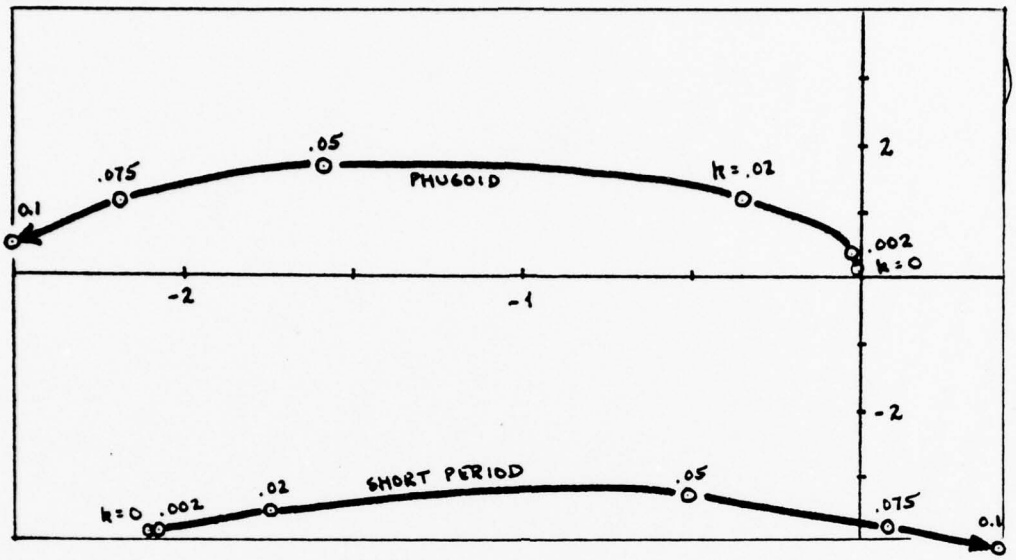
Figure 7-8

Figure 7-9 (a,b,c,d) shows how the roots vary as the feedback gain is varied and as different parameters are fed back. Complex conjugates are not shown where their omission would be confusing. These results are tabulated for more careful scrutiny in Table 7-4.

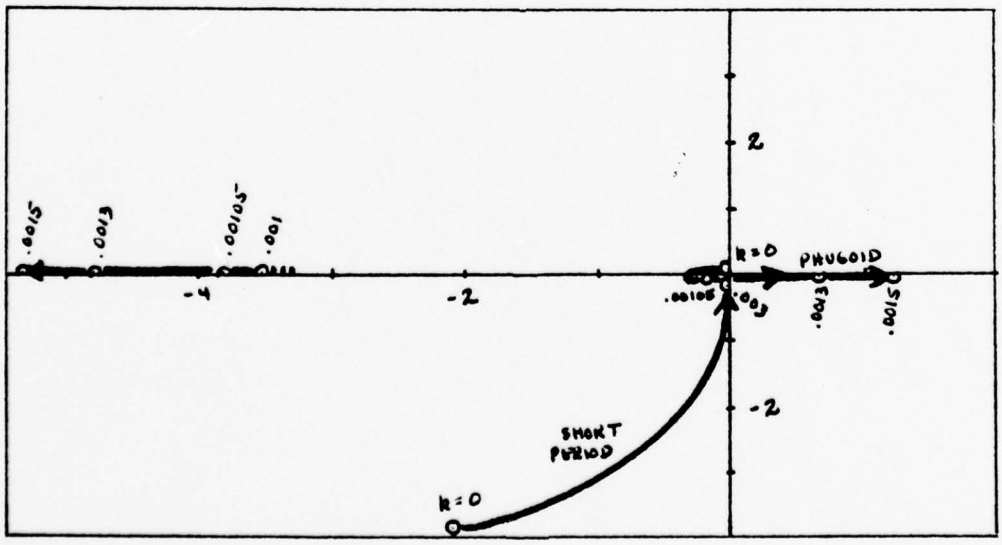
Figure 7-10(a) depicts the time history of the McRuer F-89 aircraft subject to an initial condition of vertical velocity = 10 fps. No control inputs are postulated. The parameter chosen to display system response is pitch angle; it was chosen because of its good definition of short period and phugoid motion.

Feedback of horizontal velocity error can substantially increase phugoid damping before the short period mode is much affected. However, a further increase in the gain of this error signal will drive the short period to instability. The sensitivity of the system in this regime is shown by Figure 7-10(b); here, with $k_u = 0.02$, the short period motion is less than critically damped and oscillates several times before dying out. The damping effect on the phugoid is readily apparent.

Feedback of vertical velocity (or angle of attack),

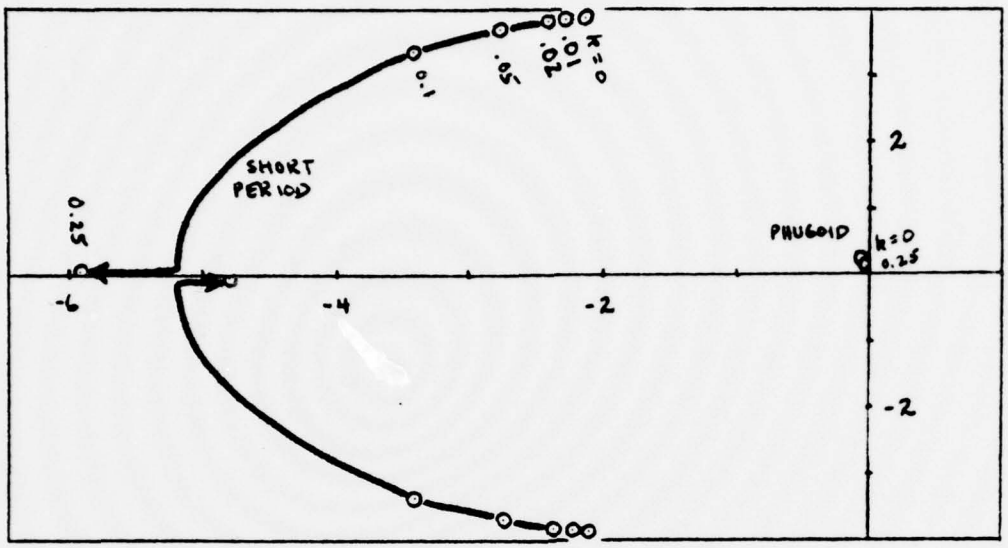


(a) k_u feedback

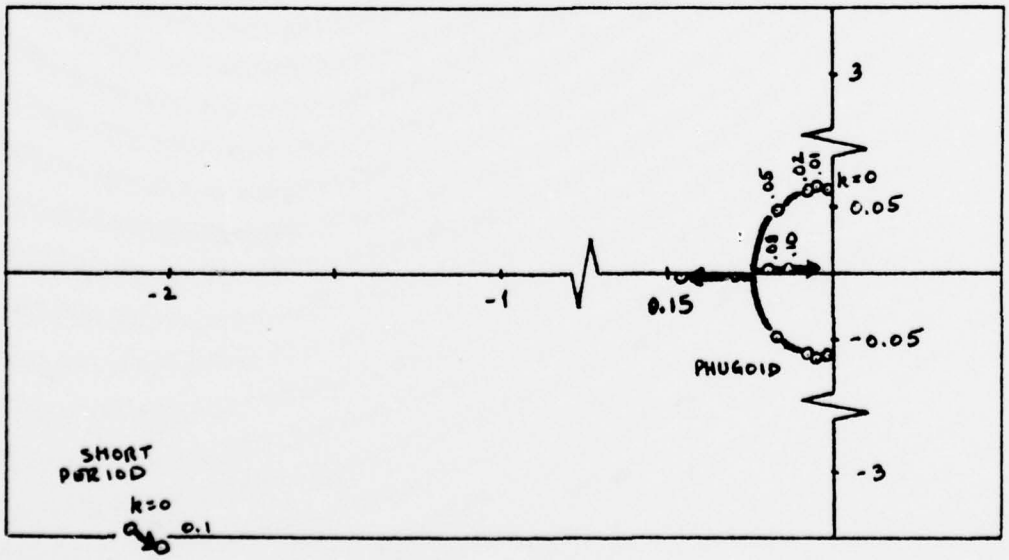


(b) k_w feedback

Figure 7-9



(c) k_q feedback



(d) k_θ feedback

Figure 7-9 (continued)

Feedback parameter: HORIZONTAL VELOCITY (u)

gain	0	0.002	0.02	0.05	0.075	0.1
T(sp)	1.42	1.44	1.60	1.89	1.67	1.52
ζ(sp)	0.477	0.475	0.444	0.154	-0.02	-0.10
T(ph)	99.35	17.86	5.16	2.76	2.55	2.43
ζ(ph)	0.072	0.097	0.297	0.702	0.888	0.980

Feedback parameter: VERTICAL VELOCITY (w)

gain	0	0.001	.00105	.0013	.0015	.003
T(sp)	1.42	1.77	1.65	1.32	1.18	0.78
ζ(sp)	0.477	1	1	1	1	1
T(ph)	99.35	165.17	75.04	68.11	78.43	89.15
ζ(ph)	0.072	1	1	0.108	0.082	0.072
T_3	-	254.69	112.48	-	-	-
ζ_3	-	-1	-1	-	-	-
T_4	-	10.54	20.14	9.56	5.10	1.55
ζ_4		1	1	-1	-1	-1

Feedback parameter: PITCH RATE (q)

gain	0	0.01	0.02	0.05	0.1	0.25
T(sp)	1.42	1.41	1.40	1.36	1.31	1.31
ζ(sp)	0.477	0.502	0.526	0.598	0.710	1
T(ph)	99.35	100.25	101.14	103.75	107.97	119.69
ζ(ph)	0.072	0.072	0.073	0.074	0.076	0.084
T_3	-	-	-	-	-	1.06
ζ_3	-	-	-	-	-	1

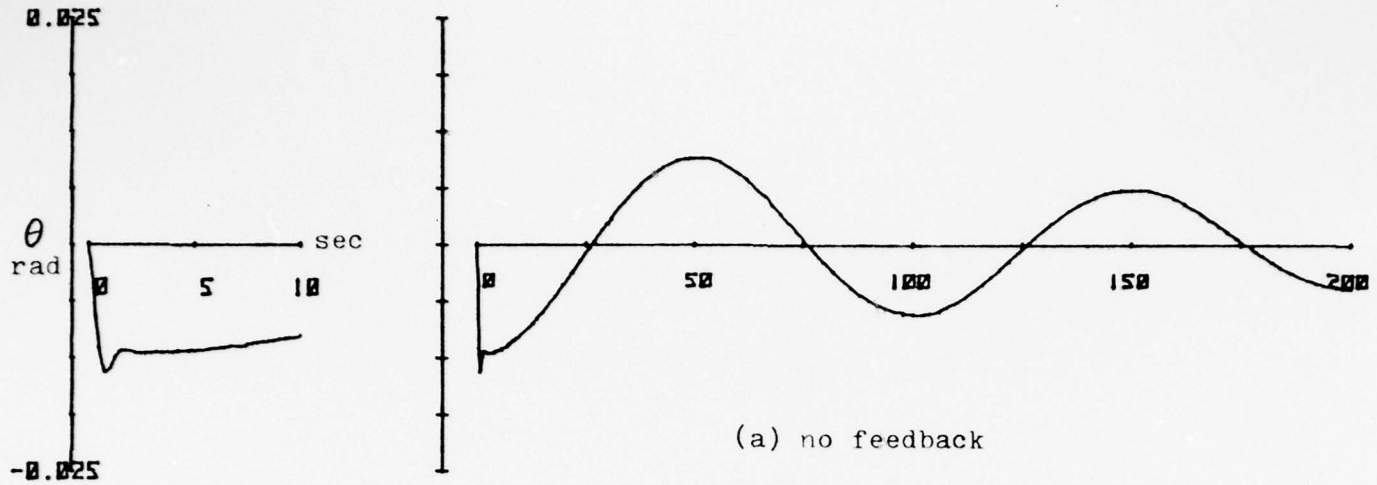
Feedback parameter: PITCH ANGLE (θ)

gain	0	0.01	0.02	0.05	0.08	0.1
T(sp)	1.42	1.42	1.41	1.39	1.37	1.36
ζ(sp)	0.477	0.473	0.469	0.456	0.445	0.437
T(ph)	99.35	97.71	96.18	92.16	73.18	45.98
ζ(ph)	0.072	0.211	0.343	0.702	1	1
T_3	-	-	-	-	107.12	163.04
ζ_3	-	-	-	-	1	1

Table 7-4

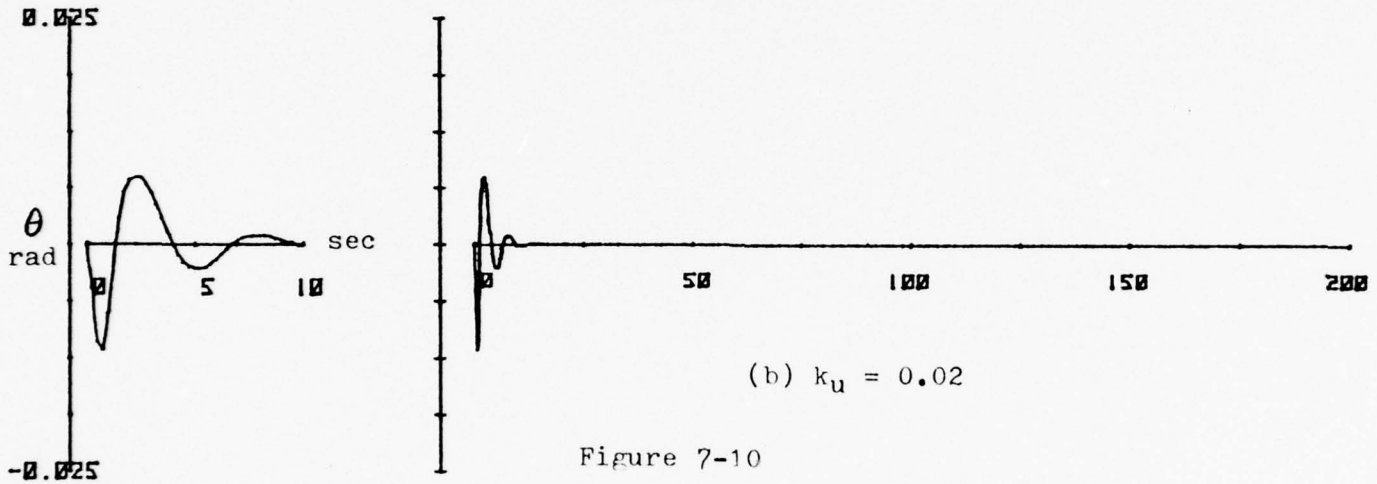
if the gain is small, will increase the frequency and damping ratio of the short period mode. Since the angle of attack signal is 1/660th of the vertical velocity signal, it would be a better parameter from which to obtain an error signal. Increasing the gain of this feedback will cause a third mode to go unstable; however, its period is so great that no problem would be anticipated in controlling it manually. A further increase in gain will cause a fourth mode of significantly shorter period to go unstable. Since its period decreases rapidly with an increase in gain, it may be assumed that values of gain in this region are to be avoided. Figure 7-10 (c) shows a time history of pitch angle versus time with $k_w = 0.0001$ and $w_o = 10$fps.

Feedback of pitch rate has almost no effect upon the phugoid motion but appreciably increases the short period damping. This very desirable feature makes this parameter useful in speed, altitude, and attitude hold modes for auto-pilots. Figure 7-10(d) shows a time history of pitch angle against time with $k_q = 0.1$ and $w_o = 10$fps.



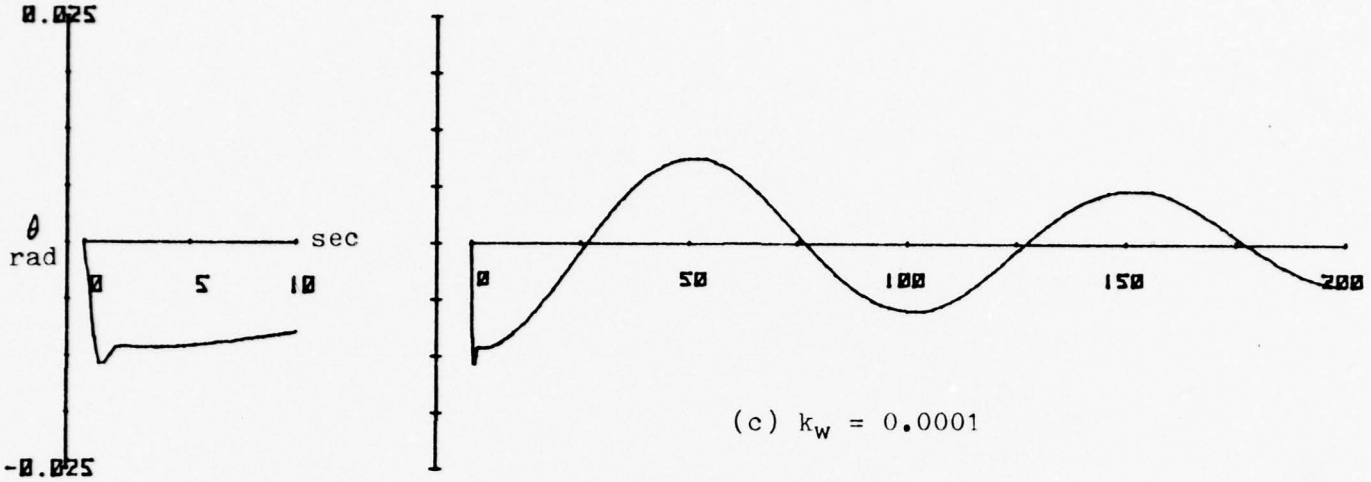
(a) no feedback

short period phugoid



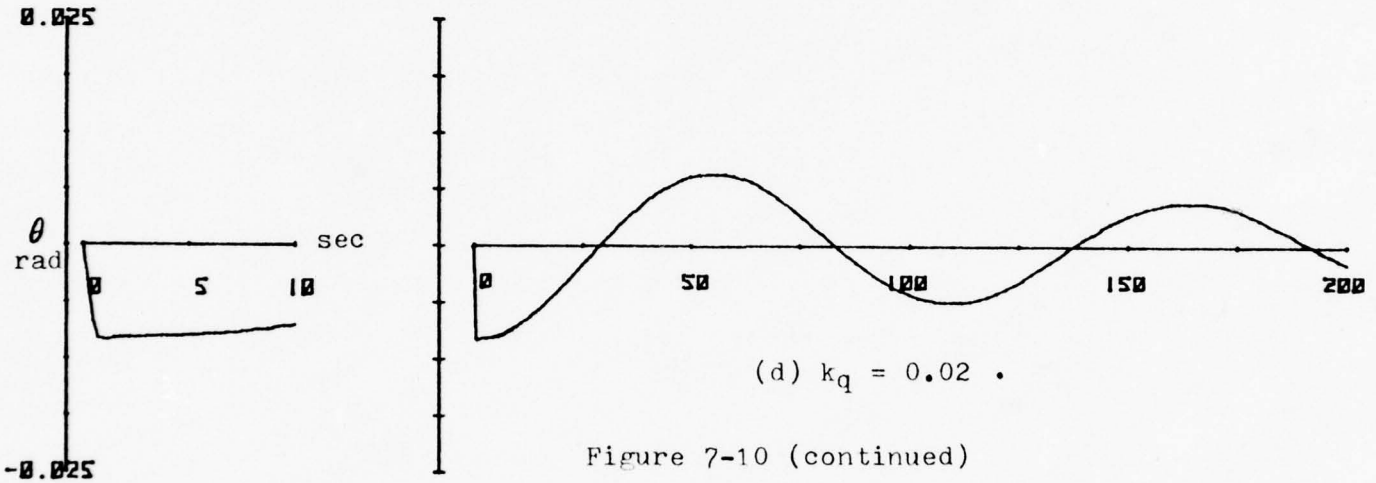
(b) $k_u = 0.02$

Figure 7-10



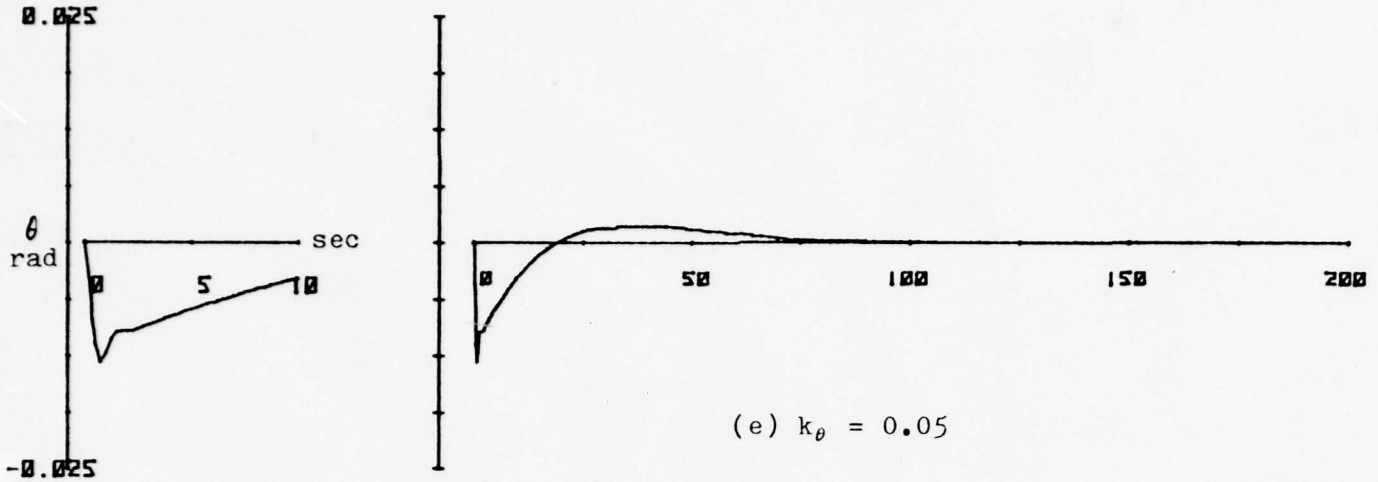
(c) $k_w = 0.0001$

short period phugoid



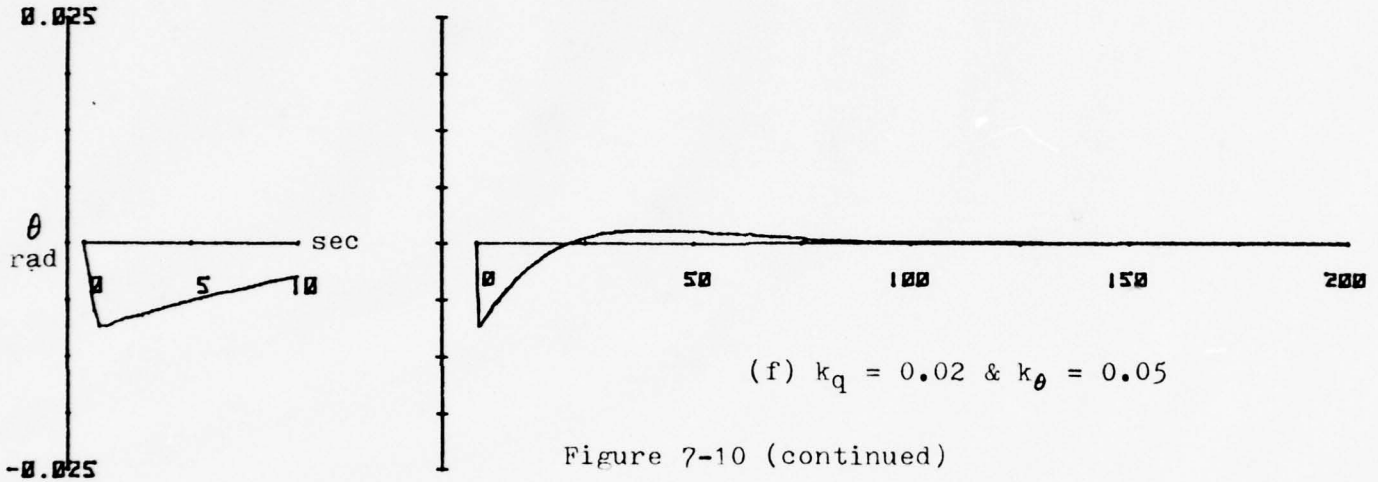
(d) $k_q = 0.02$.

Figure 7-10 (continued)



short period phugoid

(e) $k_\theta = 0.05$



(f) $k_q = 0.02$ & $k_\theta = 0.05$

Figure 7-10 (continued)

Pitch angle feedback is also an excellent method of improving longitudinal response. In this case, the phugoid damping is significantly increased at the expense of short period damping. If short period damping is marginal to begin with, use of this feedback may cause an instability in that mode. Figure 7-10(e) shows the effects of $k_\theta = 0.05$ on the time history of the pitch angle perturbations with $w_o = 10$fps.

Use of both pitch rate and pitch angle feedback together should provide an ideal system with maximum increase in damping ratios and minimum increase in frequency. Using the same feedback gains as above, the response is shown in Figure 7-10(f).

The equations of state for each of the above examples were obtained by entering BASMAT with the modified plant matrix $\left[A - \underline{b}\underline{k}^T\right]$ and multiplying the resulting state transition matrix by the initial condition vector in accordance with the equation

$$\dot{\underline{x}}(t) = \Phi(t)\underline{x}(0) \quad \text{where} \quad \underline{x}(0) = \begin{Bmatrix} 0 \\ 10 \\ 0 \\ 0 \end{Bmatrix}.$$

One further conclusion was reached in this treatment

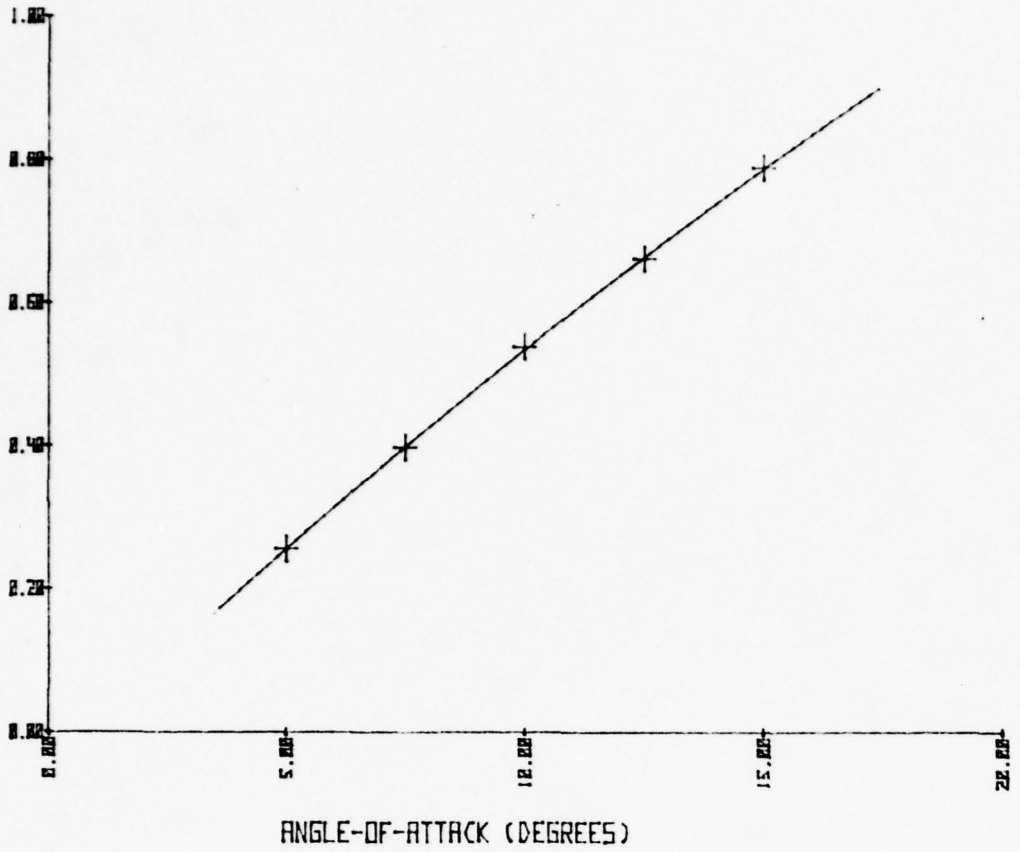
of feedback: the two parameters which are most affected in phugoid motion, forward velocity and pitch angle, were the two whose feedback most affected that motion. Their effect on the short period was minimal. Likewise, the two parameters which are relatively constant in the phugoid but which vary considerably in the short period, angle of attack and pitch rate, had little effect on the phugoid but significantly damped the short period.

VIII. THE ORBITER

The Aerodynamic Design Data Book was obtained from NASA's Lyndon B. Johnson Space Center in order to obtain data necessary to calculate the stability derivatives and to acquire the block diagram of the longitudinal control system (automatic mode) of the space shuttle orbiter.

The environment chosen for the study was the area at which the Mach number was 1.05. This area was chosen because the aerodynamics are undergoing rapid change here, and it would provide a testing challenge for programming and solution.

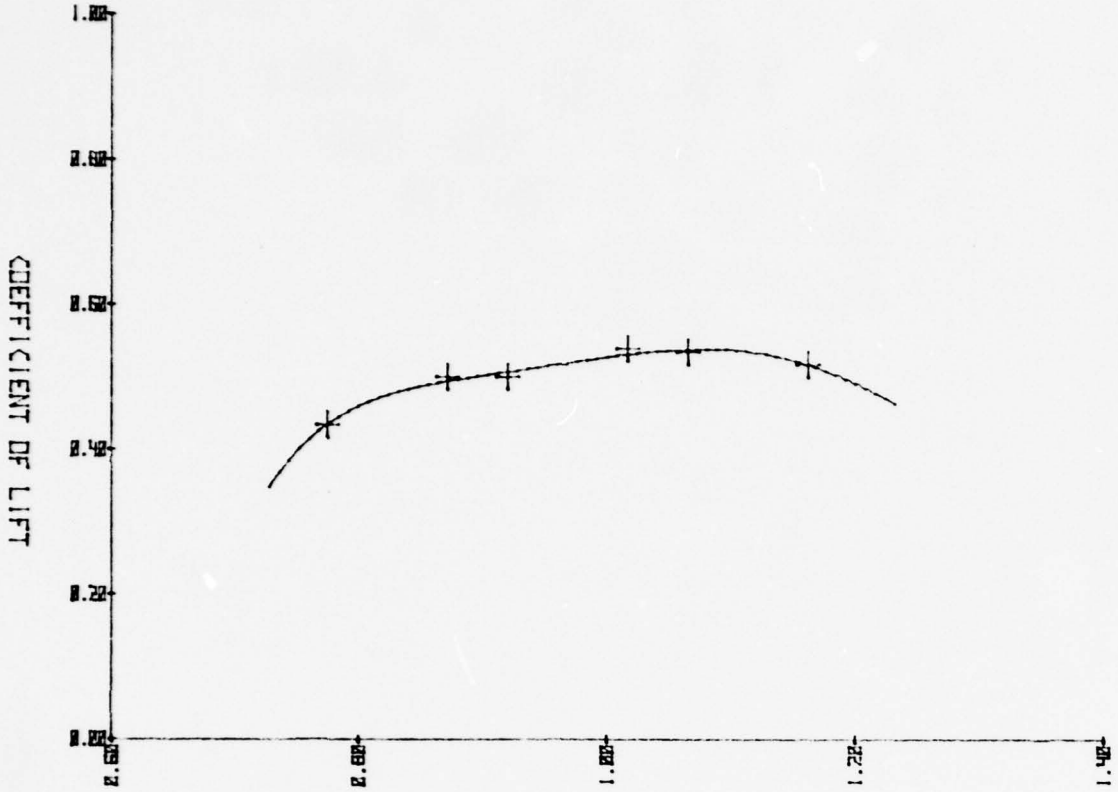
The stability derivatives were found by plotting the force and moment coefficients with respect to velocity (U) and angle of attack and then measuring the slope; see Figures 8-1 through 8-6. By choosing points close together where the slope was rapidly changing, piecewise linearity could be assumed between them. The results are shown in Table 8-1. The derivatives with respect to δ_e were also taken from the publication; the graph of ΔC_{D_e} -vs- δ_e is shown, as an example, in Figure 8-7. The δ_e derivatives are listed in Table 8-2.



AOA (DEG)	C_L
5.0	0.256
7.5	0.397
10.0	0.538
12.5	0.661
15.0	0.788

Figure 8-1

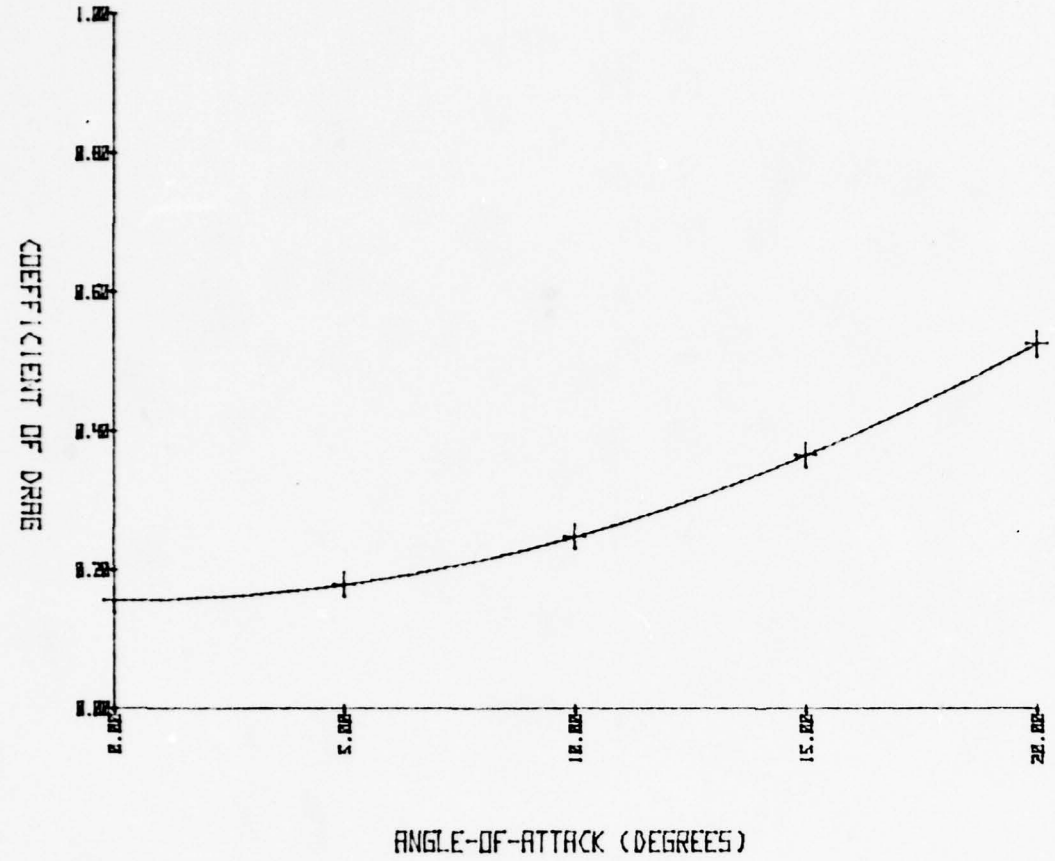
AOA -VS- COEFF OF LIFT (MACH=1.05)



MACH	VEL(FPS)	C_L
0.80	774.8	0.434
0.90	871.6	0.500
0.95	920.0	0.500
1.05	1016.9	0.539
1.10	1065.3	0.534
1.20	1162.2	0.517

Figure 8-2

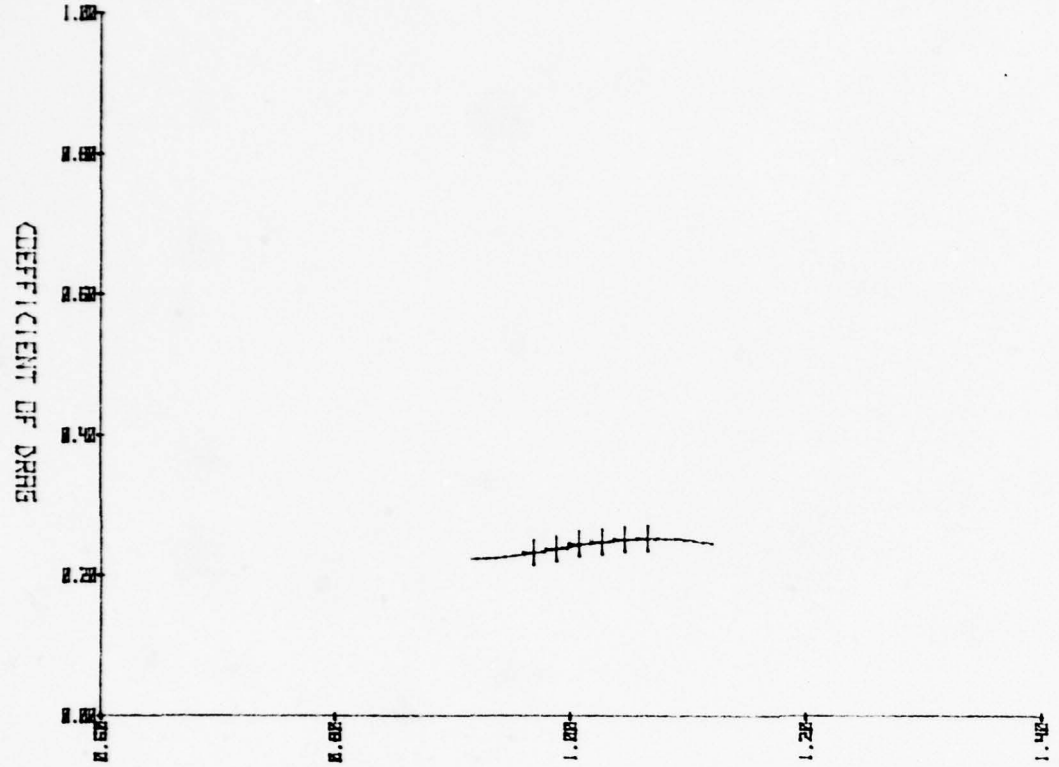
VEL -VS- COEFF OF LIFT (AOA=10 DEG)



AOA(DEG)	C_D
0	0.156
5	0.179
10	0.248
15	0.365
20	0.525

Figure 8-3

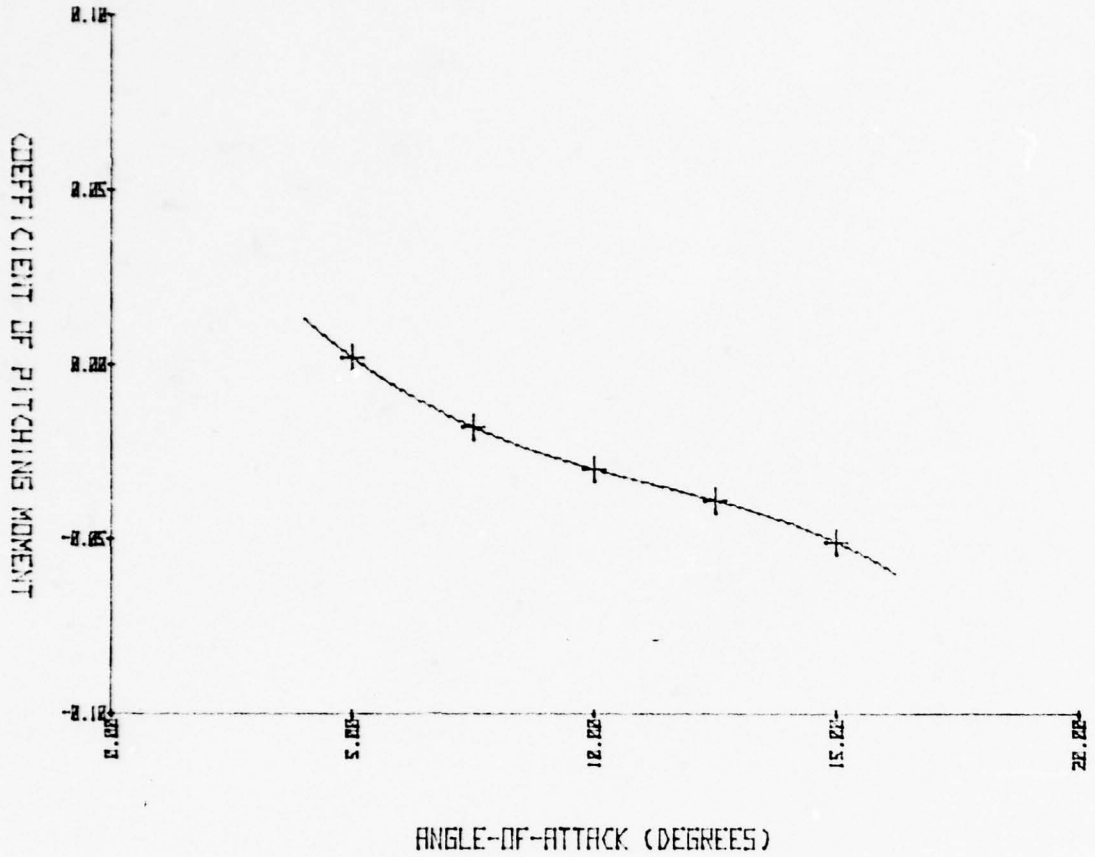
AOA -VS- COEFF OF DRAG (MACH=1.05)



MACH	VEL(FPS)	C_D
1.00	968.5	0.233
1.02	987.8	0.238
1.04	1007.2	0.245
1.06	1026.6	0.248
1.08	1045.9	0.252
1.10	1065.3	0.253

Figure 8-4

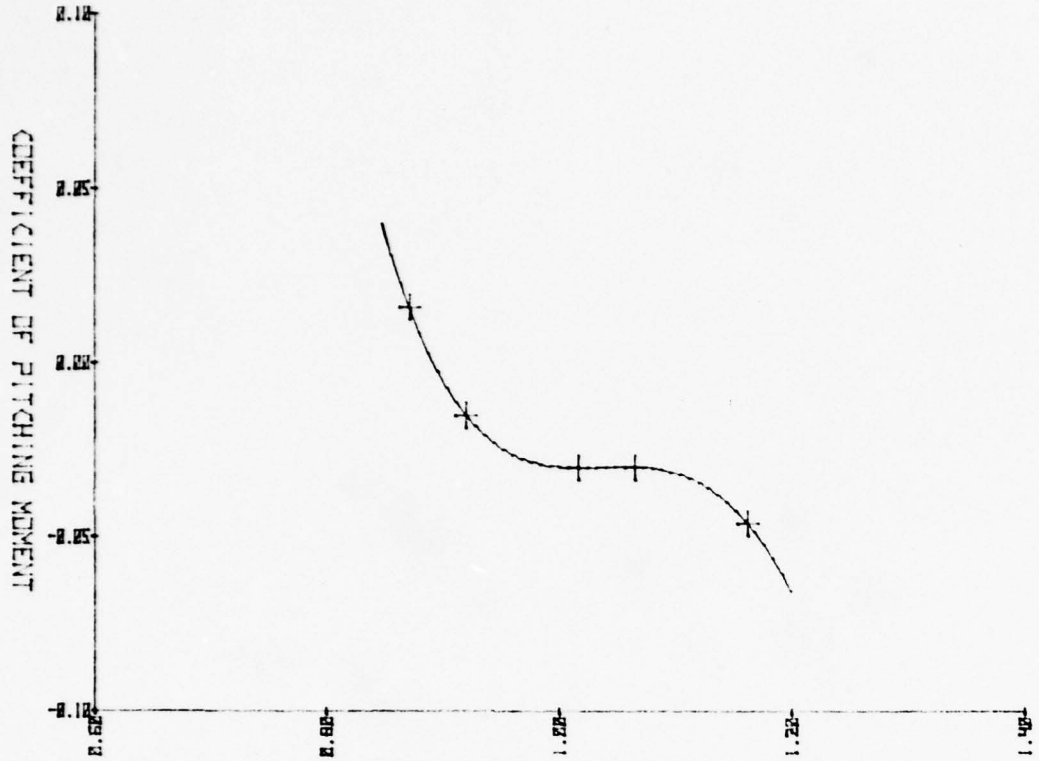
VEL. -VS- COEFF OF DRAG (ALPH=10 DEG)



AOA(DEG)	C_M
5.0	+0.002
7.5	-0.018
10.0	-0.030
12.5	-0.039
15.0	-0.051

Figure 8-5

AOA -VS- PITCHING MOMENT COEFF (MACH=1.05)



MACH	VEL(FPS)	C_M
0.90	871.6	+0.016
0.95	920.0	-0.015
1.05	1016.9	-0.030
1.10	1065.3	-0.030
1.20	1162.2	-0.046

Figure 8-6

VEL -VS- PITCHING MOMENT COEFF (AOA=10DEG)

AOA (deg)	C_{L_α}
5	0.0564
7.5	0.0564
10	0.0528
12.5	0.0500
15	0.0500

U (fps)	C_{L_u}
920.1	0.0
1016.9	7.23E-4
1065.3	-1.24E-4
1162.2	-1.75E-4

AOA (deg)	C_{D_α}
5	0.0046
10	0.0138
15	0.0234
20	0.0320

U (fps)	C_{D_u}
968.5	5.79E-4
1016.9	3.10E-4
1065.3	1.24E-4
1113.7	-2.10E-5

AOA (deg)	C_{M_α}
7.5	-0.0080
10	-0.0048
12.5	-0.0036
15	-0.0048

U (fps)	C_{M_u}
920.1	-6.40E-4
1016.9	-1.55E-4
1065.3	0.0
1162.2	-1.65E-4

Table 8-1

δ_e	$C_{L_{\delta_e}}$
-20°	0.0057
-17.5	0.0072
-15	0.0076
-10	0.0086
0	0.0108
20	0.0142

δ_e	$C_{D_{\delta_e}}$
-25°	-0.0018
-20	-0.0014
-15	-0.0012
-10	0.0024
-5	0.0050
0	0.0080

δ_e	$C_{M_{\delta_e}}$
-30°	-0.0010
-25	-0.0016
-20	-0.0026
-15	-0.0042
-10	-0.0058
0	-0.0067
20	-0.0089

Table 8-2

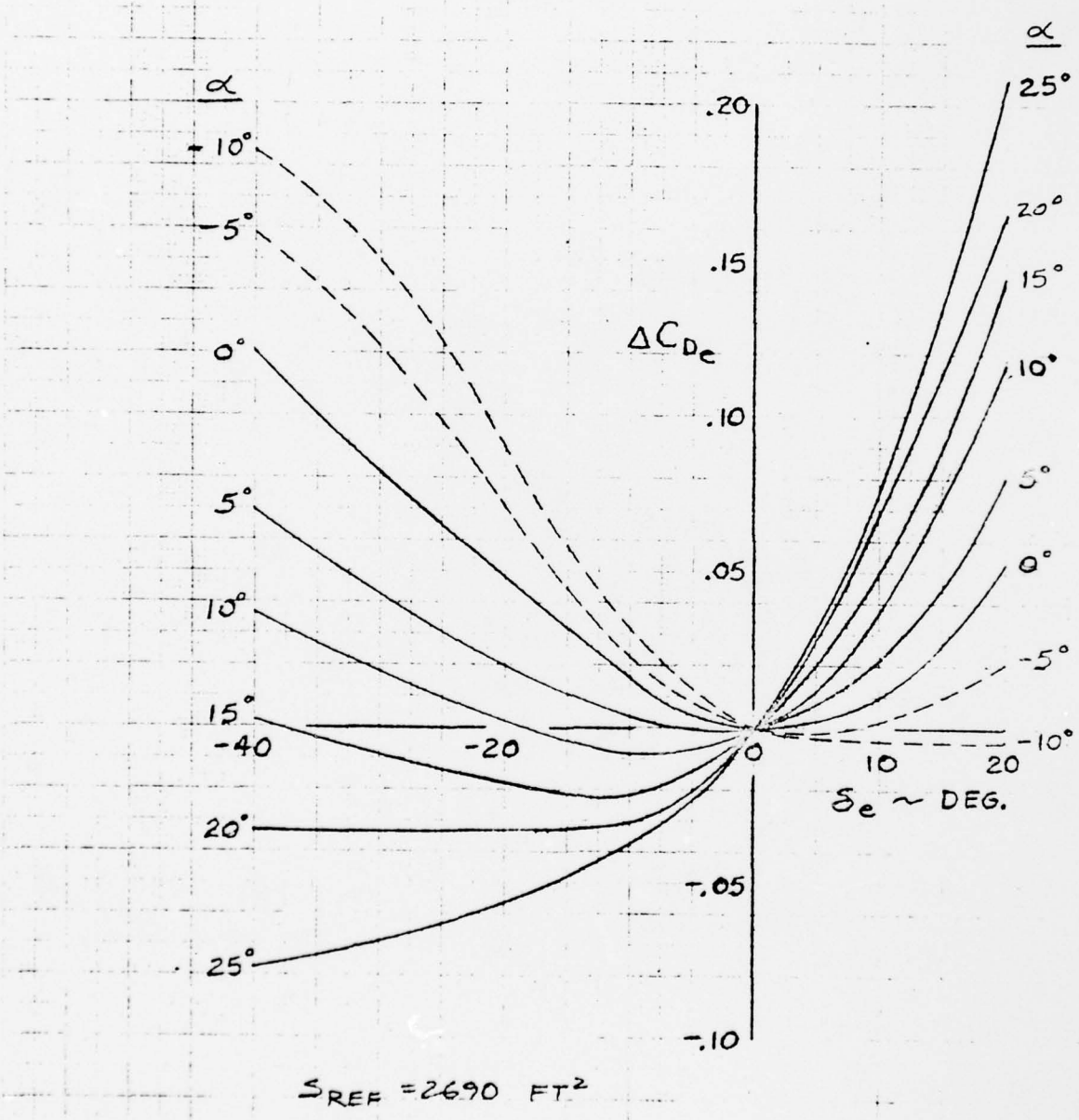


FIG 3.5-1L ELEVON EFFECTIVENESS DRAG INCREMENT ($M_\infty = 1.05$)

Figure 8-7

In cases where U was the independent variable, angle of attack was assumed to be 10°; where angle of attack was the independent variable, U was 1016.9 fps (Mach = 1.05). The δ_e derivatives were based upon an angle of attack of 10°.

The point in the design reentry trajectory where the Mach number is 1.05 occurs at approximately 62000 feet in altitude. Also, at this point, the load factor n_z = 1.09, and the air density ρ = 2.0325E-4 slugs/ft^3.

Other constants which are required for computations are:

wing area = S = 2690 ft^2

wing M.A.C. = $\bar{c}$ = 39.56 ft

moment of inertia = I_y = 5.7830E+6 slug-ft^2

gravity = g = 32.073 ft/sec^2 (corrected for altitude and latitude)

pitch angle = Θ = 9.0 deg

mass = m = 5839 slugs

For the condition of Mach = 1.05 and angle of attack = 10°, the stability derivatives take on the following values:

$$X_u = \frac{\rho U S}{m}\left(-\frac{U}{2}C_{D_u} - C_D\right) = -0.04410$$

$$X_w = \frac{\rho U S}{2m}\left(C_L - C_{D_\alpha}\right) = 0.02849$$

$$X_q = X_{\dot{w}} = \emptyset$$

$$X_{\delta_e} = -\frac{\rho U^2 S}{2m} C_{D_{\delta e}} = -0.44219$$

$$Z_u = \frac{\rho U S}{m}\left(-\frac{U}{2} C_{L_u} - C_L\right) = -0.09845$$

$$Z_w = \frac{\rho U S}{2m}\left(-C_{L_\alpha} - C_D\right) = -0.01635$$

$$Z_q = Z_{\dot{w}} = \emptyset$$

$$Z_{\delta_e} = -\frac{\rho U^2 S}{2m} C_{L_{\delta e}} = -0.78489$$

$$M_u = \frac{\rho U S \bar{c}}{I_y}\left(\frac{U}{2} C_{M_u} + C_M\right) = -4.725\,E\text{-}4$$

$$M_w = \frac{\rho U S \bar{c}}{2 I_y} C_{M_\alpha} = -1.042\,E\text{-}5$$

$$M_q = \frac{\rho U S \bar{c}^2}{4 I_y} C_{M_q} = -0.05583$$

$$M_{\dot{w}} = \frac{\rho S \bar{c}^2}{4 I_y} C_{M_{\dot{\alpha}}} = -4.223\,E\text{-}5$$

$$M_{\delta_e} = \frac{\rho U^2 S \bar{c}}{2 I_y} C_{M_{\delta e}} = -0.01479$$

Entering these values into the plant matrix (see page 54) yields

$$[A] = \begin{bmatrix} -0.04410 & 0.02849 & 0.0 & -32.073 \\ -0.09845 & -0.01635 & 1016.9 & 0.0 \\ -4.683E\text{-}4 & -9.730E\text{-}6 & -0.09877 & 0.0 \\ 0.0 & 0.0 & 1.0 & 0.0 \end{bmatrix}$$

$$\{B\} = \begin{Bmatrix} -0.44219 \\ -0.78489 \\ -0.01476 \\ 0.0 \end{Bmatrix}$$

Entering BASMAT with [A] yields the results shown in Figure 8-8. Using the GRAPH program developed in Chapter VI (see page 71), the time response to an initial condition of w_o = 10 fps was plotted. The results are shown in Figure 8-9. The vehicle is clearly unstable in the open-loop configuration.

A look at the eigenvalues printed out in Figure 8-8 showed that the phugoid had disappeared, being replaced by two real roots, one of which was positive. Although the negative (stable) root was larger, the instability became dominant very quickly.

The eigenvalues were not widely separated, having

```
BASIC MATRIX PROGRAM
      PROBLEM IDENTIFICATION-      ORBITER MACH = 1.15

**************************************************

      THE A MATRIX

      -4.1099999E-02        2.8429999E-02        0.0                  -5.2072998E 01
      -9.8449945E-02       -1.6349997E-02        1.9148999E 03         0.0
      -4.6829996E-04       -9.7299999E-06       -9.0769963E-02         0.0
       0.0                  0.0                  1.0000000E 00         0.0

      THE DETERMINANT OF THE MATRIX

      -2.1485008E-04

      THE INVERSE OF THE MATRIX

      -1.3113022E-06        1.4524037E 01       -2.8477419E 03        -1.7181243E 03
       1.5258789E-05       -6.9998999E 01        1.4000014E 04         7.2541188E 04
       2.3283064E-10        9.3132257E-10       -1.7881393E-07         9.9999988E-01
      -3.1178858E-02       -6.3959718E-02        1.0128556E 01         6.0139084E 01

**************************************************

      THE MATRIX COEFFICIENTS OF THE NUMERATOR OF THE RESOLVENT MATRIX

      THE MATRIX COEFFICIENT OF S**3

       1.0000000E 00        0.0                  0.0                   0.0
       0.0                  1.0000000E 00        0.0                   0.0
       0.0                  0.0                  1.0000000E 00         0.0
       0.0                  0.0                  0.0                   1.0000000E 00
```

Figure 8-8

THE MATRIX COEFFICIENT OF S**2

1.1511905E-01	2.8419997E-02	0.0	-3.2672950E 01
-9.8445945E-02	1.3980993E-01	1.0158999E 03	0.0
-4.6829996E-04	-9.7299999E-06	5.7440000E-02	0.0
0.0	0.0	1.0000000E 00	1.5021990E-01

THE MATRIX COEFFICIENT OF S**1

1.1509518E-02	2.8139520E-03	-3.1015720E 01	-5.0922417E 00
-4.8593801E-01	4.0594414E-03	4.1784580E 01	3.1575842E 00
-6.6967704E-06	-1.3741708E-05	3.4700172E-02	1.5019782E-02
-4.6829996E-04	-9.7299999E-06	5.7440000E-02	1.5045584E-02

THE MATRIX COEFFICIENT OF S**0

0.0	3.1207013E-04	-5.2455508E-01	-3.0013830E-01
1.4961161E-08	-1.5019780E-02	3.1575785E 00	1.5545468E 01
7.9580786E-13	2.7284841E-12	-2.5265064E-11	2.1484983E-04
-6.6967704E-06	-1.3741708E-05	3.4700172E-02	1.4317401E-02

****

THE CHARACTERISTIC POLYNOMIAL - IN ASCENDING POWERS OF S

-2.1425308E-04	-7.0233113E-04	1.5845554E-02	1.5021990E-01	1.0000000E 00

****

THE EIGENVALUES OF THE A MATRIX

REAL PART	IMAGINARY PART
3.3441827E-02	0.0
-6.8664648E-02	-1.4253621E-01
-6.8664648E-02	1.4253621E-01
-1.0205231E-01	0.0

Figure 8-8 (continued)

```
**************************************************

     THE ELEMENTS OF THE STATE TRANSITION MATRIX

     THE MATRIX COEFFICIENT OF EXP( 9.3011835E-03)T

      2.9041117E-01      9.2157185E-02     -9.0731201E 01     -1.1135965E 02
     -5.1010100E 00     -1.6187325E 00      1.6998700E 03      1.9560210E 03
     -4.7340705E-04     -1.5024759E-04      1.5771912E-01      1.8155420E-01
     -5.6006531E-03     -1.7763208E-03      1.8547401E 00      2.1700181E 00

     THE MATRIX COEFFICIENT OF EXP(-6.8004405E-02)T*COS( 1.4253635E-01)T

      4.4712102E-01     -1.1317804E-02      4.5239740E 01      2.9353973E 01
      1.7509850E 01     -1.1415091E 00      6.9015479E 02      1.8585322E 03
     -5.8808224E-04      4.7726433E-04      6.3403190E-01     -5.1322830E-01
      1.6001858E-02     -1.3887550E-03      1.8338595E-01      2.0004153E 00

     THE MATRIX COEFFICIENT OF EXP(-6.8004405E-02)T*SIN( 1.4253635E-01)T

     -5.4532409E-02      8.2133114E-02      1.1502140E 02     -8.0481500E 01
      1.3415012E 00      2.9938374E 00      4.7473477E 03     -3.0004565E 03
     -2.5261822E-03      1.4120014E-05     -3.3033371E-01     -1.1669591E-01
      3.5700808E-03      2.0795221E-03      4.5172024E 00     -2.0089725E 00

     THE MATRIX COEFFICIENT OF EXP(-1.0215235E-01)T

      2.0240972E-01.    -8.0339034E-02      5.1402170E 01      8.2005900E 01
     -1.2208820E 01      3.7003045E 00     -2.3913224E 03     -3.8145552E 03
      1.0015524E-03     -3.2695709E-04      2.0325363E-01      3.3187404E-01
     -1.0341210E-02      3.1350271E-03     -2.0[illegible]7E 00     -3.2510371E 00
CP
```

Figure 8-8 (continued)

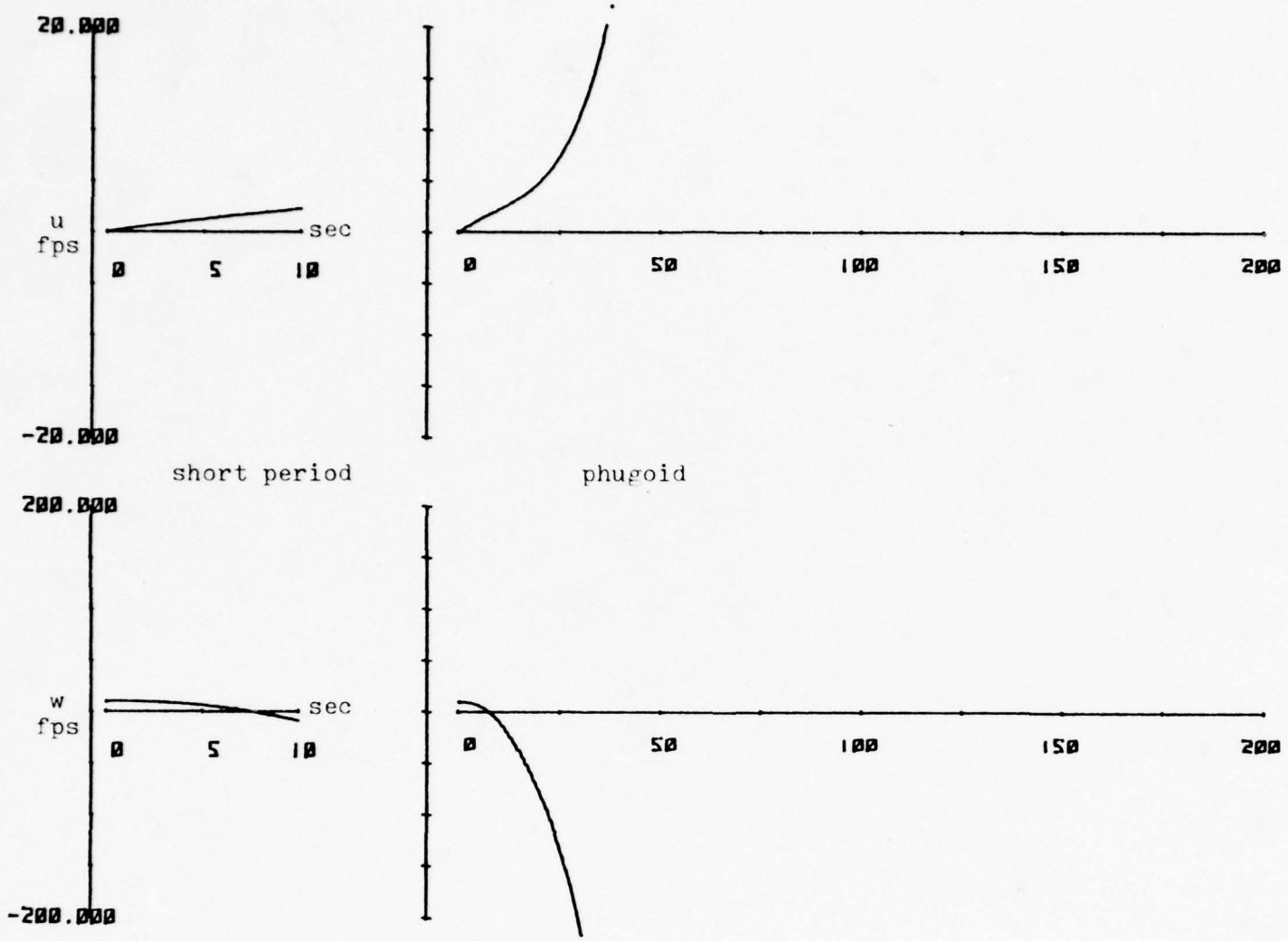

20.000
u
fps
sec
0
5
10
-20.000
0
50
100
150
200
short period
phugoid
200.000
w
fps
sec
0
5
10
-200.000
0
50
100
150
200

Figure 8-9

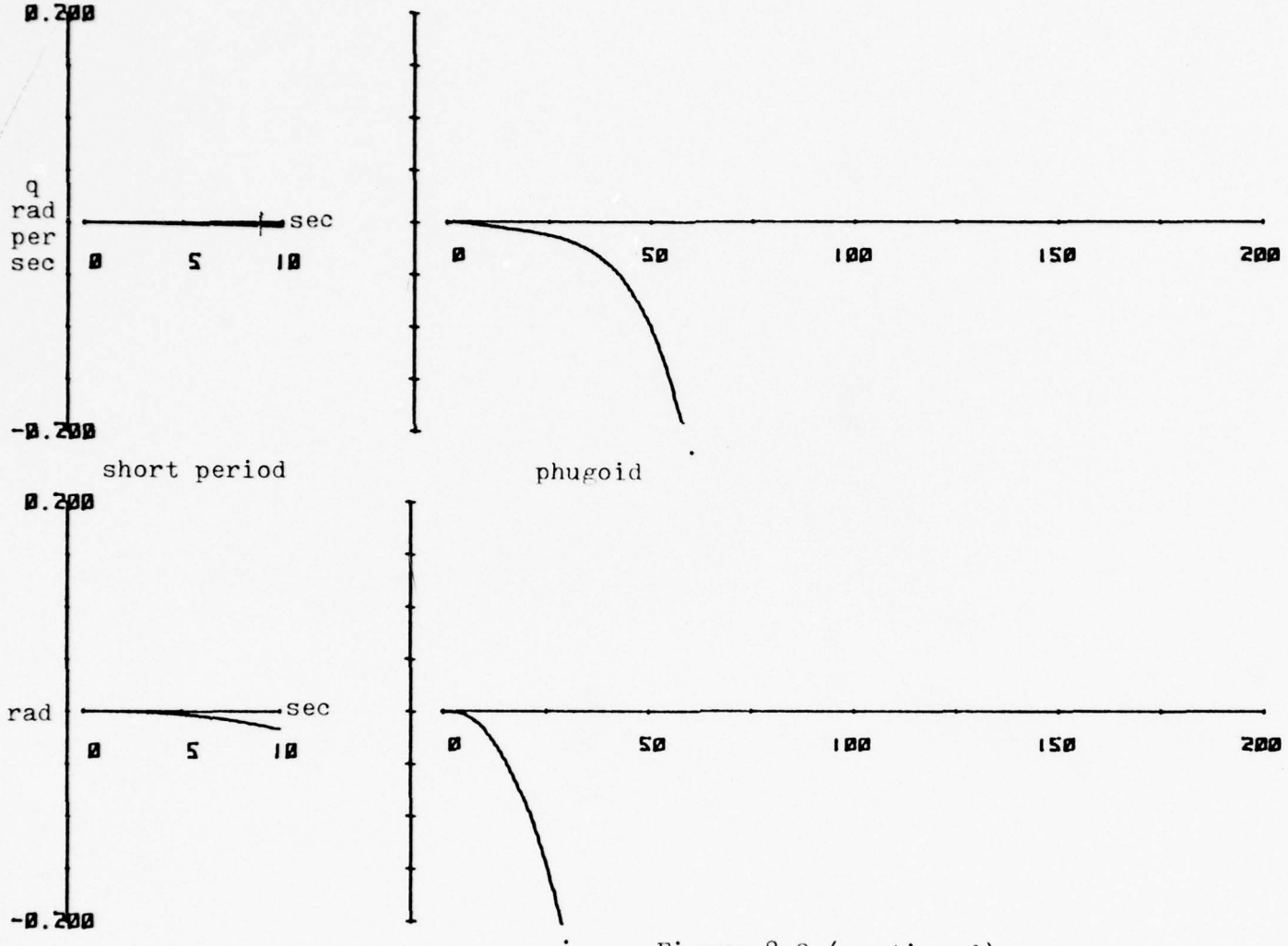


Figure 8-9 (continued)

periods of 75.1, 61.2, and 39.7 seconds, respectively, so the short period was effectively missing as well. Although its theoretical damping ratio was 0.4337, it was completely supressed by the instability of the positive real root.

It was obvious that some form of feedback network would be necessary so that the stability of the vehicle would be more in line with that of conventional aircraft. And, since the orbiter was designed to fly at the very extremes of atmospheric conditions, the system would necessarily depend upon many parameters, among them dynamic pressure, Mach number, true airspeed, load factor (which is a function of C_L), pitch angle and rate, angle of attack, and elevon deflection angle. Other factors could have been used, e.g., vertical velocity, descent angle, to name a few, but the ones chosen appeared to be those most easily obtainable and from which other necessary information could be computed. The end result of the engineering design is shown in Figure 8-10.

In order to solve the equations of motion as they were modified by the various gains, feedbacks, lead-lag elements, and limits, the Continuous System Modeling Program (version III), as incorporated on the IBM360, was utilized.

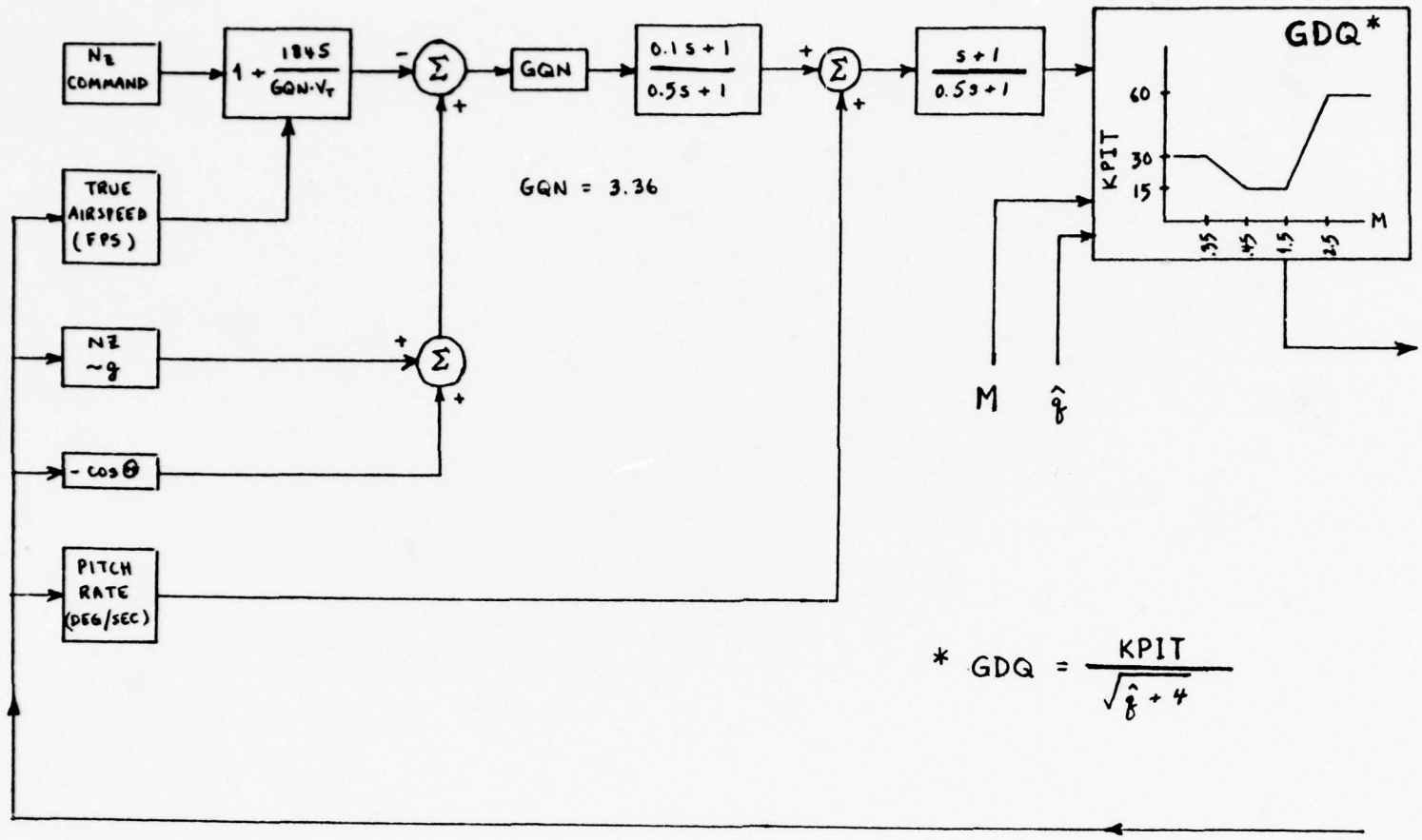

N_z COMMAND
$1 + \frac{1845}{GQN \cdot V_T}$
GQN
$\frac{0.1s+1}{0.5s+1}$
$\frac{s+1}{0.5s+1}$
GDQ*
KPIT
60
30
15
M
.35
.45
1.5
2.5
GQN = 3.36
TRUE AIRSPEED (FPS)
NZ ~g
$-\cos\theta$
PITCH RATE (DEG/SEC)
M
$\hat{q}$
* GDQ = $\frac{KPIT}{\sqrt{\hat{q}+4}}$

Figure 8-10

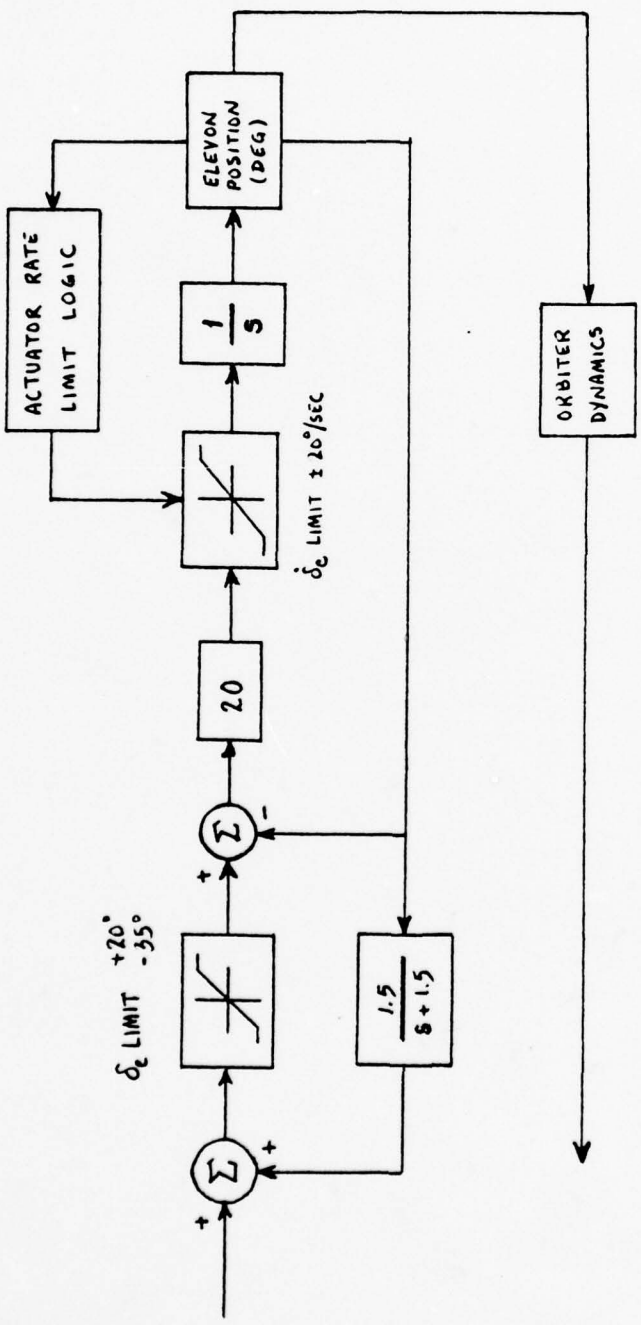


Figure 8-10 (continued)

The system variables were assigned names as follows:

N_z command = GCMD

true airspeed = U1

$N_z \sim g$ = NZ

Θ = THETA1

horizontal velocity perturbation = X1

vertical velocity perturbation = X2

pitch rate perturbation = X3

pitch angle perturbation = X4

elevon deflection perturbation = X8

The input signal to the first lead-lag element was called X5IN and its output called X5. The input to the second lead-lag element was called X6IN and its output X6.

The signal entering the δ_e LIMIT was called X8PRE1 and the limited signal X8PRE2; the signal entering the $\dot{\delta}_e$ LIMIT was called X8PRE3 and its output called X8DOT; the integration of X8DOT was X8. The signal X8 was fed back through a lag element whose output was labeled X7.

The CSMP III program is divided into three segments, INITIAL, DYNAMIC, and TERMINAL. The INITIAL part is for defining parameters whose value will not change for the

duration of the program. The DYNAMIC segment contains the equations of motion and other computations. The TERMINAL section (optional) contains any final operations which are desired. For this analysis, the following terms were assumed constant:

gravity = GRVTY = 32.073 ft/sec^2

$X_q = Z_q = 0.0$

density = RHO = 2.0325E-4 slug/ft^3

$C_{M_{\dot{\alpha}}}$ = CMADOT = -2.0

The initial values of two parameters were listed:

pitch angle = THETA = 0.1571 rad

true airspeed = U0 = 1016.9 fps

The other constants listed in the program (see Figure 8-11) are dimensional parameters or mass properties of the orbiter. AREA refers to wetted wing area; ISUBY (I_y) is the mass moment of inertia about the pitch axis; CHORD is the reference wing chord length; MASS is the mass of the vehicle with the payload out.

The FUNCTION statements enable the program to find a dependent variable knowing the value of the independent variable, much like reading a graph. The interpolation between the points listed in the statement may be linear or quadratic. Should an independent variable value fall

```
$$$CONTINUOUS SYSTEM MODELING PROGRAM III   V1M3   TRANSLATOR OUTPUT$$$

INITIAL

NOSORT
CONSTANT GRVTY = 32.073, XO = 0.0, ZO = 0.0, THETA = ...
         0.1571, UO = 1016.9, RHO = 2.0325E-4, AREA = 2690., ...
         CHORD = 39.56, MASS = 5839., ISUBY = 5.783JE+6, ...
          CMADOT = -2.0, PI = 3.14159

FUNCTION F1 = (-.5236,-.3573),(-.4363,-.3917),(-.3491,-.4493),...
              (-.2618,-.24061,(-.1745,-.33231,(0.0,-.38391,(.3491,...
              -.5099)
FUNCTION F2 = (-.4363,-.1331),(-.3491,-.0802),(-.2618,-.0688),...
              (-.1745,-.0573),(-.0873,.0229),(0.0,.0802),(.0873,...
              .1375),(.1745,.2865),(.3491,.4584)
FUNCTION F3 = (-.3491,.3266),(-.3054,.4125),(-.2618,.4354),...
              (-.1745,.4927),(0.0,.6188),(.3491,.8136)
FUNCTION F4 = (0.),(1.)), ((10.),(1.35), (20.),(1.04), (30.),(1.)), ...
              (40.0,1.0), (50.0,1.065), (60.0,1.08), (200.0,1.22)
FUNCTION F5 = (.0873,3.2317),(.1309,3.2317),(.1745,3.0254),(.2182,...
              2.865)),(.2618,2.865))
FUNCTION F6 = (0.0,0.155),(.0873,0.180),(.1745,0.247),(.2618,0.367),...
              (.3491,0.524)
FUNCTION F7 = (920.1,0.0), (1016.9,7.23E-4), (1065.3,-1.24E-4), ...
              (1162.2,-1.75E-4)
FUNCTION F8 = (.0873,.)256),(.1309,).397),(.1745,).538),(.2182,).661)...
              ,(.2618,C.788))
FUNCTION F9 = (.0873,0.2636),(.1745,0.7907),(.2618,1.3408),...
              (.3491,1.8336)
FUNCTION F10 = (968.5,5.79E-4), (1016.9,3.1E-4), (1065.3,1.24E-4), ...
               (1113.7,-2.1E-5)
FUNCTION F11 = (920.0,-6.,0E-4), (1016.9,-1.55E-4), (1065.3,0.0), ...
               (1162.2,-1.65E-4)
FUNCTION F12 = (.0873,0.332),(.1309,-0.318),(.1745,-).330),...
               (.2182,-0.039),(.2618,-0.051)
FUNCTION F13 = (.1309,-0.4584),(.1745,-0.2750),(.2182,-0.2063),...
               (.2618,-).2750)
FUNCTION F14 = (.1396,-2.25),(.1745,-1.30),(.1920,-1.00),(.2094,-1.00)

DYNAMIC

SORT

U1 = UO + X1
THETA1 = THETA + X4
QHAT = 0.5*RHO*U1**2
GDQ = 15.0/SQRT(QHAT+4.0)
AOA = X2/U1 + 0.2316
CMDE = AFGEN(F1,X8)
MDE = RHO*U1**2*AREA*CHORD*CMDE/(2*ISUBY)
CDDE = AFGEN(F2,X8)
XDE = -RHO*U1**2*AREA*CDDE/(2*MASS)
CLDE = AFGEN(F3,X8)
ZDE = -RHO*U1**2*AREA*CLDE/(2*MASS)
GCMD = AFGEN(F4,TIME)
ZW = RHO*U1*AREA*(-CLA-CD)/(2.0*MASS)
CLA = AFGEN(F5,AOA)
CD = AFGEN(F6,AOA)
```

Figure 8-11

```
ZU = RHO*UI*AREA*(-UI*CLU/2.0-CL)/MASS
CLU = AFGEN(F7,UI)
CL = AFGEN(F8,ADA)
XW = RHO*UI*AREA*(CL-CDA)/(2.0*MASS)
CDA = AFGEN(F9,ADA)
XU = RHO*UI*AREA*(-UI*CDU/2.0-CD)/MASS
CDU = AFGEN(F10,UI)
MU = RHO*UI*AREA*CHORD*(UI*CMU/2.0*CM)/ISUBY
CMU = AFGEN(F11,UI)
CM = AFGEN(F12,ADA)
MW = RHO*UI*AREA*CHORD*CMA/(2.0*ISUBY)
CMA = AFGEN(F13,ADA)
MQ = RHO*UI*AREA*CHORD**2*CMQ/(4.0*ISUBY)
CMQ = AFGEN(F14,ADA)
MWDOT = RHO*AREA*CHORD**2*CMADOT/(4.0*ISUBY)

X8PRE1 = GDQ*X6 + X7
X8PRE2 = LIMIT(-.6109,.3491,X8PRE1)
X8PRE3 = 2.3491*(X8PRE2 - X8)
X8DOT = LIMIT(-.3491..3491,X8PRE3)

X1DOT = XU*X1 + XW*X2 + XQ*X3 - GRVTY*X4 + XDE*X8
X2DOT = ZU*X1 + ZW*X2 + (ZQ+UI)*X3 + ZDE*X8
X3DOT = (MU+ZU*MWDOT)*X1 + (MW+ZQ*MWDOT)*X2 + (MQ+MWDOT*(UI+ZQ))*X3 ...
      + (MDE+ZDE*MWDOT)*X8
X4DOT = X3
X7DOT = 1.5*(X8 - X7)

N5IN = 3.36*(NZL - COS(THETA1) - GCMD*(1.0+549.1/UI))
N6IN = N5 + N3

METHOD STIFF
X1 = INTGRL(0.,X1DOT)
X2 = INTGRL(0.0,X2DOT)
X3 = INTGRL(0.0,X3DOT)
X4 = INTGRL(0.,X4DOT)
N5 = LEDLAG(0.1,0.5,N5IN)
N6 = LEDLAG(1.0,0.5,N6IN)
X7 = INTGRL(0.0,X7DOT)
X8 = INTGRL(-0.048,X8DOT)
H = INTGRL(823.,X2)

NZL = CL*QHAT*AREA/(MASS*GRVTY)

NOSORT
ADADEG = ADA*180./PI
X3DEG = X3*180./PI
X4DEG = X4*180./PI
X8DEG = X8*180./PI
X8DODEG = X8DOT*180./PI
THETAD = THETA1*180./PI
W = X2 + 11.74

TIMER FINTIM = 10.0, OUTDEL = 0.125
PRTPLT ADADEG
LABEL ANGLE OF ATTACK (DEGREES)
PRTPLT UI
LABEL HORIZONTAL VELOCITY RESPONSE (FPS)
PRTPLT W
```

Figure 8-11 (continued)

```
LABEL VERTICAL VELOCITY RESPONSE (FPS)
PRTPLT X3DEG
LABEL PITCH RATE RESPONSE (DEG/SEC)
PRTPLT THETAD
LABEL PITCH ANGLE RESPONSE (DEGREES)
PRTPLT X8DEG
LABEL ELEVON DEFLECTION (DEGREES)
PRTPLT X8DDEG
LABEL ELEVON DEFLECTION RATE (DEGREES/SEC)
PRTPLT NZL
LABEL LOAD FACTOR (NZ)
PRTPLT QHAT
LABEL DYNAMIC PRESSURE
PRTPLT GDQ
LABEL GAIN GDQ
PRTPLT H
LABEL ALTITUDE
PRTPLT CLA
LABEL LIFT COEFF WRT ACA
PRTPLT CLU
LABEL LIFT COEFF WRT VELOCITY
PRTPLT CLDE
LABEL LIFT COEFF WRT ELEVON DEFLECTION
PRTPLT CDA
LABEL DRAG COEFF WRT ACA
PRTPLT CDU
LABEL DRAG COEFF WRT VELOCITY
PRTPLT CDDE
LABEL DRAG COEFF WRT ELEVON DEFLECTION
PRTPLT CMA
LABEL PITCHING MOMENT COEFF WRT ACA
PRTPLT CMU
LABEL PITCHING MOMENT COEFF WRT VELOCITY
PRTPLT CMQ
LABEL PITCHING MOMENT COEFF WRT PITCH RATE
PRTPLT CMDE
LABEL PITCHING MOMENT COEFF WRT ELEVON DEFLECTION
END
STOP

OUTPUT VARIABLE SEQUENCE
UI      COM     ATA     CD      XU      CL      CDA     XW      CDDE    XDE
X1DOT   X1      CLU     ZU      CLA     Zw      CLDE    ZDE     X2DOT   X2
CMU     CM      MU      MWDOT   CMA     MW      CMQ     MQ      CMDE    MDE
X3DOT   X3      X4DOT   X4      QHAT    NZL     THETA1  GCMD    X5IN    ZZ1008
ZZ1009  X5      X5IN    ZZ1012  ZZ1013  X7DOT   X7      GDQ     X6      X8PRE1
X8PRE2  X8PWF3  X8DOT   X8      H       ANADEG  X3DEG   X4DEG   X8DEG   X8DDEG
THETAD  W
```

Figure 8-11 (continued)

outside the range of points listed, the program will extrapolate a value based on the slope of the function at the nearest point listed.

The FUNCTION statements are entered with an AFGEN command (for linear interpolation). Since linear interpolation was used in this analysis, it was necessary to insure that the dependent variable varied linearly between the points chosen. The functions were

F1: CMDE = $C_{M_{\delta_e}}$

F2: CDDE = $C_{D_{\delta_e}}$

F3: CLDE = $C_{L_{\delta_e}}$

F4: GCMD = n_z command

F5: CLA = C_{L_α}

F6: CD = C_D

F7: CLU = C_{L_u}

F8: CL = C_L

F9: CDA = C_{D_α}

F10: CDU = C_{D_u}

F11: CMU = C_{M_u}

F12: CM = C_M

F13: CMA = C_{M_α}

F14: CMQ = C_{M_q}

These coefficients were in turn used to compute the stability derivatives. As the values of the independent variables changed, so did the dependent variables and so also did the stability derivatives. In this manner, the stability derivatives were modified due to changing flight conditions, and thus an important facet of the model was maintained. The stability derivatives were then used to write the equations of motion (the X1DOT through X4DOT equations).

The modeling of the system was completed by writing four other equations as the block diagram signified. X5 and X6 were written simply as lead-lag (LEDLAG) functions of X5IN and X6IN, respectively, where the parameters listed were the coefficients of s in the numerator and denominator.

The term X7 was found by writing the lag compensation from which it came as a differential equation. Since output divided by input equals the transfer function,

$$\frac{X7}{X8} = \frac{1.5}{s + 1.5}$$

$$(X7)s + 1.5(X7) = 1.5(X8)$$

Taking the inverse Laplace transform,

$$\dot{X7} = 1.5(X8) - 1.5(X7)$$

$$\text{and } X7 = \int \dot{X7}$$

Writing this in the CSMP III language,

X7 = INTGRL(0.0,X7DOT)

where the 0.0 refered to the initial condition.

The equation to find X8 was somewhat more complex. The signal was first the sum of GDQ*X6 + X7 = X8PRE1; this was then limited to -35/+20°, compared to X8, and the difference multiplied by 20 (here, in radians). After limiting this signal to -20/+20° per second, it was integrated to find X8.

The eight equations were solved simultaneously using the STIFF method of integration, and, after converting some of the parameters into degrees, the results were printed.

It may be seen from the block diagram that the forcing function is the command load factor, GCMD. This value, plotted as FUNCTION F4, was available from the Aerodynamic Design Data Book and was programmed accordingly.

The value of CMADOT was not available from the above publication. To arrive at the value of -2.0, several aircraft were studied, considering wing planform, aircraft size, airspeed, and altitude. The larger aircraft (C-47 and DC-8) had values of -10 and -6.8, respectively, the DC-8 figure being at Mach 0.88 and 33000 feet. The A-4D, having a delta planform, had a C_{M_α} of -2.1 at 15000 feet and -1.4 at 35000 feet. Considering the size of the orbiter and its altitude for this study, the value of -2.0 was deemed appropriate.

Several equations to compute the load factor on the vehicle were considered. The one chosen was derived from the lift equation:

$$n_z = \frac{L}{W} \qquad \text{where } L = C_L \hat{q} S$$

$$\text{so, } n_z = C_L \hat{q} S / mg$$

$$= CL*QHAT*AREA/(MASS*GRVTY)$$

This equation was chosen as it was most independent of the equations of motion and would therefore amplify to a less extent any errors due to integration round-off or to other sources during the solution of the simultaneous equations.

The results are shown in Figure 8-12 (short period) and Figure 8-13 (phugoid). Inasmuch as both modes were evidently stable, the steady state magnitudes were extremely high. Several causes must be considered.

One, the equations of motion were written as perturbed motions. This was necessary in order to justify their linearization. The parameter values were treated as perturbations throughout the program, being added to the large scale motion where necessary for computation (as in the case of THETA1 and U1) and for output plots. Their initial conditions were collectively zero. The initial conditions for the other parameters, X5 through X7, were <u>not</u> zero, however, and a method for incorporating (or even deriving) their initial value was not available. The initial condition for X8 was available from the Data Book and was so used. It is not known if the lack of initial conditions for these parameters caused the large excursions in the response; it is doubtful that this was the case because the steady state values should still have been reasonable; they were not.

Two, the simulation was begun at some point other than t=0 in the trajectory. That is, the vehicle had

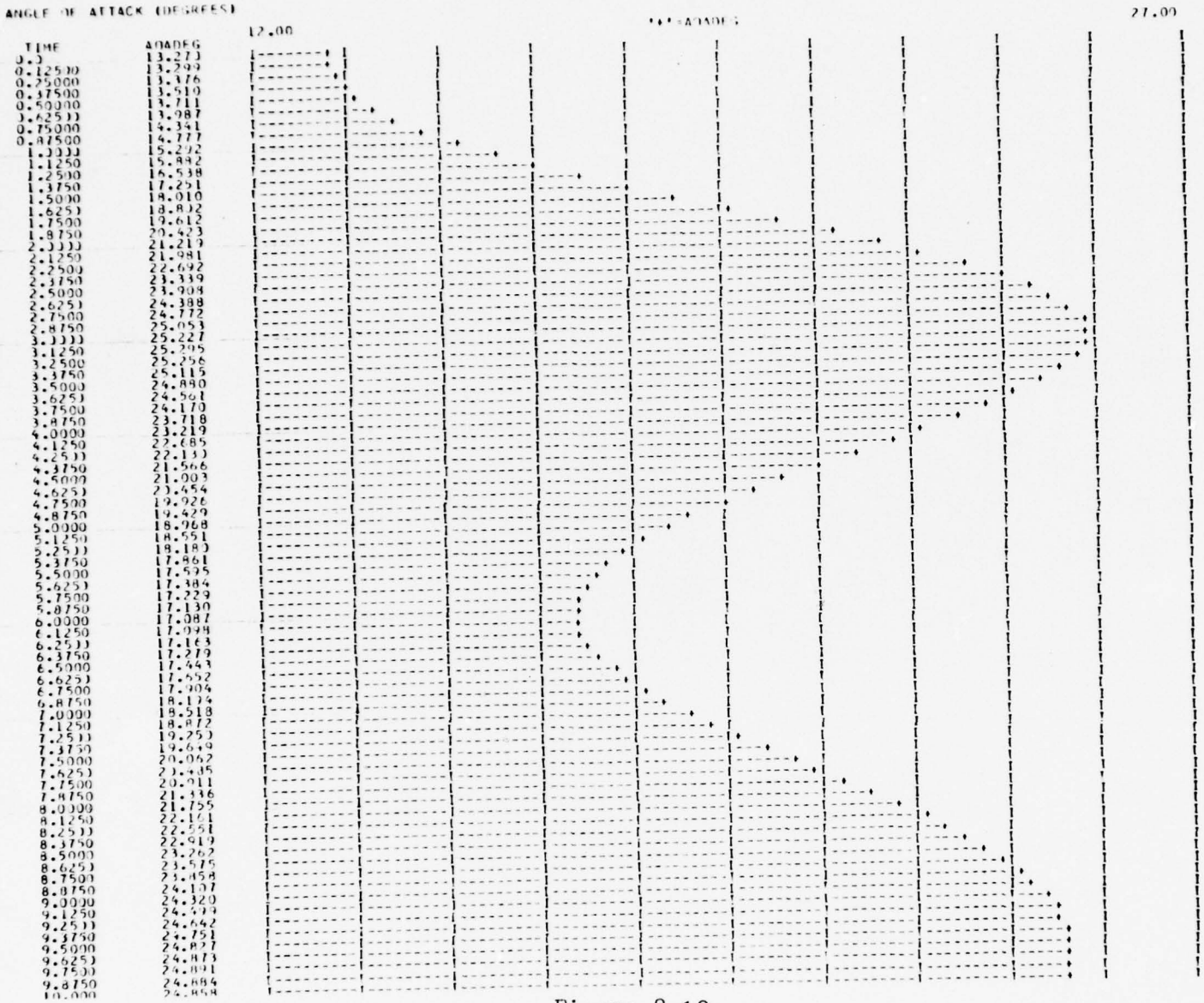

ANGLE OF ATTACK (DEGREES)
12.00
*** ADADEG ***
27.00
TIME ADADEG
0.0 13.273
0.12500 13.299
0.25000 13.476
0.37500 13.510
0.50000 13.711
0.62500 13.987
0.75000 14.341
0.87500 14.777
1.0000 15.292
1.1250 15.882
1.2500 16.538
1.3750 17.251
1.5000 18.010
1.6250 18.802
1.7500 19.612
1.8750 20.423
2.0000 21.219
2.1250 21.981
2.2500 22.692
2.3750 23.339
2.5000 23.908
2.6250 24.388
2.7500 24.772
2.8750 25.053
3.0000 25.227
3.1250 25.295
3.2500 25.256
3.3750 25.115
3.5000 24.880
3.6250 24.561
3.7500 24.170
3.8750 23.718
4.0000 23.219
4.1250 22.685
4.2500 22.133
4.3750 21.566
4.5000 21.003
4.6250 20.454
4.7500 19.928
4.8750 19.429
5.0000 18.968
5.1250 18.551
5.2500 18.180
5.3750 17.861
5.5000 17.595
5.6250 17.384
5.7500 17.229
5.8750 17.130
6.0000 17.087
6.1250 17.099
6.2500 17.163
6.3750 17.279
6.5000 17.443
6.6250 17.652
6.7500 17.904
6.8750 18.174
7.0000 18.518
7.1250 18.872
7.2500 19.250
7.3750 19.649
7.5000 20.062
7.6250 20.485
7.7500 20.911
7.8750 21.336
8.0000 21.755
8.1250 22.161
8.2500 22.551
8.3750 22.919
8.5000 23.262
8.6250 23.575
8.7500 23.858
8.8750 24.107
9.0000 24.320
9.1250 24.499
9.2500 24.642
9.3750 24.751
9.5000 24.827
9.6250 24.873
9.7500 24.891
9.8750 24.884
10.000 24.858

Figure 8-12

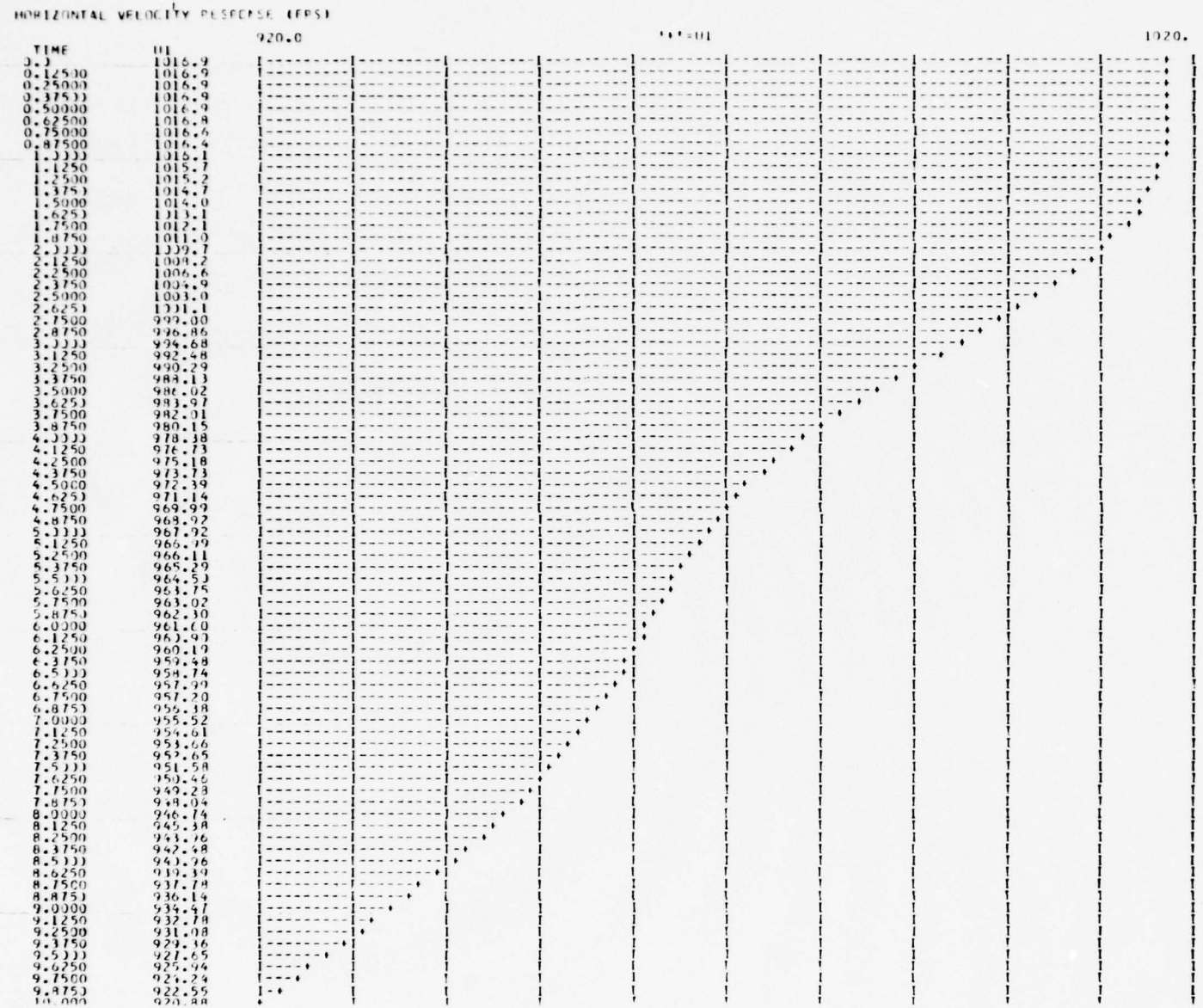


Figure 8-12 (continued)

VERTICAL VELOCITY RESPONSE (FPS)

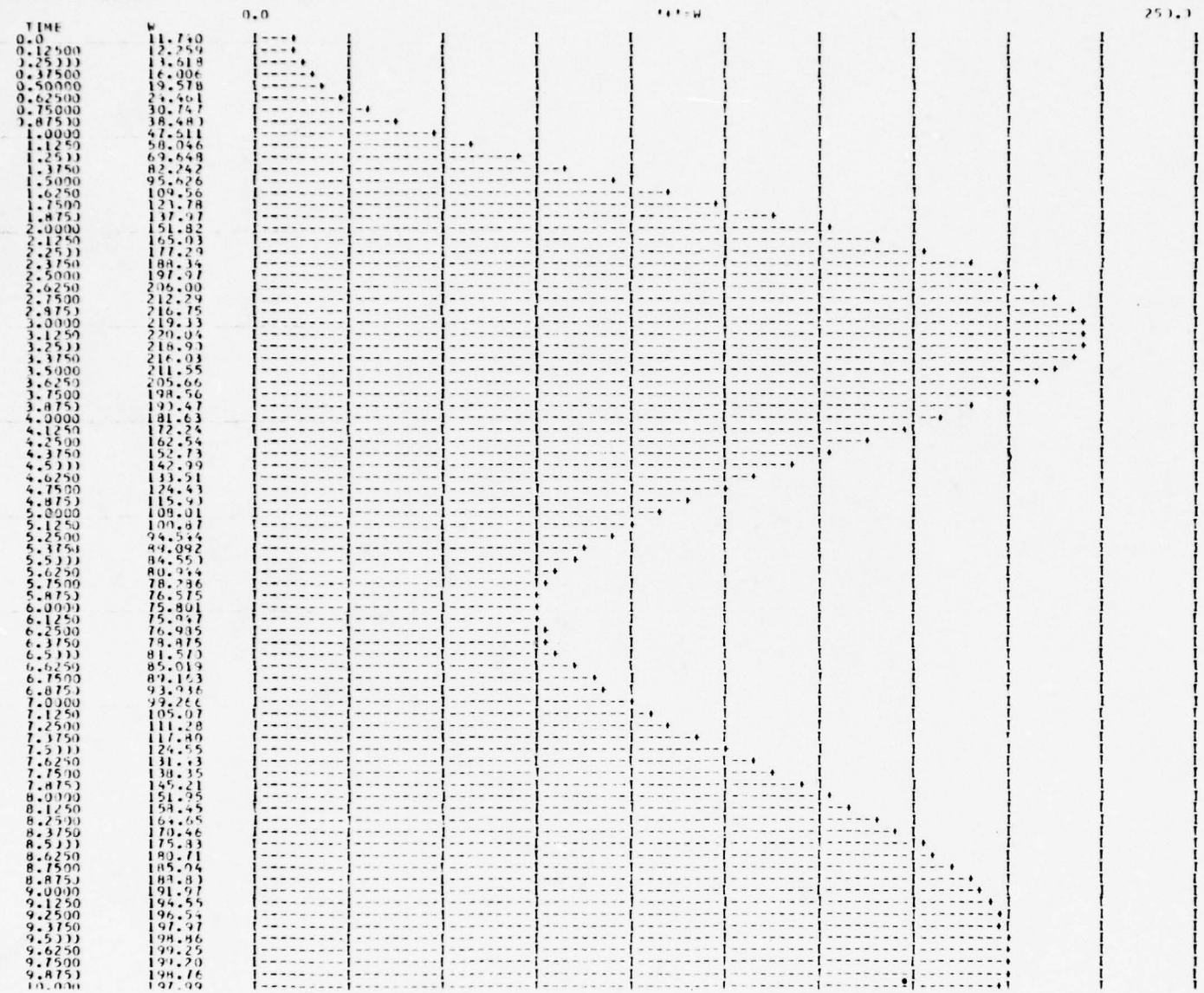


Figure 8-12 (continued)

PITCH RATE RESPONSE (DEG/SEC)

TIME	X30EG
0.0	0.0
0.12500	0.30107
0.25000	0.73515
0.37500	1.1949
0.50000	1.7692
0.62500	2.4028
0.75000	3.0858
0.87500	3.7835
1.0000	4.4563
1.1250	5.0942
1.2500	5.6756
1.3750	6.1827
1.5000	6.5930
1.6250	6.9086
1.7500	7.0974
1.8750	7.1555
2.0000	7.0733
2.1250	6.8483
2.2500	6.4829
2.3750	5.9994
2.5000	5.4105
2.6250	4.7300
2.7500	3.9749
2.8750	3.1652
3.0000	2.3224
3.1250	1.4698
3.2500	0.62621
3.3750	-0.18430
3.5000	-0.93819
3.6250	-1.6152
3.7500	-2.2049
3.8750	-2.6946
4.0000	-3.0928
4.1250	-3.3864
4.2500	-3.5817
4.3750	-3.6837
4.5000	-3.6963
4.6250	-3.6256
4.7500	-3.4812
4.8750	-3.2724
5.0000	-3.0076
5.1250	-2.6958
5.2500	-2.3431
5.3750	-1.9631
5.5000	-1.5570
5.6250	-1.1334
5.7500	-0.69841
5.8750	-0.25744
6.0000	0.18436
6.1250	0.62227
6.2500	1.0519
6.3750	1.4691
6.5000	1.8699
6.6250	2.2505
6.7500	2.6074
6.8750	2.9368
7.0000	3.2354
7.1250	3.5001
7.2500	3.7281
7.3750	3.9171
7.5000	4.0648
7.6250	4.1695
7.7500	4.2307
7.8750	4.2492
8.0000	4.2259
8.1250	4.1500
8.2500	4.0337
8.3750	3.8899
8.5000	3.7075
8.6250	3.4960
8.7500	3.2605
8.8750	3.0068
9.0000	2.7409
9.1250	2.4691
9.2500	2.1975
9.3750	1.9321
9.5000	1.6788
9.6250	1.4427
9.7500	1.2286
9.8750	1.0435
10.000	0.88153

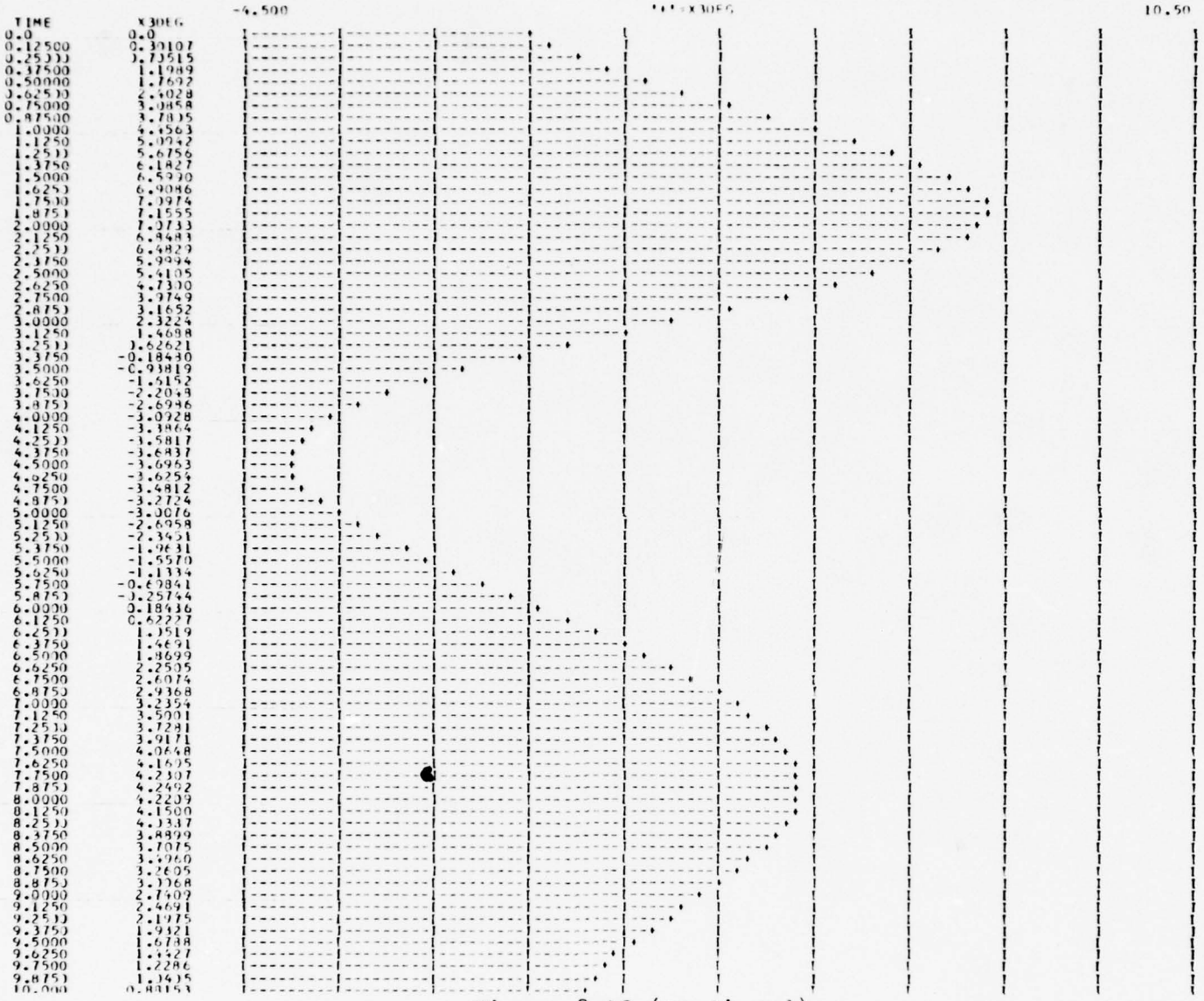
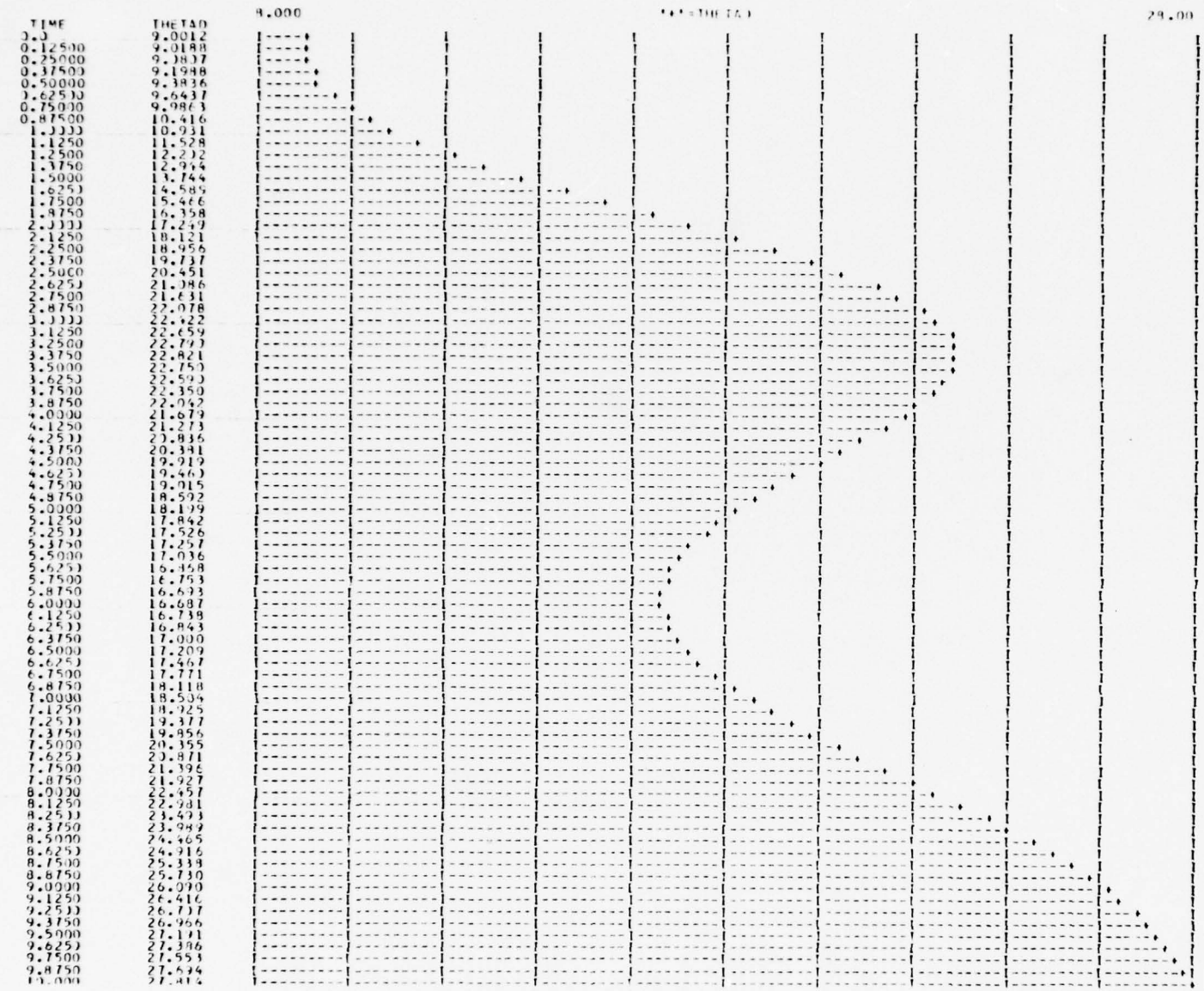


Figure 8-12 (continued)

PITCH ANGLE RESPONSE (DEGREES)



TIME	THETAD
0.0	9.0012
0.12500	9.0188
0.25000	9.3837
0.37500	9.1988
0.50000	9.3836
0.62500	9.6437
0.75000	9.9863
0.87500	10.416
1.0000	10.931
1.1250	11.528
1.2500	12.202
1.3750	12.944
1.5000	13.744
1.6250	14.589
1.7500	15.466
1.8750	16.358
2.0000	17.249
2.1250	18.121
2.2500	18.956
2.3750	19.737
2.5000	20.451
2.6250	21.086
2.7500	21.631
2.8750	22.078
3.0000	22.422
3.1250	22.659
3.2500	22.793
3.3750	22.821
3.5000	22.750
3.6250	22.593
3.7500	22.350
3.8750	22.042
4.0000	21.679
4.1250	21.273
4.2500	20.836
4.3750	20.381
4.5000	19.919
4.6250	19.460
4.7500	19.015
4.8750	18.592
5.0000	18.199
5.1250	17.842
5.2500	17.526
5.3750	17.257
5.5000	17.036
5.6250	16.868
5.7500	16.753
5.8750	16.693
6.0000	16.687
6.1250	16.738
6.2500	16.843
6.3750	17.000
6.5000	17.209
6.6250	17.467
6.7500	17.771
6.8750	18.118
7.0000	18.504
7.1250	18.925
7.2500	19.377
7.3750	19.856
7.5000	20.355
7.6250	20.871
7.7500	21.398
7.8750	21.927
8.0000	22.457
8.1250	22.981
8.2500	23.493
8.3750	23.989
8.5000	24.465
8.6250	24.916
8.7500	25.338
8.8750	25.730
9.0000	26.090
9.1250	26.416
9.2500	26.707
9.3750	26.966
9.5000	27.191
9.6250	27.386
9.7500	27.553
9.8750	27.694
10.000	27.812

Figure 8-12 (continued)

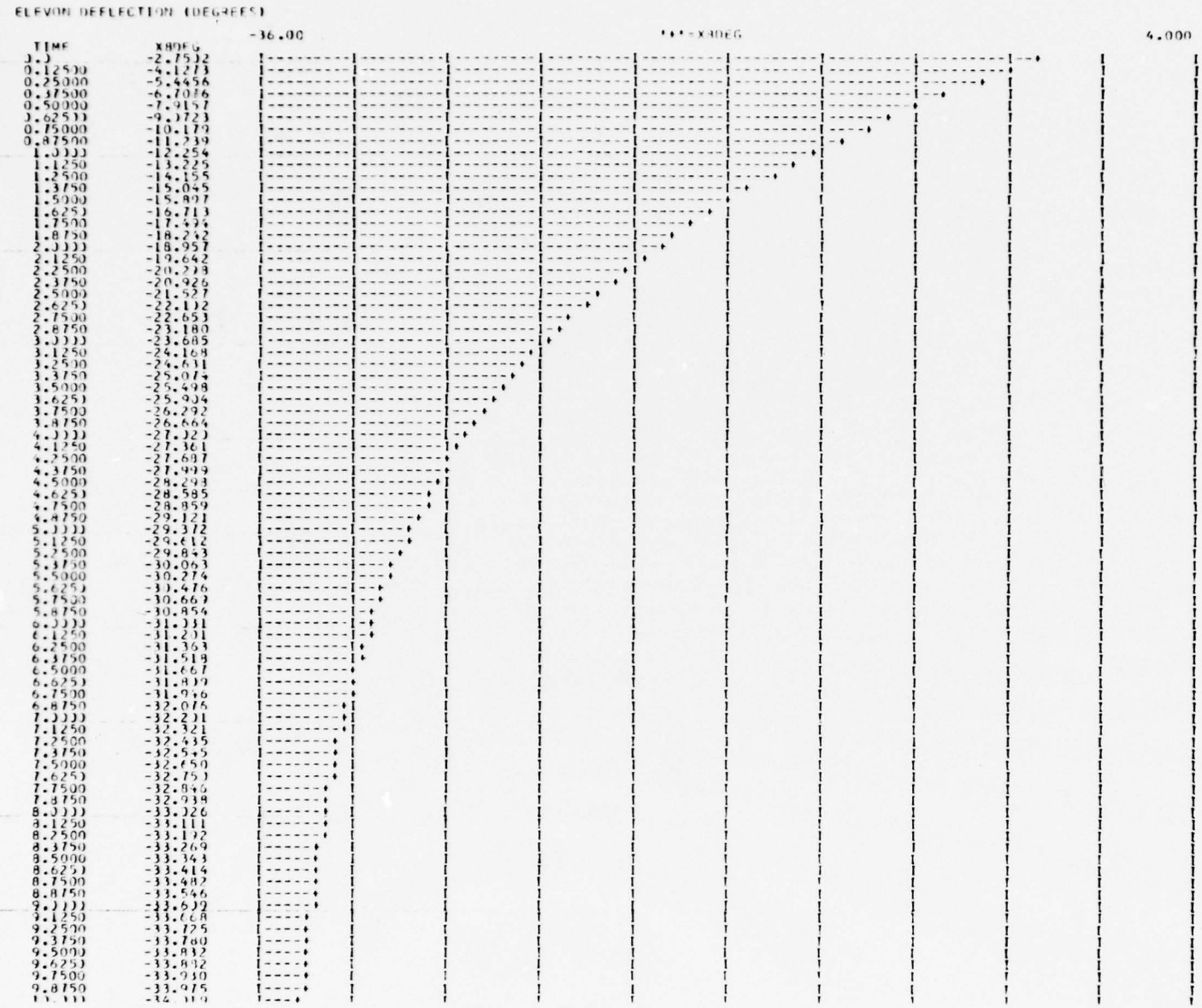


Figure 8-12 (continued)

ELEVON DEFLECTION RATE (DEGREES/SEC)

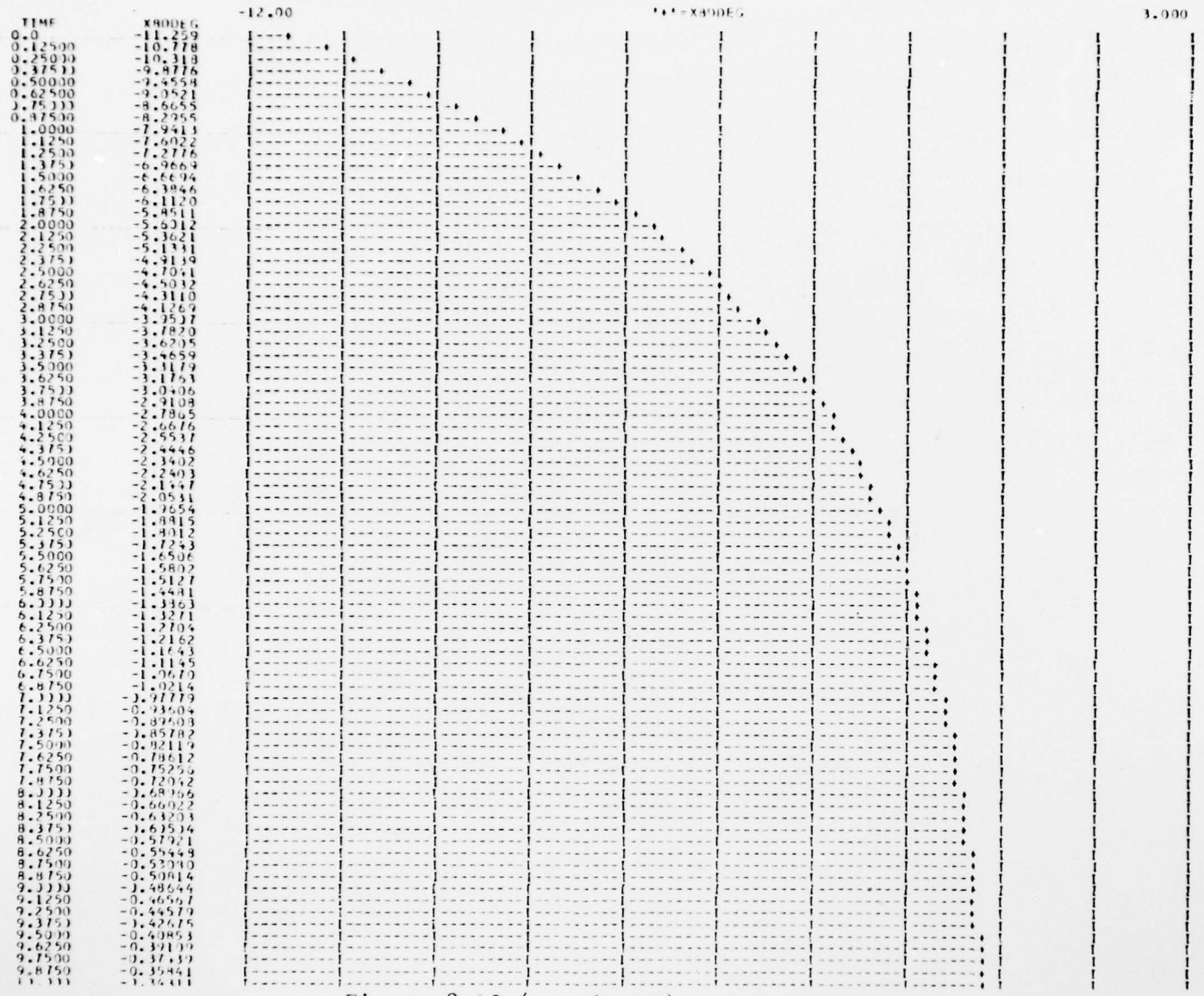


Figure 8-12 (continued)

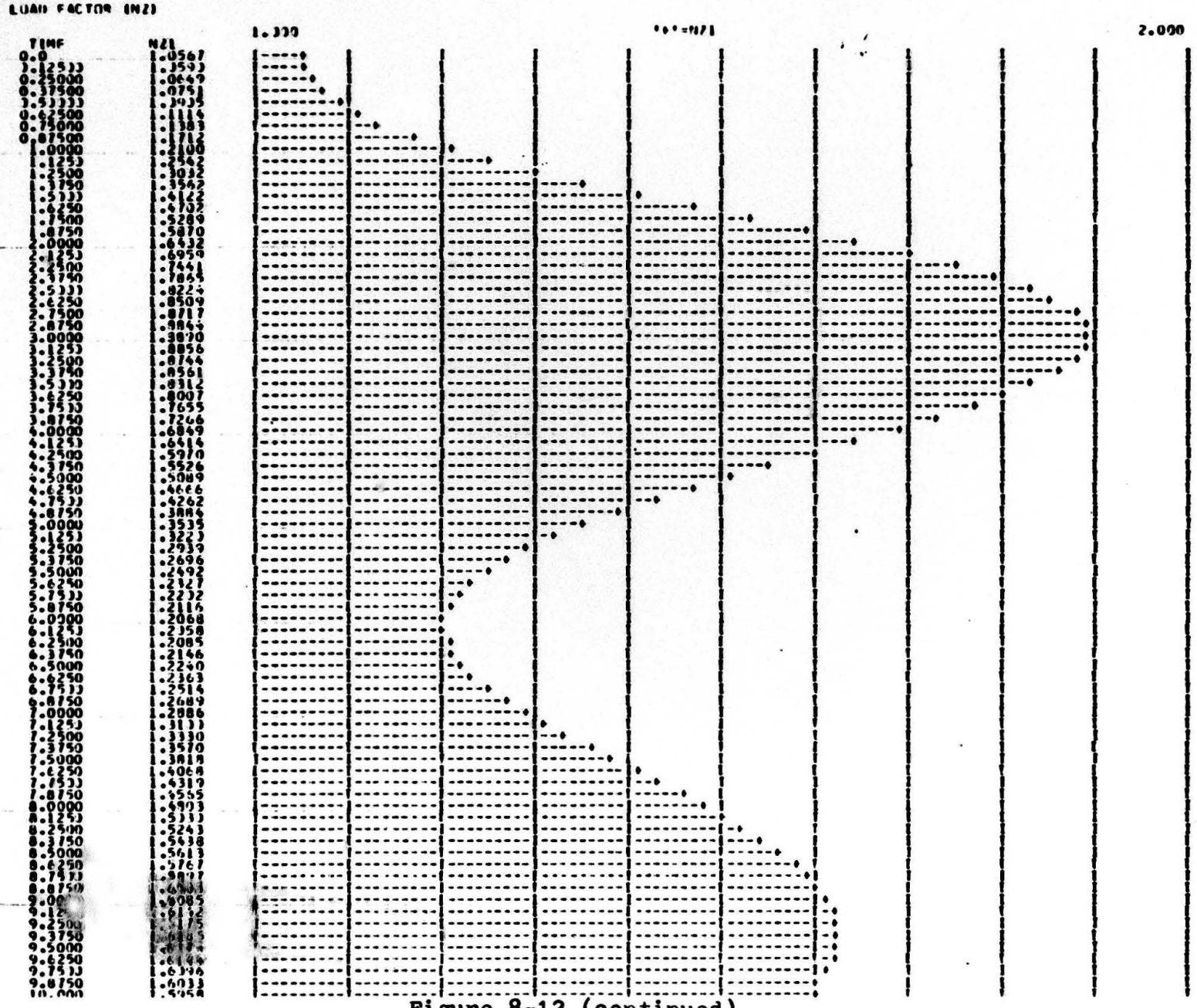


Figure 8-12 (continued)

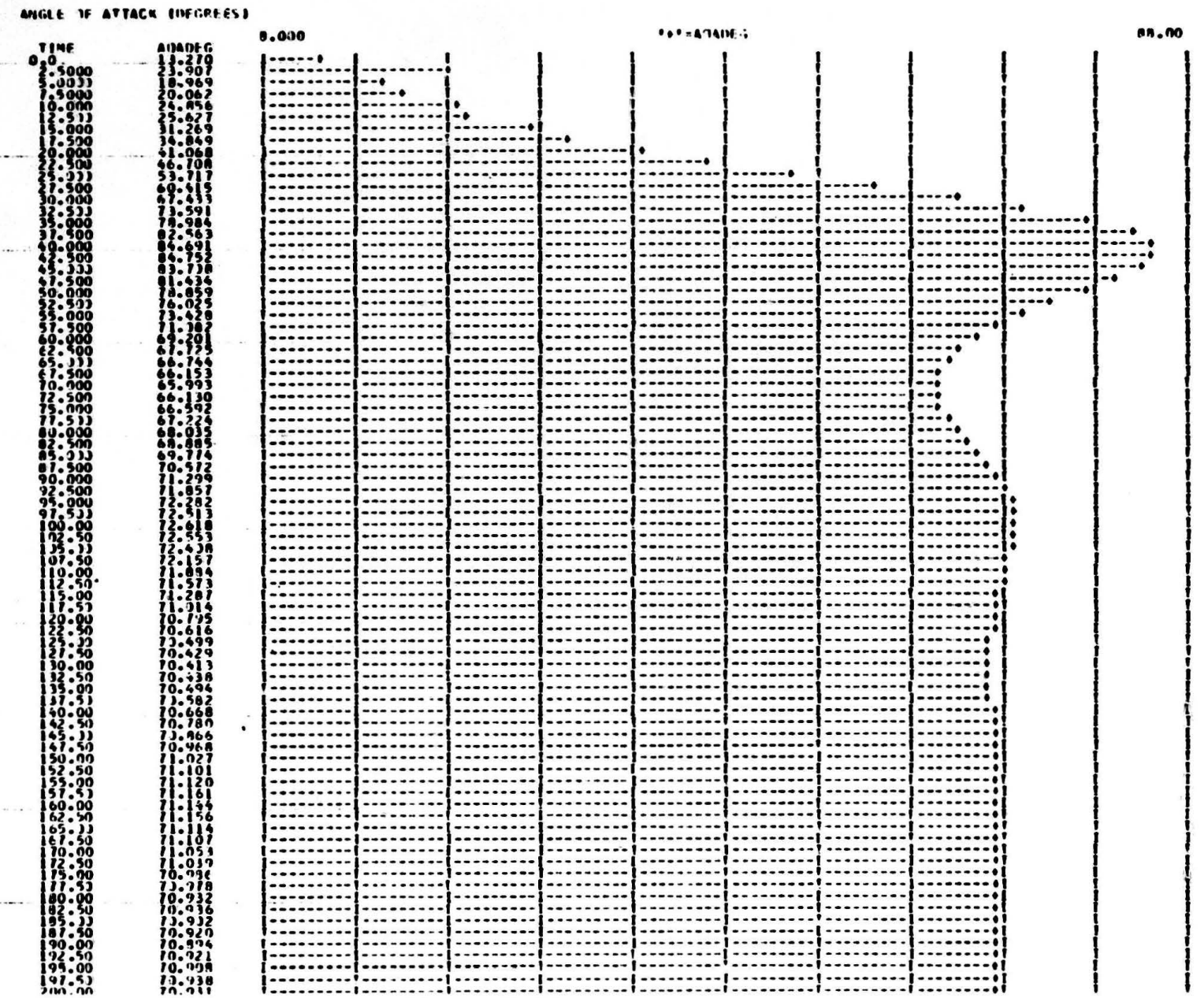


Figure 8-13

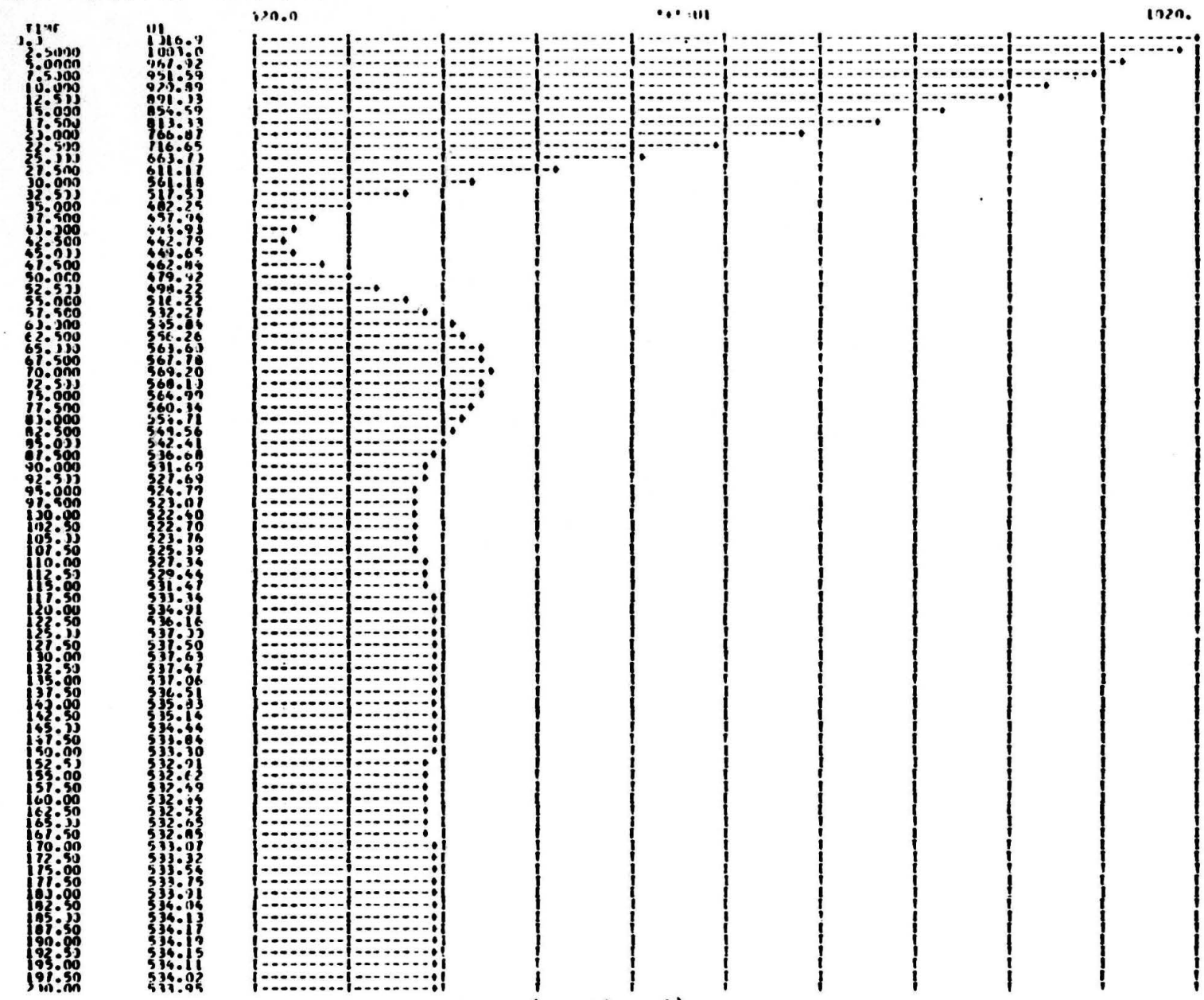


Figure 8-13 (continued)

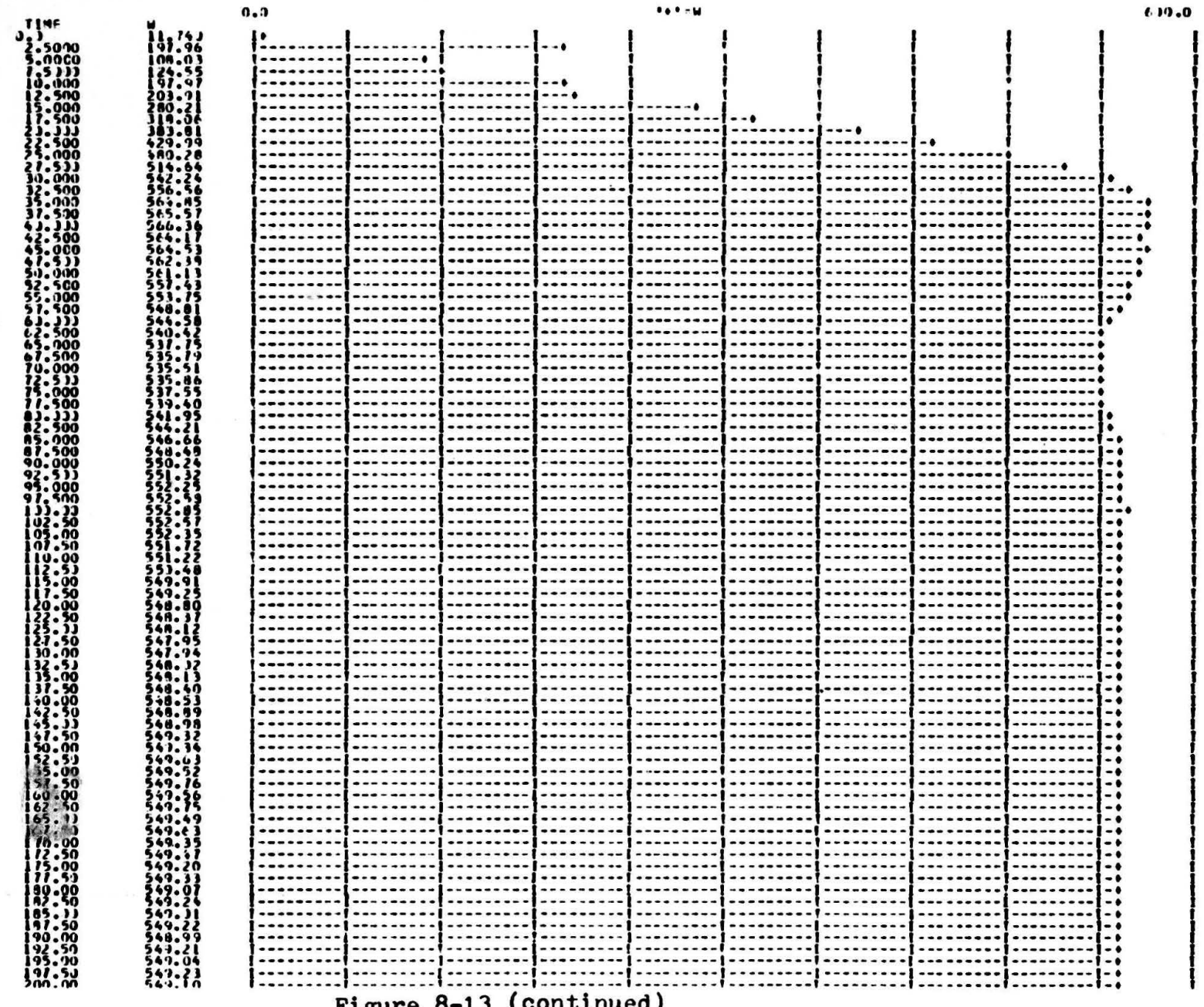


Figure 8-13 (continued)

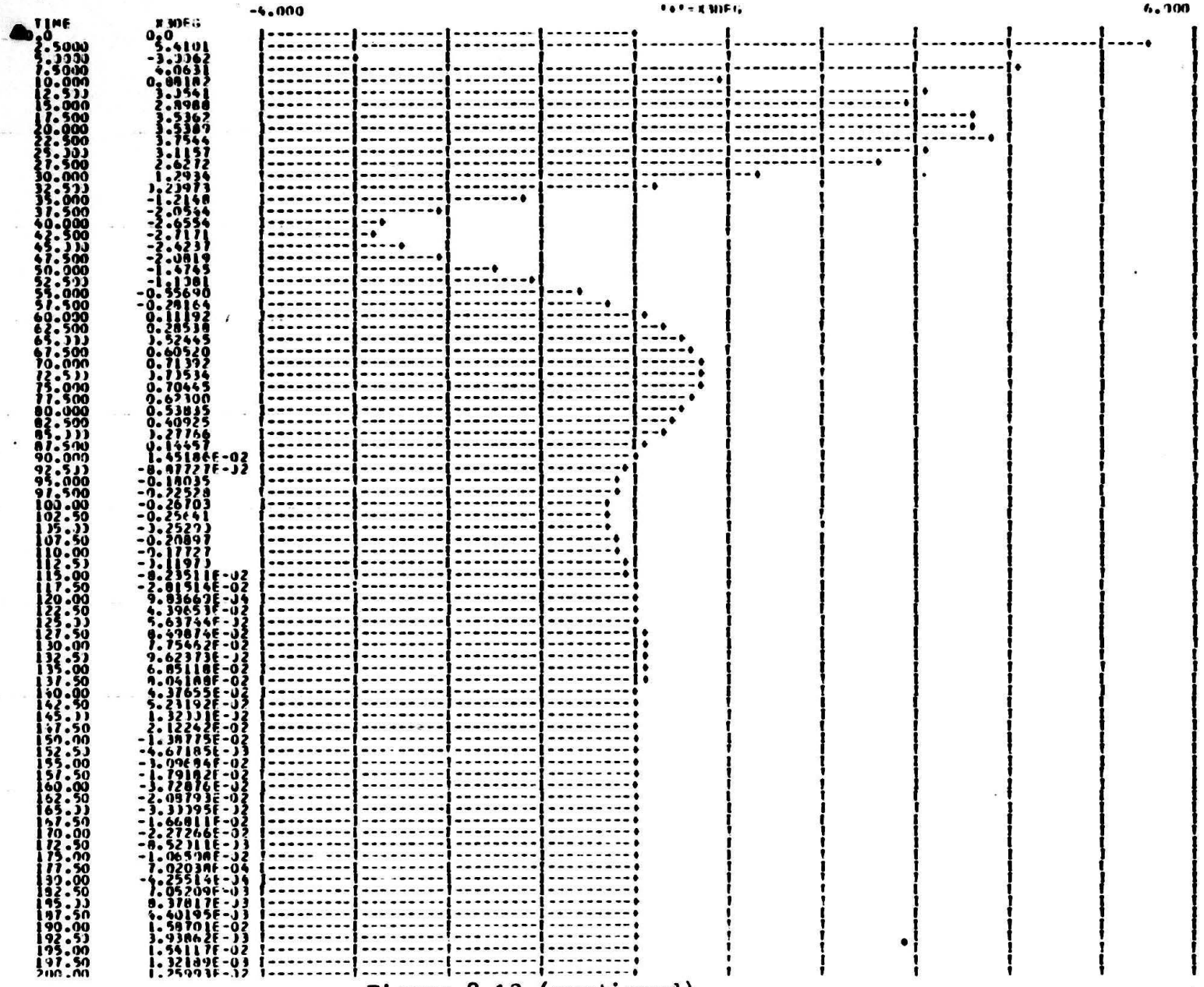


Figure 8-13 (continued)

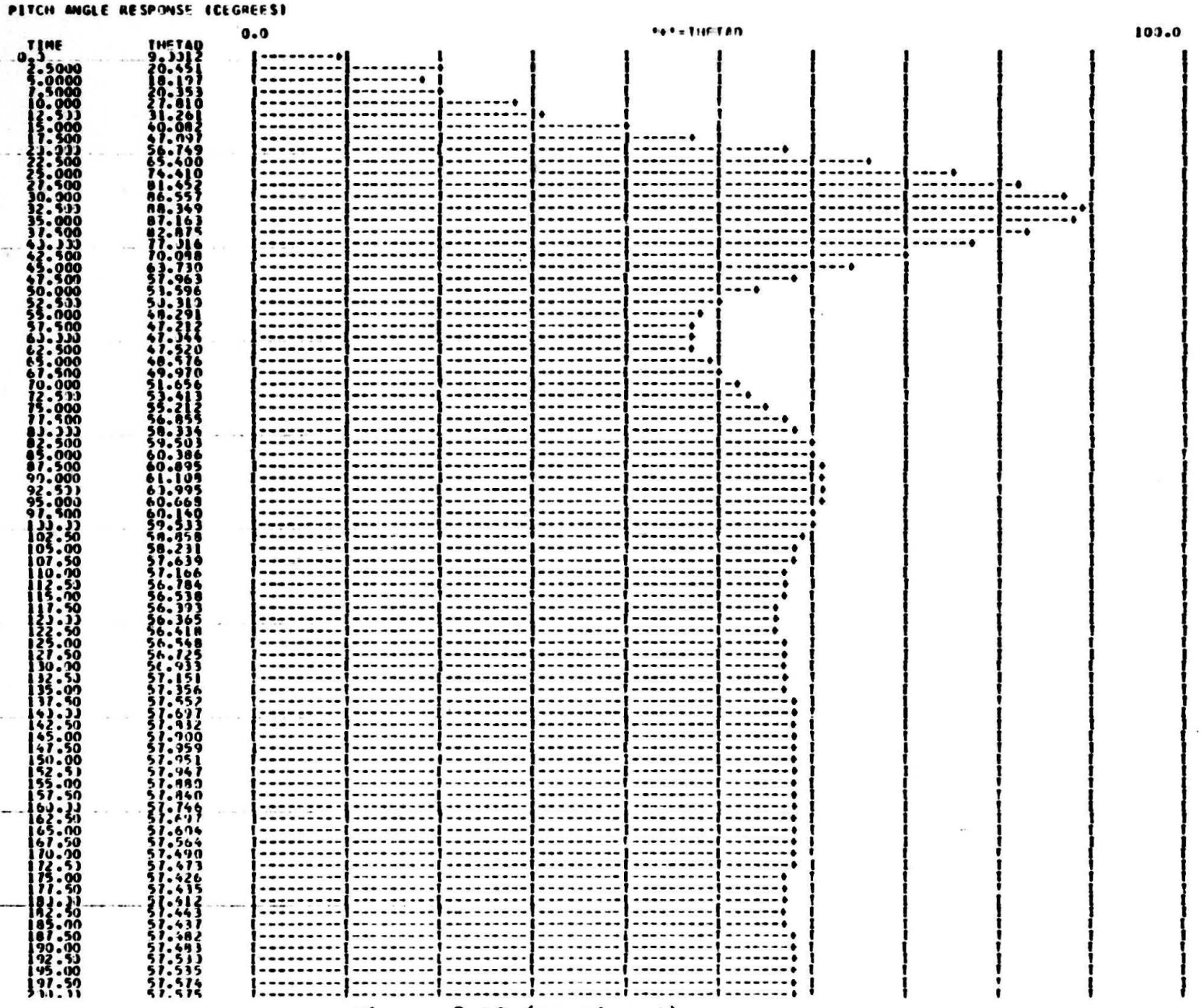


Figure 8-13 (continued)

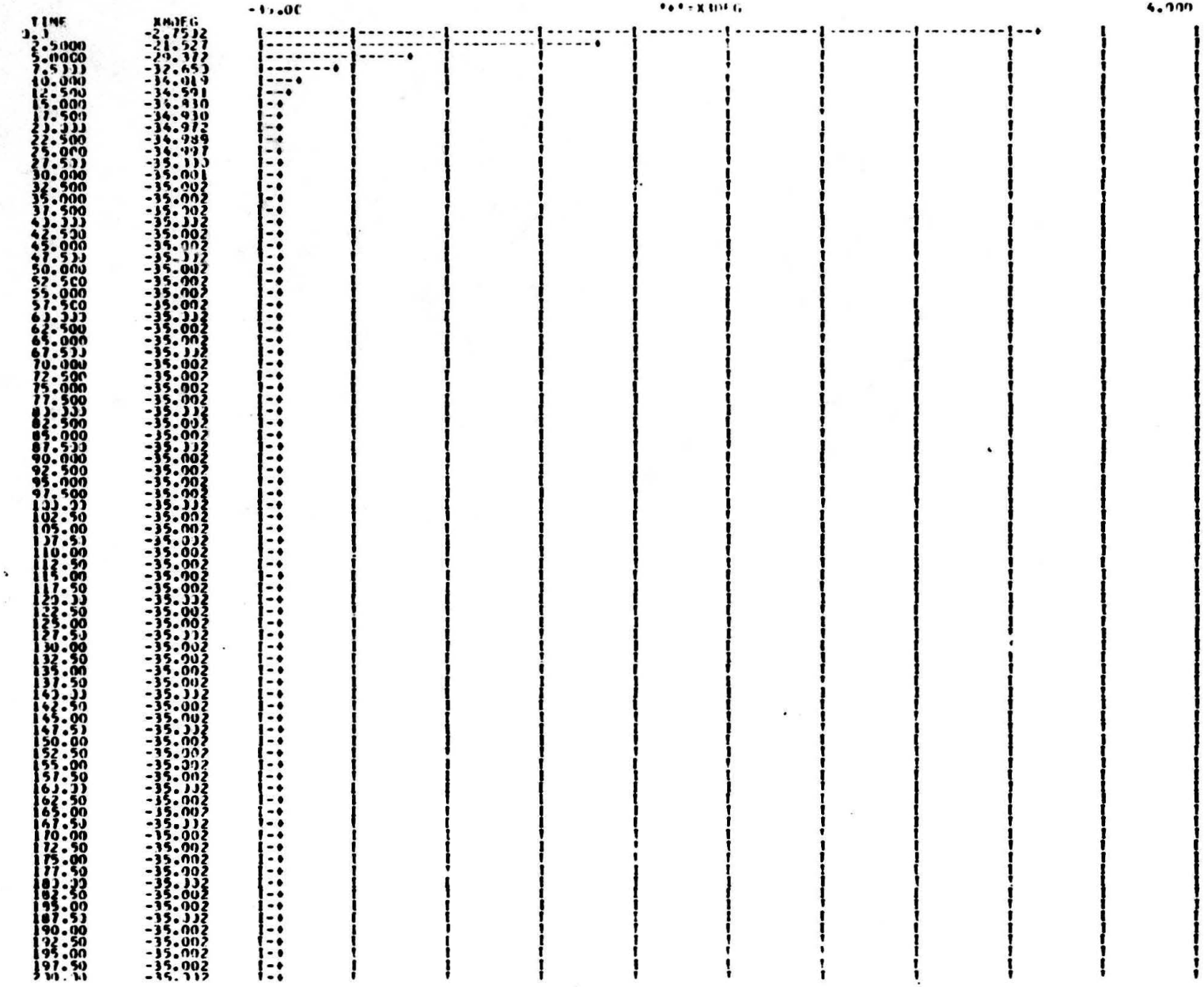


Figure 8-13 (continued)

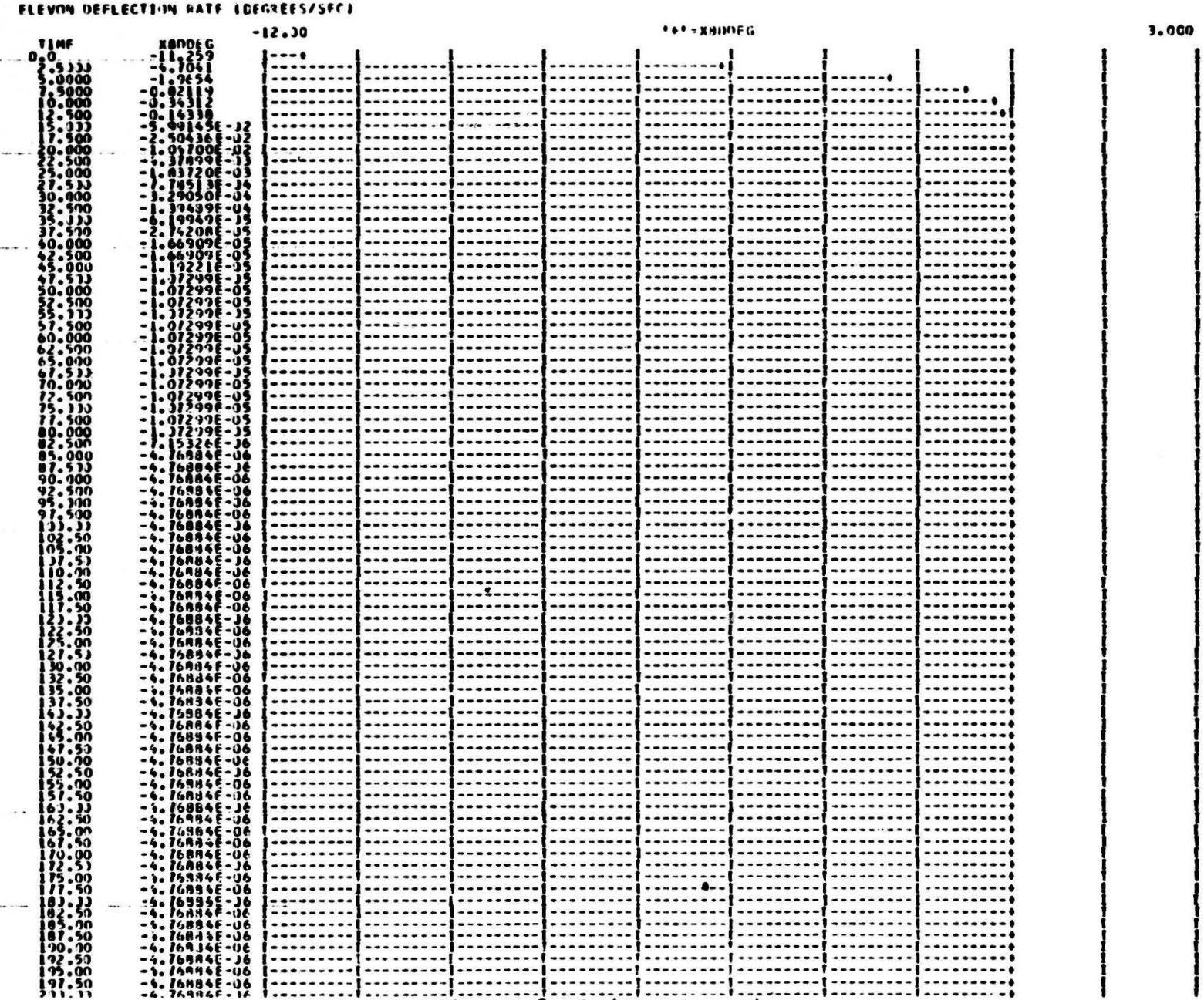


Figure 8-13 (continued)

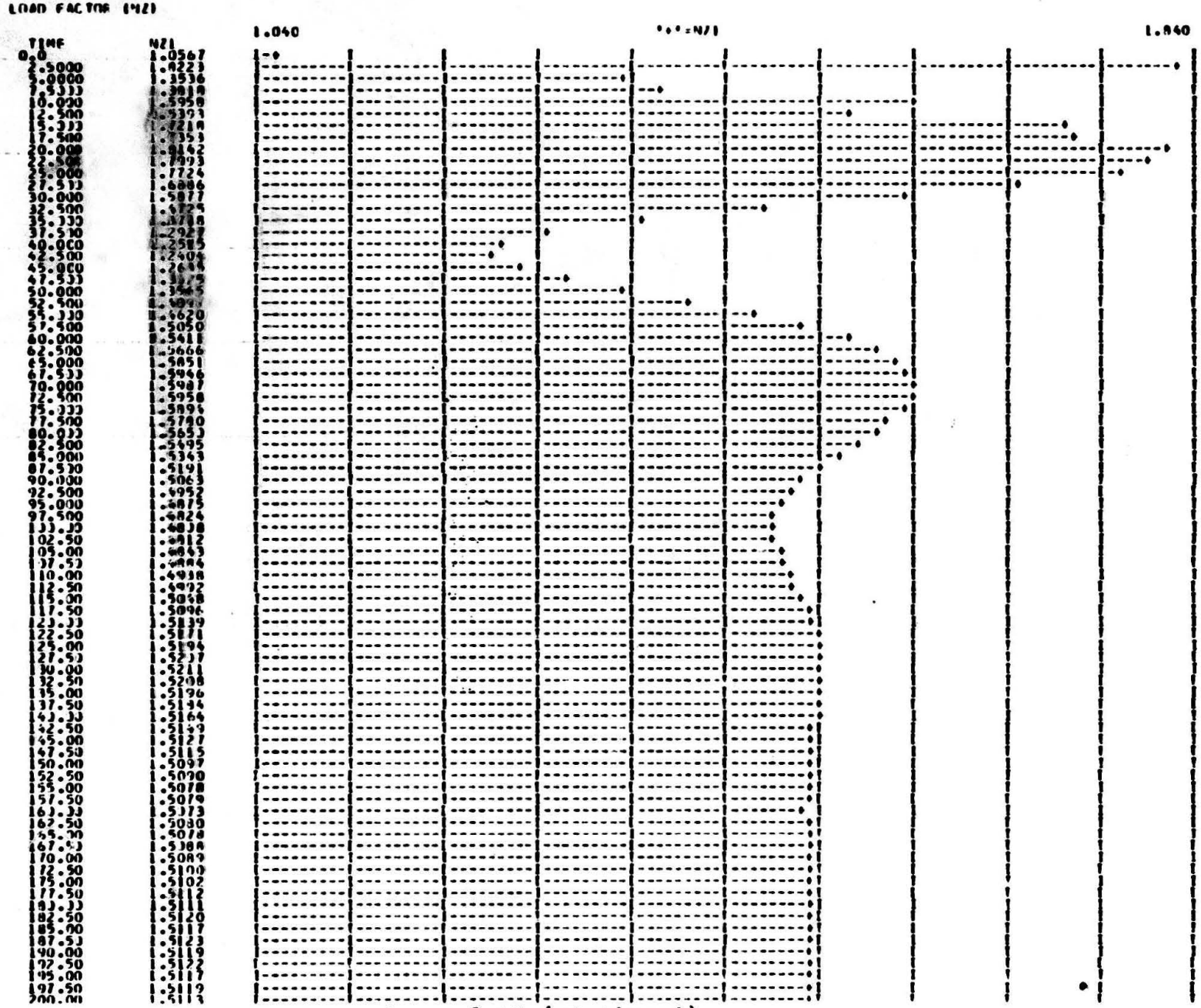


Figure 8-13 (cOntinued)

already entered the atmosphere, was flying aerodynamically, being commanded, responding, etc., in short, was in a dynamic environment when this program started. Unless the parameters existing at t_o for this simulation can be precisely ascertained, it is doubtful that meaningful results can be expected.

To this end, angle of attack corresponding to the commanded load factor at t_o was calculated:

$$n_z = 1.09 = C_L(\tfrac{1}{2}\rho V^2)S/mg$$

Solving for C_L yielded 0.722. Since the angle of attack at 1.0 "g" was 10^o with a C_L of 0.544, the angle of attack at 1.09 "g" was found to be $10^o(0.722/0.544)$ or 13.27^o (0.2316 rad).

An initial pitch rate would affect the X2 coefficient in the X1DOT equation and the X1 coefficient in the X2DOT equation, so it was computed using $n_z = Q_oU_o/g + 1.0$ and found to be 0.0344 rad/sec.

Both of these modifications were made to the program with negligible effect on the results.

To analyze the results as they stand:

The angle of attack first exceeded the limits of the

FUNCTION statements (requiring interpolation of the force coefficients well outside the linear range of the functions) at approximately 2 seconds, oscillated in and out of the range, and left the range for good at approximately 10 seconds. All stability derivatives dependent upon angle of attack must be considered suspect after this time. The angle of attack was computed by dividing the vertical velocity perturbation by the horizontal velocity and adding this to the initial angle of attack.

The vertical velocity response (positive is downward) reached an extremely high value very quickly, and if applied to altitude, would have the orbiter impacting the ground before the simulation period was half over. Such a rate of descent would also cause a rapid change in air density, which was originally assumed constant, leading to very different values of those stability derivatives proportional to RHO. The assumption of a constant RHO should be valid for the three minute duration of the simulation.

The pitch rate magnitudes are not unusual, perhaps a bit high, but the steady state pitch angle is much too high. The steady state values of 58° pitch angle and 71° angle of attack indicate a glide angle of 13°, also much too high.

The elevon deflection, going to the trailing edge up limit in just over ten seconds, indicated that the vehicle sensed an insufficient nose up pitching moment with a GCMD of 1.09 and was trying vainly to create that moment. The result of the full trailing up deflection was instead a stalling angle of attack and a high rate of descent.

The actual load factor experienced by the vehicle in the simulation was only slightly higher than expected; the large elevon deflection was undoubtedly the cause of the initial rapid rise in this parameter. However, since the program computed n_z as a function of ρ, the steady state value was meaningless.

Taking the above observations into consideration, the program appeared to be consistent. Many possible reasons for the magnitude discrepancies were examined, but no changes in the program made more than a modicum of change in the results. It appeared that the error was basic in nature and not related to the model as presented or to the CSMP program. The most likely cause is, as was mentioned earlier, the fact that the simulation is not commencing at t=0.

BIBLIOGRAPHY

National Aeronautics and Space Administration Technical Memorandum TM X-2804, Supersonic Aerodynamic Characteristics of the North American Rockwell ATP Shuttle Orbiter, by G. M. Ware, B. Spencer, Jr., and R. H. Fournier, August 1973

National Aeronautics and Space Administration Technical Memorandum TM X-2786, Subsonic Aerodynamic Characteristics of a Space Shuttle Orbiter, by J. C. Ellison, July 1973

Greensite, A. L., Elements of Modern Control Theory, Spartan Books, 1970

Space Division, North American Rockwell, Aerodynamic Design Data Book, v. 1, SD 72-SH-0060-1I

Melsa, J. L. and Jones, S. K., Computer Programs for Computational Assistance, 2d ed., McGraw-Hill Book Company, 1973

Arden, B. W. and Astill, K. N., Numerical Algorithms, Origins, and Applications, Addison-Wesley Publishing Company, 1970

Organick, E. I. and Meissner, L. P., Fortran IV, Addison-Wesley Publishing Company, 2d ed., 1974

Ogata, K., Modern Control Engineering, Prentice-Hall, Inc., 1970

McRuer, D., Ashkenas, I., and Graham, D., Aircraft Dynamics and Automatic Control, Princeton University Press, 1973

Dommasch, D. O., Sherby, S. S., and Connolly, T. F., Airplane Aerodynamics, 4h ed., Pitman Publishing Corp., 1967

Melsa, J. L. and Schultz, D. G., Linear Control Systems, McGraw-Hill Book Co., 1969

Etkin, B., Dynamics of Flight, John Wiley & Sons, Inc., 1959

DiStefano, J. J., III, Stubberud, A. R., and Williams, I. J., Feedback and Control Systems, McGraw-Hill Book Co., 1967

Standard Mathematical Tables, 22d ed., CRC Press, 1974

Fullerton, C. G., LTCOL, USAF, "Space Shuttle Orbiter Approach and Landing Test Program," The Society of Experimental Test Pilots, 1975 Report

INITIAL DISTRIBUTION LIST

	No. Copies
1. Defense Documentation Center Cameron Station Alexandria, Virginia 22314	2
2. Library, Code 0142 Naval Postgraduate School Monterey, California 93940	2
3. Department Chairman, Code 67 Department of Aeronautics Naval Postgraduate School Monterey, California 93940	1
4. Professor D. J. Collins Department of Aeronautics Naval Postgraduate School Monterey, California 93940	1
5. LCDR C. J. Pierce, USN Code 50 Naval Air Development Center Warminster, Pennsylvania 18974	1